

# **Determining the initial design parameters of a radial-inflow turbine**

**Abrie Rossouw**

**M. Eng**

**North-West University**

**December 2006**

**Supervisor: Dr. B.W. Botha  
Potchefstroom campus**

## EXECUTIVE SUMMARY

The development of computer technology makes it increasingly possible to start designs through simulation and making it possible to address technical problems before manufacturing. This not only saves cost, but also the design time needed to develop a new product. In order to stay competitive within the market, designers are forced to make use of simulation in various fields by means of specialist software packages.

Specialist software packages usually have the disadvantage of being expensive and that the designer must already have a good basis in order to significantly make use of it. Thus, a need exists to guide young turbo-machine designers in making reasonable assumptions during the design of a new turbo-machine, in this case a radial-inflow turbine.

The aim is to give the designer meaningful initial design parameters making it possible for the designer to start a new design within a current available simulation package with some degree of assurance that it will solve. This is achieved by completing the following three steps:

1. Do a thorough literature study concerning radial-inflow turbines in order to determine which parameters are important during the design of a radial-inflow turbine.
2. Develop a simple tool to determine the initial design parameters of a radial-inflow turbine by making use of the Engineering Equation Solver (EES).
3. Verify the constructed EES radial-inflow turbine design tool.

After these steps have been completed, the designer will be able to determine "ball-park" values for the design of a radial-inflow turbine and in doing so, will be able to state the economical feasibility of a system before proceeding to a detail design.

## Acknowledgements

I would like to acknowledge those who supported me during the completion of this thesis, my family as well as my mentor for his guidance. In particular to my wife Charmaine, for her patience and support during the moments of frustration. Finally, I would like to thank the Lord for his blessings.

## TABLE OF CONTENTS

### CHAPTER 1

#### INTRODUCTION

1.1	Need of study.....	1
1.2	Problem statement.....	2
1.3	Aim of study.....	2
1.4	Methodology of study.....	2

### CHAPTER 2

#### LITERATURE STUDY

2.1	Types of turbines.....	4
2.2	Introduction to radial turbines.....	6
2.2.1	Cantilever-type radial-inflow turbine.....	11
2.2.2	Mixed-flow-type radial-inflow turbine.....	12
2.3	Detail operation of a radial-inflow turbine.....	13
2.3.1	The Collector.....	14
2.3.2	Nozzle blades.....	14
2.3.3	The rotor.....	15
2.3.4	The outlet diffuser / exhaust diffuser.....	15
2.4	Losses in radial-inflow turbines.....	16
2.4.1	Losses.....	16
2.4.1.1	Passage loss.....	16
2.4.1.2	Tip clearance loss.....	17
2.4.1.3	Trailing edge loss.....	17
2.4.1.4	Windage loss.....	17
2.4.2	Loss coefficients in 90° IFR turbines.....	18
2.4.2.1	Nozzle loss coefficients.....	18
2.4.2.2	Rotor loss coefficient.....	19
2.5	The temperature range of a radial-inflow turbine.....	19
2.6	Limiting factors in turbine design.....	19
2.7	Rotor flow processes.....	20
2.7.1	The inlet region.....	20
2.7.2	The exducer region.....	22
2.8	Conclusion.....	23

### CHAPTER 3

#### PRELIMINARY DESIGN OF A RADIAL-INFLOW TURBINE

3.1	Basic analysis of a stage.....	24
3.1.1	Velocity triangles.....	25
3.2	Nozzle vanes.....	31
3.2.1	The nozzle vane design.....	31
3.2.2	Deviation.....	33
3.3	The nozzle-rotor interspace.....	35



3.4	Radial-inflow turbine design.....	36
3.4.1	Rotor preliminary design.....	36
3.4.2	Rotor design optimization.....	43
3.4.2.1	Rotor inlet.....	44
3.4.2.2	Rotor exit.....	46
3.4.3	Scaling.....	48
3.4.4	EES radial-inflow turbine design.....	53
3.4.5	Volute preliminary design.....	55
3.4.5.1	Flange to Critical Section.....	56
3.4.5.2	Scroll section.....	57
3.4.6	Blade loading and blade number.....	59
3.4.7	Meanline analysis.....	60
3.5	Conclusion.....	63

## CHAPTER 4

### EES VERIFICATION AND GUIDELINES

4.1	EES verification.....	64
4.1.1	Example 1.....	65
4.1.2	Garrett GT42.....	66
4.1.3	Concepts NREC Rital.....	68
4.1.3.1	Rotational speed variation.....	69
4.1.3.2	Mass-flow variation.....	71
4.1.3.3	Inlet temperature variation.....	74
4.1.3.4	Summary and Conclusion.....	76
4.2	Design guidelines.....	78
4.2.1	EES input parameters.....	78
4.2.2	Materials.....	80
4.2.3	Bearings.....	81
4.3	Conclusion.....	83

## CHAPTER 5

### CONCLUSION AND RECOMMENDATIONS

5.1	Conclusion.....	84
5.2	Recommendations.....	85

References.....	86
Appendix A.....	90
Appendix B.....	99
Appendix C.....	101
Appendix D.....	102
Appendix E.....	103
Appendix F.....	115

## NOMENCLATURE

B	Blockage	
b	Blade height	
C	Absolute velocity	
C <sub>p</sub>	Specific heat	
C <sub>s</sub>	Isentropic 'spouting' velocity	
h	Enthalpy	
i	Incidence angle	
k	Specific heat ratio	
M	Mach number	
m	Mass flow rate	
N	Rotational speed	
N <sub>s</sub>	Specific speed	
P	Power, Pressure	
PR	Pressure ratio	
R	Gas constant	
r	Radius	
Re	Reynolds number	
SC	Swirl coefficient	
T	Temperature	
t	Blade thickness	
U	Blade speed	
V	Velocity	
W	Relative velocity	
Z	Blade number	
$\alpha$	Absolute flow angle	(Alpha)
$\beta$	Relative flow angle	(Beta)
$\Delta$	Difference	(Delta)
$\delta$	Deviation angle, difference	(delta)
$\eta$	Efficiency	(Eta)
$\theta$	Angle	(Theta)
$\rho$	Density	(Rho)
$\Phi$	Flow coefficient	(Phi)
$\Psi$	Loading coefficient	(Psi)

## LIST OF FIGURES

- Figure 1: Illustration of a radial-inflow turbine used in turbochargers.
- Figure 2: An illustration of an axial-flow turbine.
- Figure 3: Illustration of the components of a turbo-charger.
- Figure 4: Cross section of a gas turbine engine with single-stage radial turbine.
- Figure 5: A cryogenic radial-inflow turbine.
- Figure 6: A cryogenic radial-inflow turbine.
- Figure 7: Cantilever-type radial-inflow turbine.
- Figure 8: Mixed-flow-type radial-inflow turbine.
- Figure 9: Components of a radial-inflow turbine.
- Figure 10: Volute flow.
- Figure 11: Photograph of the exducer on to the rotor.
- Figure 12: Observed path lines in a radial-flow rotor at various inlet flow angles.
- Figure 13: Recirculation in the inlet region of a radial turbine rotor passage.
- Figure 14: Passage vortex development in an axial turbine blade passage.
- Figure 15: Components of a radial turbine.
- Figure 16: Rotor inlet velocity triangle.
- Figure 17: Rotor exit velocity triangle.
- Figure 18: Uncambered and cambered radial turbine nozzle guide vanes.
- Figure 19: Co-ordinated transformation of blade design from Cartesian to radial plane.
- Figure 20: Swing-vane variable-geometry turbine.
- Figure 21: Comparison of predicted and measured deviation.
- Figure 22: Correlation of blade loading and flow coefficients for radial-inflow turbines.
- Figure 23: Rotor inlet velocity triangle.
- Figure 24: Rotor blade geometry.
- Figure 25: Rotor exit velocity triangle.
  
- Figure 26: Rotor exit Mach numbers for zero exit swirl.
- Figure 27: Constructed EES design window.
- Figure 28:  $A/r$  ratio of a volute.
- Figure 29: Volute sections.
- Figure 30: Sketch of the volute showing the velocity vectors.
- Figure 31: Flow angle at rotor inlet as a function of the number of rotor vanes.

- Figure 32: Rotational speed at 20 000 rpm.  
 Figure 33: Rotational speed at 50 000 rpm.  
 Figure 34: Rotational speed at 80 000 rpm.  
 Figure 35: Rotational speed at 110 000 rpm.  
 Figure 36: Mass-flow rate at 0.1 kg/s.  
 Figure 37: Mass-flow rate at 0.125 kg/s.  
 Figure 38: Mass-flow rate at 0.15 kg/s.  
 Figure 39: Inlet temperature at 400 K.  
 Figure 40: Inlet temperature at 600 K.  
 Figure 41: Inlet temperature at 800 K.  
 Figure 42: Inlet temperature at 1000 K.  
 Figure 43: Speed response of a Ball bearing and a Sleeve bearing.  
 Figure A1: An illustration of a turbo-charger.  
 Figure C1: Example 1 EES design window.  
 Figure D1: GT42 EES design window.  
 Figure F1: Design window for a radial-inflow turbine rotor in EES.  
 Figure F2: Correlation of blade loading and flow coefficients for radial-inflow turbines.  
 Figure F3: Results of three different relative inlet-flow angles.

## LIST OF TABLES

- Table 1: Comparison of EES and Example 1 results.  
 Table 2: Comparison of EES and GT42 results.  
 Table 3: Input parameters and their influences  
 Table 4: Properties of turbine materials.  
 Table A1: Results for the preliminary design of a radial-inflow turbine.

## CHAPTER 1

### INTRODUCTION

#### 1.1 *Need of study*

Blanchard and Fabrycky (1998) states: "Technological growth and change are occurring continuously and are stimulated by an attempt to respond to some unmet current need and by attempting to perform ongoing activities in a more effective and efficient manner". The development of computer technology makes it increasingly possible to start designs through simulation and making it possible to address technical problems before manufacturing. This not only saves cost, but also the design time needed to develop a new product. In order to stay competitive within the market, designers are forced to make use of simulation in various fields. One such a field is the design of turbo-machines where the ability to simulate can save months of development time merely by making use of design software packages such as *Concepts NREC*®.

Specialist software packages usually have the disadvantage of being expensive and that the designer must already have a good basis in order to significantly make use of it. Although the software package delivers good results, it however means that a new designer does not always know which meaningful input parameters to use in order to reach the initiated design. Without meaningful input parameters, designers will usually discover that their designs are different to execute. This presents the designer with the alternative of starting the design procedure with a currently available design and then modifying it until reasonable results are reached. Although this method usually works, it is exposed to the danger of transferring flaws from the current design to that of the new design.

In many cases a detail design is not yet necessary and a simple software package can contribute by first reaching "ball-park" values and in doing so,

stating the economical feasibility of a system before proceeding to a detail design.

## **1.2 Problem statement**

The use of currently available turbo-machine simulation packages has indicated that a need exists to guide young turbo-machine designers in making reasonable assumptions, based on previous experience, during the design of a new turbo-machine. The goal is to help develop the designer's background concerning radial-inflow turbine design and to help prevent flaws carried over from an existing design to that of a new design by making use of a radial-inflow turbine design tool. It will also make it possible to determine the feasibility of a system before continuing with a detail design through the much more expensive turbo-machine software packages.

## **1.3 Aim of study**

The aim of this study is to develop a tool to assist designers with the initial "ball-park" design of new radial-inflow turbine rotors. The aim is to give the designer meaningful initial design parameters making it possible for the designer to start a new design within a current available simulation package with some degree of assurance that it will solve, from where further fine-tuning will be possible.

## **1.4 Methodology of study**

In order to reach this goal, the first step will be to do a thorough literature study in order to determine which parameters are important during the design of a radial-inflow turbine. The second step will be to develop a simple tool by making use of the Engineering Equation Solver (EES) in order to determine the initial design parameters of a radial-inflow turbine. This will make it possible for users to reach a first order design. In order to create trust within this tool, it will have to be verified. The third step will be accomplished through two different methods, the first being to compare it to design samples sourced from turbo-machine literature.

The second method will be to make use of the *Concepts NREC*<sup>®</sup> software package, which is accepted worldwide for the design of turbo-machines.

Chapter 2 will address the first step towards reaching the specified goal, a thorough literature study regarding radial-inflow turbines.

## CHAPTER 2

### LITERATURE STUDY

The first step in reaching the aim of the study is to do a thorough literature study in order to determine which parameters are important during the design of a radial-inflow turbine. This chapter will present the designer with the necessary literature by discussing the following topics:

- Types of turbines
- Introduction to radial turbines
- Detail operation of radial-inflow turbines
- Losses and temperature range of radial-inflow turbines
- Limiting factors and rotor flow processes in radial-inflow turbines

#### **2.1 Types of turbines**

Gas turbines are heat engines based on the Brayton thermodynamic cycle, which is one of four that account for most of the heat engines in use (Miller, 1998). Two types of turbines are currently being used, namely the radial-flow turbine (Figure1) and the axial-flow turbine (Figure 2).

A radial-flow turbine is a turbo machine unit consisting of a rotating rotor and other extras such as a volute and a nozzle. The flow through a radial turbine can either be radial inwards or radial outwards (Saravanamuttoo, 2001). The main difference between a radial-flow turbine and an axial-flow turbine is that the flow of the gas (water or air) is directed to a 90° flow from the original flow direction over the blades of the rotor unit.

Inward-flow radial (IFR) turbines can provide efficiencies equal to that of the best axial-flow turbines, but only over a very limited specific speed range. The significant advantages offered by the IFR turbine compared to the axial-flow



turbine are the higher work that can be obtained per stage, the ease of manufacture and its superior ruggedness.

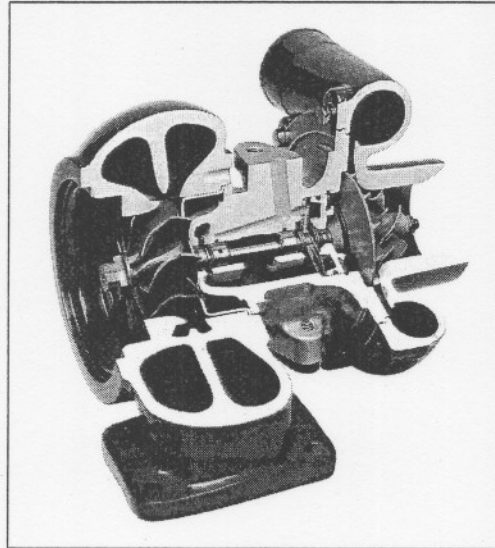


**Figure 1:** *Illustration of a radial-inflow turbine used in turbochargers. (Author)*

A summary comparison between radial-flow turbines and axial-flow turbines reveals the following:

- Small radial-inflow gas turbines have efficiencies comparable to axial-flow turbines that could be substituted.
- Axial flow turbines usually have better efficiencies than radial flow turbines.
- Radial-flow turbines are usually smaller than axial flow turbines giving nearly the same power output, because radial-inflow turbines have a greater power per unit mass flow rate of gas.

Figure 2 is an illustration of an axial-flow turbine.

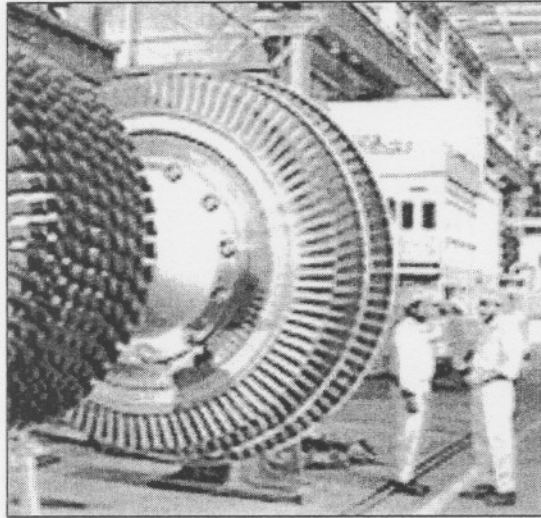


Figure 2: An illustration of an axial-flow turbine. (From Saravanamuttoo, 2001)

## 2.2 Introduction to radial turbines

The following paragraph will give the reader a short background concerning radial-inflow turbines and how it operates. Interesting facts regarding radial-inflow turbine design will also be mentioned.

Radial-inflow turbines have a long history and were used before axial machines were even discovered. The first truly effective radial turbines were water turbines and the development of the radial turbine can be traced from the Roman Empire 70 B.C. to the modern Francis turbine (Wilson, 1998). The study will mainly be looking at turbines working with compressible fluids.

Today the compressible flow radial turbine is used in many different applications such as small gas turbines, turbochargers for cars, buses and trucks, railway locomotives, diesel power generators, cryogenic and process expanders, rocket engine turbo-pumps and specialty steam turbines.

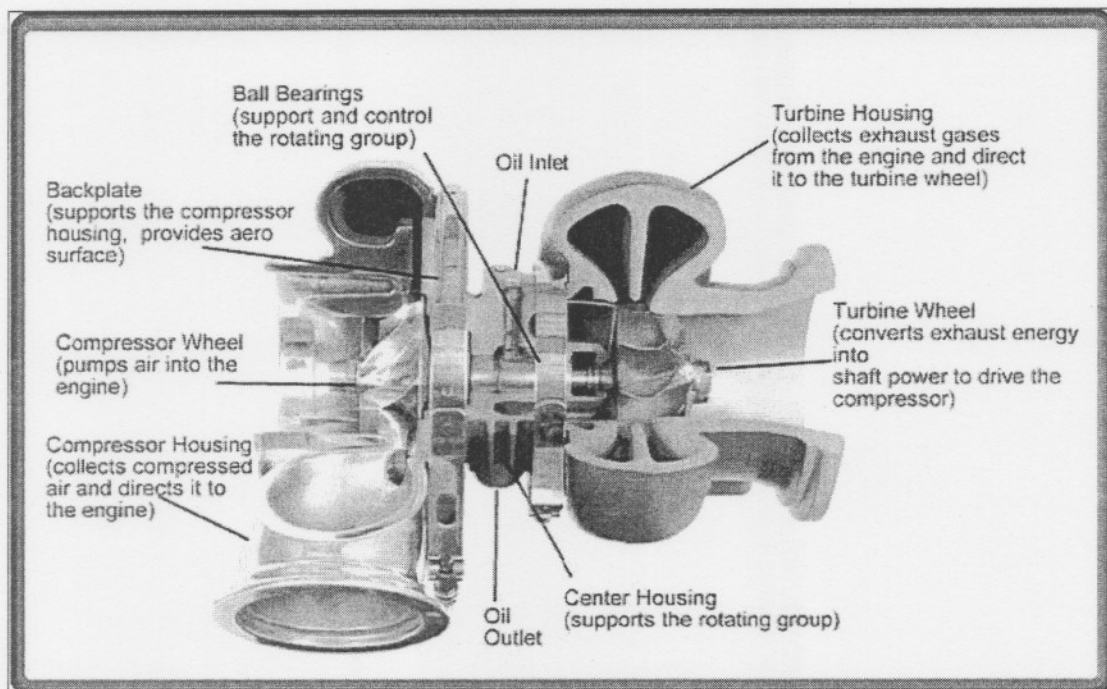
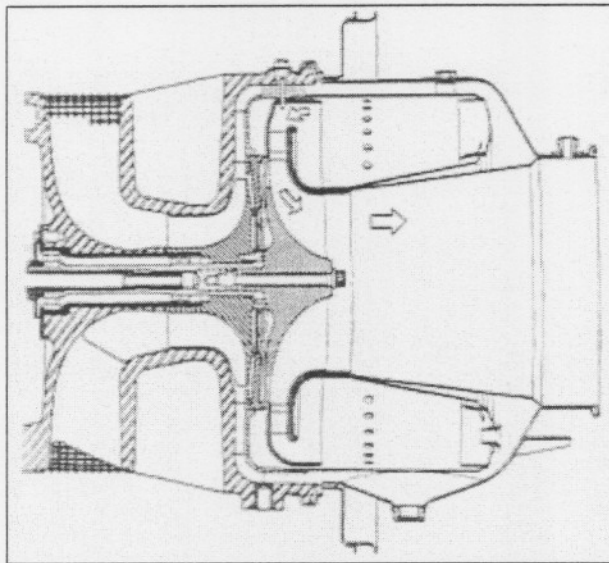


Figure 3: Illustration of the components of a turbo-charger. (From Garrett, 2005)

In some designs a split-inlet exhaust housing (Figure 3) permits the exhaust pulses to be grouped or separated by cylinder all the way to the turbine, as used in combustion engines. The merit of doing this is in keeping the individual package of energy, an exhaust putt, intact and unmolested by other putts all the way to the turbine (Bell, 1997).

A radial turbine stage is distinguished from an axial stage by the fact that the fluid undergoes a significant radius change in passing through the rotor. In a conventional radial stage the fluid enters the rotor in the radial inward direction, it is then turned in the axial-radial plane and leaves in the axial direction. The radial stage consists of two essential parts: a *stator* in which the working fluid is expanded and turned to give it a circumferential velocity about the axis of the machine and a *rotor* through which the flow passes and in doing so, generates work (Baines, 2003).





**Figure 4:** Cross section of a gas turbine engine with single-stage radial turbine.  
(From Baines, 2003)

The stator may take a number of forms that may depend on factors such as the application and the installation. Figure 4 is an illustration of a gas turbine making use of a radial turbine stage. The gas leaving the combustion chamber flows to the turbine through ducting and finally approaches it from a radial direction. In order to accelerate the gas and give it the necessary tangential velocity at entry to the rotor, a ring of nozzle vanes is used.

Different arrangements of stators, but with the same basic design of rotor, can be seen in Figure 5 and Figure 6.

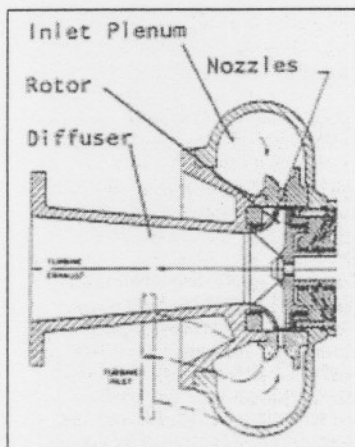


**Figure 5:** A cryogenic radial-inflow turbine. (From Baines, 2003)

In Figure 5 the flow enters the turbine via an annular plenum that has a constant cross-section and sufficient volume so that the gas velocity is very low in this region. The fluid leaves the plenum through a set of nozzle vanes. These vanes accelerate the flow from effectively stagnant conditions in the plenum to high velocity at the inlet to the rotor (Baines, 2003). Thus, a radial-inflow turbine translates high-energy flow to low-energy flow by extracting energy. The aim is to get the inlet flow velocity as high as possible by transmitting flow from a high pressure to a low pressure.

In Figure 6 the first element of the turbine is a volute, also known as an inlet scroll. The flow enters through a pipe and is dispersed evenly around the annulus of the turbine in the volute. The cross-sectional area of the volute linearly reduces in the streamwise direction from a maximum at the inlet to nearly zero after the full 360° of annulus have been traversed.

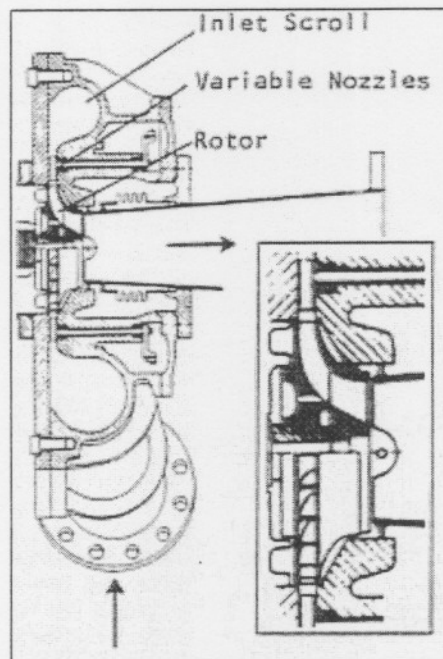


Figure 6: A cryogenic radial-inflow turbine. (From Baines, 2003)

By steadily reducing the area, the reduced area causes the flow to be accelerated and to acquire some considerable swirl (tangential velocity) before it enters the nozzle. Because the flow has already been turned to a significant degree in the volute, the nozzle vanes here have to do less turning. The turbine stator thus consists of two component parts, the volute and the nozzle.

A radial turbine stage can deliver a greater specific power (power per unit mass flow rate of gas) than an equivalent axial stage, thus giving the same power, but with less space needed. This is explained by the Euler turbo-machinery equation and the velocity triangle (Figure 16).

The former equation is (Baines, 2003):

$$W_x = U_4 C_{\theta 4} - U_6 C_{\theta 6} \quad (2.1)$$

(Station 4 is the rotor inlet and 6 the rotor exit)

The geometry of the velocity triangles gives the following relation:

$$W^2 = U^2 + C^2 - 2UC \sin \alpha$$

which can be combined with Eq. (2.1) to give:

$$W_x = 0.5 [(U_4^2 - U_6^2) - (W_4^2 - W_6^2) + (C_4^2 - C_6^2)] \quad (2.2)$$

From Equation 2.2 one can clearly see the contribution made to the work output by the change in blade tip speed  $(U_4^2 - U_6^2)$  and hence the radius, in the radial turbine.  $U$  is approximately constant in an axial stage and there is no significant contribution. Several other designs that are necessary in order to achieve a high specific work output  $W_x$ , is also shown by this equation. The relative velocity term  $(W_4^2 - W_6^2)$  is subtracted and so it must be arranged that  $W_6 > W_4$  so that this term makes a net positive contribution to the work output. The absolute velocity term  $(C_4^2 - C_6^2)$  is then added. In order to maximize the stator exit velocity, and hence the rotor inlet velocity  $C_4$ , the stator has to be designed to accelerate the flow at inlet. The exit velocity triangle should be arranged in order to minimize the absolute velocity at exit  $C_6$  (Baines, 2003).

There are two types of radial-inflow turbines: the cantilever radial-inflow turbine and the mixed-flow radial-inflow turbine, as shown in Figure 7 and Figure 8.

### 2.2.1 Cantilever-type radial-inflow turbine

Non-radial inlet angles are used on Cantilever blades and they are often two-dimensional. It is similar to impulse or low-reaction turbines because there is no acceleration of the flow through the rotor. The cantilever-type radial-inflow turbine is not used frequently because of low efficiency and production difficulties. Rotor blade flutter problems are common to this type of turbine (Boyce).



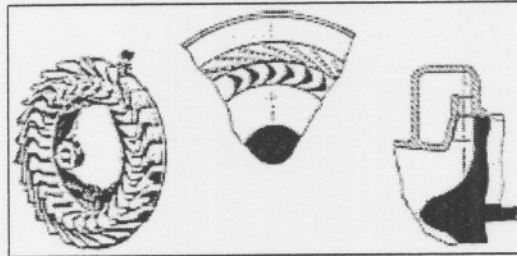


**Figure 7:** *Cantilever-type radial-inflow turbine. (From Boyce)*

### 2.2.2 Mixed-flow-type radial-inflow turbine

One of the most widely used turbines is the mixed-flow radial-inflow turbine. The scroll that receives the flow from a single duct usually has a decreasing cross-sectional area around the circumference. In some designs, the scrolls are used as vaneless nozzles and create the necessary flow angles. The nozzle vanes are neglected for economical reasons and also to avoid erosion in turbines where fluid or solid particles are trapped in the airflow. Frictional flow losses are greater in vaneless designs than in vaned nozzle designs, because of the non-uniformity of the flow and because of the greater distance the accelerating airflow must travel. Vaneless nozzle configurations are widely used in turbochargers where efficiency is not that important, because in most engines the amount of energy in the exhaust gasses far exceeds the energy needed by the turbocharger (Boyce).

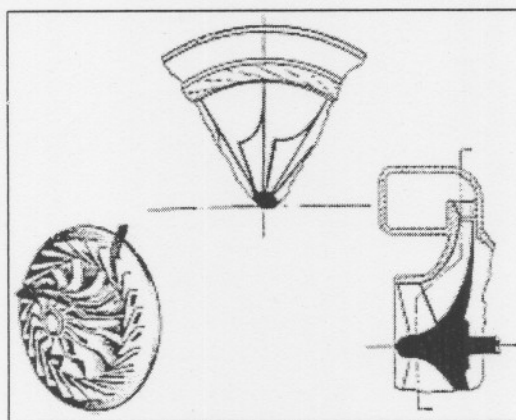


**Figure 8:** *Mixed-flow-type radial-inflow turbine. (From Boyce)*



In some designs, it is preferred that the turbine has no nozzle. In these designs the vanes are dispensed with altogether and the volute alone is responsible for accelerating and swirling the flow. The attraction of this is that by dispensing with the nozzle ring a lower cost assembly can be achieved (Baines, 2005). The disadvantages are that the volute alone is rarely as aerodynamically efficient as a nozzle and that the larger the expansion ratio, the larger the volute that is required to achieve the necessary acceleration.

### 2.3 Detail operation of a radial-inflow turbine

In order to construct an EES design tool for the calculation of the input parameters needed by most radial-inflow turbine design software to do a preliminary and detail design, it will be necessary to understand the design method used. After this has been completed, the designer will be able to operate the constructed EES design tool and will better understand the importance of each design parameter.

The following paragraphs will give a quick recap on the different components of a radial-inflow turbine, some components already mentioned, as well as a more detailed description of each component.

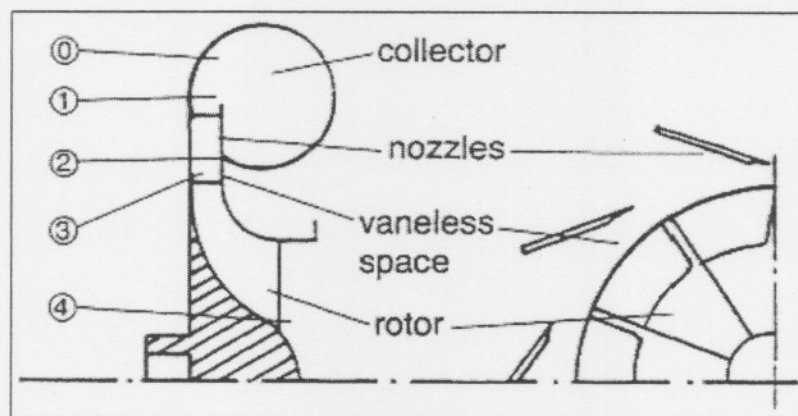


Figure 9: Components of a radial-inflow turbine. (From Boyce)

### 2.3.1 The collector

The collector (Figure 9) is the first part of a radial-inflow turbine that receives the working fluid. It consists of a scroll that has a large diameter at the inlet and steadily decreases until its diameter is nearly zero at the outlet. The working fluid enters the scroll (Figure 10) at the larger diameter and is guided by it as it spread evenly around the turbine rotor. In some designs where a vaneless nozzle is used, the scroll must direct the flow to the correct angle as necessary by the rotor inlet. The fluid or gas that does not enter the rotor the first time will complete the full length of the scroll and re-enter with the incoming fluid. The collector must be designed in conjunction with the rotor, as both must be able to collect and receive the same volume of working fluid.

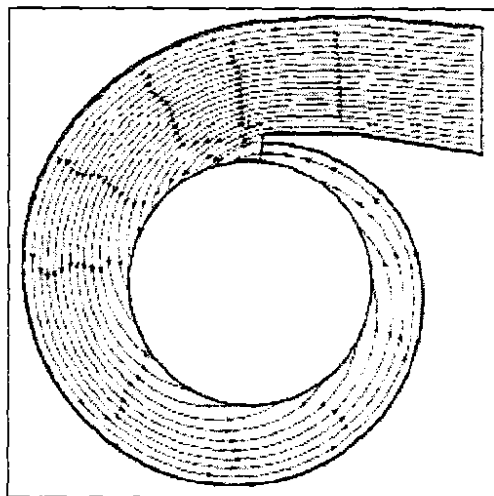


Figure 10: Volute flow. (From Gu, Engeda and Benisek)

### 2.3.2 Nozzle blades

The nozzle blades in a vaned turbine design are usually fitted around the rotor to direct the flow inward with the desired swirl component in the inlet velocity. The flow is accelerated through these blades. In low-reaction turbines the entire acceleration occurs in the nozzle vanes.

### 2.3.3 The rotor

The rotor of the radial-inflow turbine (Figure 11) is made up of a hub, blades and in some cases, a shroud. The hub is the solid axisymmetrical portion of the rotor and defines the inner boundary of the flow passage (also called the disc (Boyce)). The blades are integral to the hub and the flow stream exerts a normal force on it. The exit section of the blading is called an exducer and it is constructed separately like an inducer in a centrifugal compressor. The exducer is curved in order to remove some of the tangential velocity force at the outlet (Boyce).

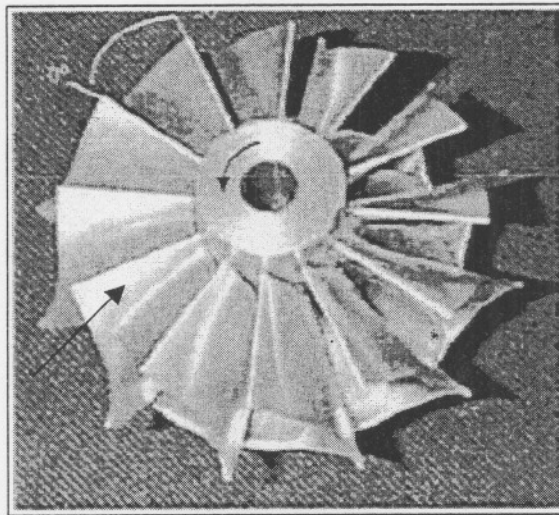


**Figure 11:** *Indication of the exducer region of a rotor.*  
(From Karamanis and Martinez-Botas)

### 2.3.4 The outlet diffuser / exhaust diffuser

The outlet diffuser is used to convert the high absolute velocity leaving the exducer into static pressure, according to Boyce. If this conversion is not done, the efficiency of the unit will be low. The conversion of the flow to a static head must be done carefully since the low-energy boundary layers cannot tolerate great adverse pressure gradients.

As stated by Whitfield and Baines (1990), the other purpose of an exhaust diffuser downstream of the turbine is to recover the exhaust kinetic energy that would otherwise be wasted. This device in effect increases the expansion ratio across the turbine and hence the total to static efficiency. The gains can be quite significant, particularly where the rotor exit has to be made smaller than is aerodynamically desirable for example, to reduce inertia or the blade root stress. According to them, the blade diffuser will normally have either a conical or an annular geometry and may be straight sided or profiled, depending on the requirements of the installation and the desired performance.

## **2.4 Losses in radial-inflow turbines**

### **2.4.1 Losses**

Various losses exist within radial turbines resulting in a significant number of parameters affecting the design of radial turbines. Although the effects of these losses are important, they are second order in determining the basic turbine rotor configuration. However, they are too important to ignore in the detail design of a radial-inflow turbine.

In order to reduce the complexity of the EES design tool, it was decided not to incorporate the various losses into the EES design procedure. The most important losses, however, will be discussed.

#### **2.4.1.1 Passage loss**

The generic term 'passage loss' is sometimes used for all the losses occurring internally in the blade passage. This includes the losses due to cross-stream or secondary flows as well as the mixing these bring about and the blockage and loss of kinetic energy due to the growth of boundary layers in a radial turbine rotor.

[For a more detail discussion on passage loss in a radial turbine, refer to Baines (2003).]

#### **2.4.1.2 Tip clearance loss**

Due to the fact that the rotor has to turn, together with manufacturing difficulty, a clearance gap must be provided between the rotor and its shroud and as a result, leakage from the rotor blade pressure to suction surfaces occurs. The effect of tip clearance on the turbine efficiency has been demonstrated in studies done by Krylov and Spunde (1936), Futral and Holeski (1970) and by Watanabe et al (1971). The results of the studies done by Futral and Holeski also showed significant effects on the exit flow conditions.

[For a more detail discussion on tip clearance loss in a radial turbine, refer to Baines (2003).]

#### **2.4.1.3 Trailing edge loss**

Passage loss occurs between the inlet and the throat of the rotor and requires the addition of a trailing edge loss. This loss is modelled as a sudden expansion from the throat to a plane just downstream of the trailing edge. It is assumed that the tangential component of velocity is constant and a total pressure loss is based on a sudden expansion from the rotor throat to an area just downstream of the trailing edge.

#### **2.4.1.4 Windage loss**

Windage loss is another loss process, but one which does not relate directly to the blade passage flows. It occurs on the back face of the turbine disk as fluid leaks between the rotor and the backplate. The disk friction is most commonly expressed as a power loss. The equations from Daily and Nece (1960) are probably the most common approach to use. In constructing these equations, they considered the simple case of a disk rotating in an enclosed casing, which is discussed in Baines (2003). Four flow regimes were identified, which corresponded to laminar and turbulent flows with unmerged or merged boundary layers. In the case of a radial turbine design, these can generally be simplified to two regimes determined by a Reynolds number.

## 2.4.2 Loss coefficients in 90° IFR turbines

The losses in the passages of 90° IFR turbines can be represented in a number of ways. There is, in addition to the nozzle and rotor passage losses, a loss at rotor entry at off-design conditions. This occurs when the relative flow entering the rotor is at some angle of incidence to the radial vanes so that it can be called an *incidence loss*. It is also often referred to as a “shock loss”, although there is no shock wave (Dixon, 1998).

The following two losses are also used in the detail design of radial-inflow turbines, but are not incorporated in the EES preliminary design tool.

### 2.4.2.1 Nozzle loss coefficients

According to Dixon, the enthalpy loss coefficient that normally includes the inlet scroll losses is defined by,

$$\zeta_N = (h_2 - h_{2s}) / (0.5c_2^2).$$

Also given is the *velocity coefficient*,

$$\Phi_N = c_2 / c_{2s}$$

and the *stagnation pressure loss coefficient*,

$$\gamma_N = (p_{01} - p_{02}) / (p_{02} - p_2).$$

This can be related to the enthalpy loss coefficient  $\zeta_N$  by,

$$\zeta_N = (1 + 0.5\gamma_N M_2^2).$$

Practical values of  $\Phi_N$  for well-designed nozzle rows in normal operation are usually in the range  $0.9 \leq \Phi_N \leq 0.97$  (Dixon, 1998).

### 2.4.2.2 Rotor loss coefficient

Rotor passage friction losses can be expressed in terms of the following coefficients at either the design condition or at the off-design condition:

The *enthalpy loss coefficient* is,

$$\zeta_R = (h_3 - h_{3s}) / (0.5w_3^2).$$

The *velocity coefficient* is,

$$\Phi_R = w_3 / w_{3s}$$

which is related to  $\zeta_R$  by,

$$\zeta_R = (1 / \Phi_R^2) - 1.$$

The normal range of  $\Phi$  for well-designed rotors is approximately  $0.75 \leq \Phi_R \leq 0.85$ , as published by Dixon.

## 2.5 The temperature range of a radial-inflow turbine

Radial-inflow turbines are usually designed to operate in temperatures lower than 650°C. If the need arises that the turbine must operate at temperatures above that mentioned, the designer is required to make use of more expensive materials that are specifically developed for these temperatures. The designer also has the option of coating the material, allowing the turbine to operate at temperatures approaching 1000°C. The materials that can be used and their temperature limitations are discussed in Paragraph 4.2.2 where the design guidelines for a radial-inflow turbine are discussed.

## 2.6 Limiting factors in turbine design

During the preliminary design of a radial-inflow turbine, there are a few basic factors that must be kept in mind, even if it will mainly form part of the detail design. By keeping these factors in mind, the detail design procedure will be less complicated. The three basic factors are:

- a) *Centrifugal stresses* in the blades are proportional to the square of the rotational speed  $N$  and the annulus area: when  $N$  is fixed, these stresses place an upper limit on the annulus area.
- b) *Gas bending stresses* are inversely proportional to the number of blades and blade section moduli, while being directly proportional to the blade height and specific work output.
- c) *Optimising the design* so that it just falls within the limits set by all these conflicting mechanical and aerodynamic requirements, will lead to an efficient turbine of minimum weight (Saravanamuttoo, 2001).

## 2.7 Rotor flow processes

The rotor may conceptually be divided into two regions: an inlet region where the meridional plane flow is primarily in the **radial** direction and an exducer region where it is primarily in the **axial** direction. This is an important simplification and it is also essential to realise that it is an artificial division that does not take into account the turning process that the fluid must undergo between these two zones.

[See Payne, Ainsworth, Miller, Moss & Harvey (2003) and Denton, Xu (1999) for detail discussions on the flow in turbine stages and 3-D flows in turbines.]

### 2.7.1 The inlet region

The dominant effect in this region, in terms of influence on turbine design, is the turning of the flow tangentially into the inlet and the negative incidence at the point of best efficiency that this implies. This effect has been recognized by designers for many years and has frequently been deduced from measurements of the turbine performance. It has been clear that optimum incidence is in the region of  $-20^\circ$  to  $-40^\circ$  (from consensus) and the incidence angle has also been occasionally measured directly by laser velocimeters (Baines, 2003).



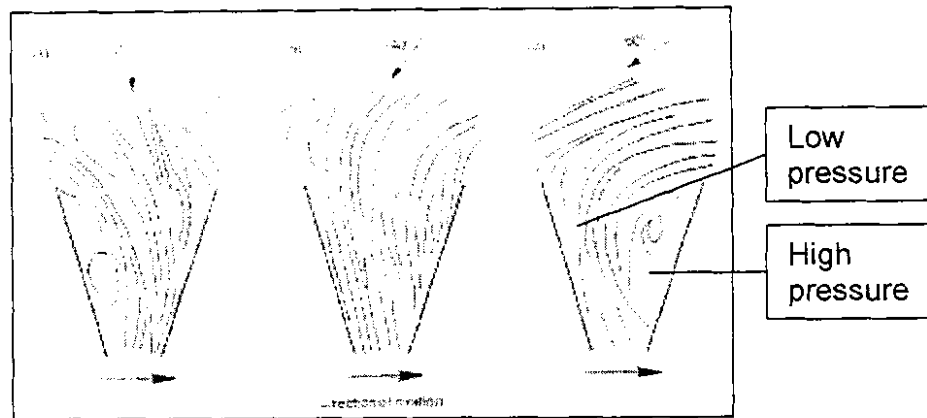


**Figure 12:** Observed path lines in a radial flow rotor at various inlet-flow angles.  
(From Baines, 2003)

In Figure 12 the flow visualizations are helpful in understanding the inlet flow field. The results for three different angles are shown. At an inlet angle of  $-40^\circ$  the most uniform flow distribution can be seen. From the radial inflow condition (a) one can see the flow separating at the leading edge of the suction surface and forming a strong recirculation that occupies the full extent of that surface without reattaching. The more negative flow angle (c) causes the flow to separate at the pressure surface leading edge and there is a region of recirculation on that surface. The path lines however, show that the flow turns sharply back toward the pressure surface and the flow reattaches before it reaches the trailing edge, at which point it is again uniform. Case (b), by contrast, shows that in spite of the incidence, the flow turns smoothly into the blade passage without any evidence of separation (Baines, 2003).

It can be seen from all three cases that there is a strong movement of the flow across the passage from the suction to the pressure surface. According to Baines, this behaviour is caused due to the fact that in the inlet region there is little or no turning of the flow in the tangential plane, so that as the flow moves inwards, the blade speed  $U$  diminishes at a faster rate than the tangential velocity  $C_\theta$ . This causes the relative velocity vector to move toward the positive direction,

which is also toward the pressure surface. The decreasing radius has the effect that it also causes a Coriolis acceleration ( $2W \times \Omega$ ), where  $\Omega$  is the angular speed of the rotor and  $W$  the relative velocity vector, to act across the passage. This becomes less intensive as the fluid moves radially inwards. The strong cross-passage force encountered near the blade tips is not matched by a similar accelerating force at lower radii and this causes a secondary flow to be set up in the blade passage in the form of a circulation in the opposite direction to the passage rotation, as shown in Figure 13.

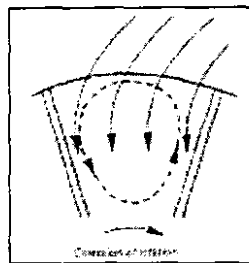


**Figure 13:** *Recirculation in the inlet region of a radial turbine rotor passage.*  
(From Baines, 2003)

The flow will separate and stagnate on the pressure surfaces of the blades if the circulation is sufficiently large. This will happen at large negative incidences. A zero or positive incidence will reduce the strength of the circulation and reduce this tendency. It will also have the effect of reducing the cross-passage pressure gradient and make the flow more likely to separate on the suction surface (Baines, 2003).

## 2.7.2 The exducer region

The flow is predominantly in the axial and tangential directions in the exducer region of the rotor and the high turning of the flow towards the trailing edge means that the largest of the main components of velocity is the tangential. This now gives rise to Coriolis acceleration in the radial direction that tends to move fluid from hub to shroud. There is also the cross passage acceleration that acts

between the blade surfaces as a result of the turning of the flow in the tangential direction (Baines, 2003).

The final result of these forces, as can be seen in Figure 14, is a complex secondary flow development in this region that typically results in non-uniform distributions of blade loading and of flow velocity at the trailing edges of the blades.

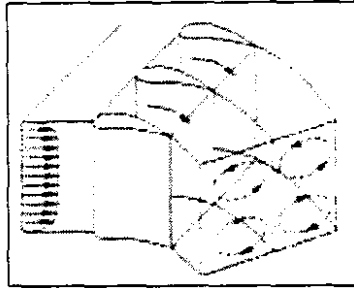


**Figure 14:** *Passage vortex development in an axial turbine blade passage.*  
(From Baines, 2003)

## 2.8 Conclusion

The chapter discussed radial turbines and their applications after which it looked at the different components of a radial-inflow turbine. It also mentioned the losses in radial turbines and the rotor flow processes associated with it.

Now that the literature study concerning radial-inflow turbines has been completed, the next step will be to discuss the basic analysis and design of a radial-inflow turbine in order to develop a tool with which to determine the initial design parameters of a radial-inflow turbine.

## CHAPTER 3

### PRELIMINARY DESIGN OF A RADIAL-INFLOW TURBINE

The aim of this chapter is to equip the designer with the necessary knowledge to do a preliminary design of a radial-inflow turbine. By using this knowledge, a simple tool will be developed in EES to determine the initial design parameters of a radial-inflow turbine. In order to achieve this goal, the chapter will discuss the following topics:

- Basic analysis and design of a radial-inflow turbine
- Nozzle vane design
- EES radial-inflow turbine design
- Volute design

#### 3.1 Basic analysis of a stage

Figure 15 illustrates the principal components and stations in a radial turbine. From the figure below, one can distinguish the volute (0-1), nozzle<sup>†</sup> (1-3), rotor (4-6) and the exhaust diffuser (6-7). Stations 2 and 5 are reserved for intermediate locations in the nozzle and rotor, which will not be used in this analysis.

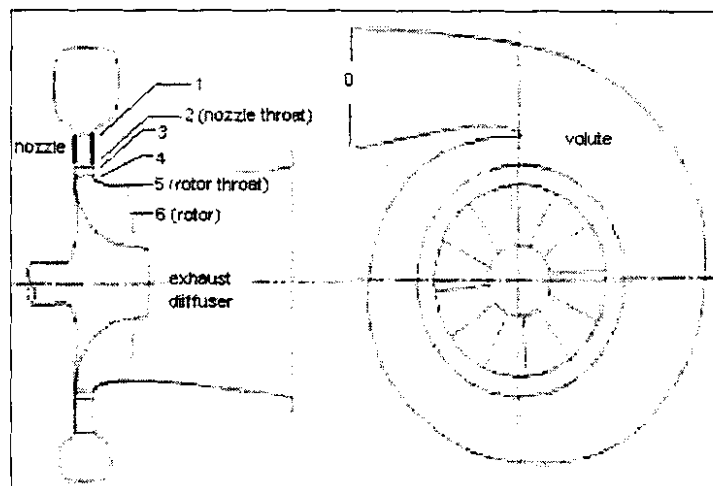


Figure 15: Components of a radial turbine. (From Baines, 2003)

The working fluid flows through the volute, nozzle and rotor and under normal operating conditions the pressure falls continuously. Some recovery of static pressure is obtained if an exhaust diffuser is fitted here. In practical machines, however, the flow is not ideal and losses do occur. For the volute, for example, the effect of loss is to reduce the exit total pressure  $p_{01}$  below the inlet total pressure  $p_{00}$ . If the volute were ideal, no loss would occur and  $p_{01} = p_{00}$ , which is usually assumed in the case of a preliminary design. The fall in total pressure is thus a measure of the loss or performance of components such as the volute or nozzle. In the rotor, however, the total pressure also falls as a result of energy being extracted from the working fluid to produce shaft power and even under ideal circumstances  $p_{04}$  is greater than  $p_{06}$  (Baines, 2003).

### 3.1.1 Velocity triangles

Firstly this study will look at the analysis of the rotor, as this is by far the most significant component in determining the overall turbine performance. For simplicity of the analysis, it is assumed that the working fluid is perfect. Figure 16 illustrates the velocity triangle relating absolute and relative velocities at inlet to the rotor, which plays an important role in the analysis and design phases.

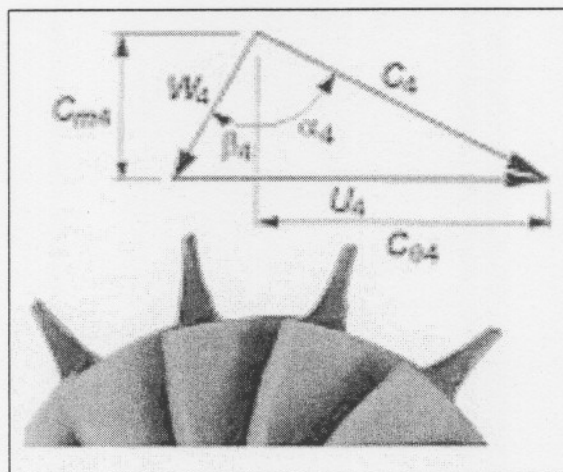


Figure 16: Rotor inlet velocity triangle. (From Baines, 2003)

According to Baines, the working fluid approaches the rotor at velocity  $C_4$  and angle  $\alpha_4$ .  $P_4$  and  $T_4$  are the corresponding static pressure and temperature at this point. It immediately follows from the first law of thermodynamics that for a perfect gas  $T_{04} = T_{00}$ , since no work transfer occurs in the stator and the assumption is made that the heat transfer is negligible. For an ideal stator the total pressure is also unchanged, so that  $p_{04} = p_{00}$ . Some total pressure loss always occurs for real stators and this must be calculated empirically or measured on the actual unit. It is now assumed that a value of  $\Delta p_0$  can be given, so that,

$$p_{04} = p_{00} - \Delta p_0. \quad (3.1)$$

It is satisfactory, for preliminary design, to assume that  $\Delta p_0 = 0$ , since the loss in the stator is usually much smaller than that in the rotor (Baines, 2003).

In determining the velocity triangle, the flow velocity and angle must be set so that the tangential component of velocity  $C_{\theta 4}$  gives the necessary work output. According to the Euler turbo-machinery equation and the radial component of velocity,  $C_{m4}$  is compatible with the mass flow rate:

$$m = \rho_4 A_4 (1 - B_4) C_{m4} \quad (3.2)$$

where  $A_4$  is the annulus area at the rotor tip and  $B_4$  is the allowance for boundary layer blockage, usually between 0 and 0.1mm (Baines, 2003). The geometry of the stator defines the flow angle. This is set mainly by the exit angle of the nozzle vanes in a nozzled turbine, but in reality the flow deviates from the vanes to some extent. This amount of deviation is known as the deviation angle:

$$\alpha_3 = \alpha_{3b} - \delta_3. \quad (3.3)$$

We take  $\alpha_4 = \alpha_3$ , because the flow angle does not normally vary appreciably between the nozzle exit and the rotor inlet, except in cases where the nozzle blades are choked and supersonic expansion occurs (Baines, 2003).

The above discussion has highlighted the three empirical quantities that are required in order to complete the analysis of the fluid flow state at this point, these being the loss, blockage and deviation.

The addition of the blade tip speed  $U_4$  makes it possible to calculate the inlet relative velocity  $W_4$  and flow angle  $\beta_4$ . The remaining equations at this station are standard gas dynamic equations as follows (Baines, 2003):

$$\rho_4 = p_4 / RT_4 \quad (3.4)$$

$$M_4 = C_4 / (kRT_4)^{1/2} \quad (3.5)$$

$$T_{04} / T_4 = 1 + ((k - 1) / 2) M_4^2 \quad (3.6)$$

$$p_{04} / p_4 = (1 + ((k - 1) / 2) M_4^2)^{k / (k - 1)} \quad (3.7)$$

In a well-designed turbine operating at its design point, the relative flow angle  $\beta_4$  at inlet will be matched to the rotor so that the flow enters the blade passages with a minimum disturbance. The blades are usually radial at the inlet to a radial turbine rotor. This region of the rotor is highly stressed and if they were not radial, there would be a bending stress in the blades generated by the centrifugal force, which could cause premature damage or failure of the rotor. If the blades are modified from the normal radial position, a material must be selected which will be able to comply with the higher stresses generated. The inlet blade angle of the rotor shown in Figure 16 is thus  $\beta_{4b} = 0$ . It might also therefore be expected that the best inlet will be achieved when  $\beta_4 = 0$ . The optimum inlet flow angle, however, is normally in the region of  $-20^\circ$  to  $-40^\circ$  (Baines, 2003). The reason for  $\beta \neq 0$  will become apparent when the flow in the inlet region of the rotor is discussed.

At the rotor exit (Station 6 in Figure 17) a similar set of equations is used and again information about the loss, blockage and deviation is required to complete the solution. However, whereas it is possible to specify the stator loss in terms of absolute total pressure, it is not helpful to specify the rotor loss by analogy in relative total pressure terms. This is because in a rotor with significant radius change, the relative total pressure is not constant, even if an isentropic flow is assumed. The rotor loss can be specified by various methods. The simplest is probably to define rotor efficiency as the ratio of the actual work output and the theoretical work output based only on the rotor pressure drop,

$$\eta_R = (h_{04} - h_{06}) / (h_{04} - h_{06s}) = (1 - T_{06} / T_{04}) / [1 - (p_{06} / p_{04})^{(k-1)/k}] \quad (3.8)$$

The loss may alternatively be expressed in terms of enthalpies or kinetic energies:

$$\zeta = (h_{06,rel} - h_6) / (h_{06,rel} - h_{6s}) = (W_6^2) / (W_{6s}^2) \quad (3.9)$$

This is the ratio of the exit relative kinetic energy of the actual rotor and that of an equivalent ideal rotor. Losses may also be defined in terms of the difference, rather than the ratio of these terms:

$$L = W_{6s}^2 - W_6^2 \quad (3.10)$$

then,

$$\zeta = 1 - (W_{6s}^2 - W_6^2) / W_{6s}^2 = 1 - [L / (h_{06,rel} - h_{6s})] \quad (3.11)$$

The static temperature at the rotor exit is then given by:

$$T_6 / T_{06,rel} = 1 - \zeta [1 - (T_{04,rel} / T_{06,rel})(p_6 / p_{04,rel})^{(k-1)/k}] \quad (3.12)$$



Either Equation (3.8) or (3.12) can be used in conjunction with the following equations to calculate the rotor exit state:

The mass-flow rate:

$$m = \rho_6 \pi (r_{6t}^2 - r_{6h}^2) (1 - B_6) W_6 \cos \beta_6 \quad (3.13)$$

The density:

$$\rho_6 = p_6 / RT_6 \quad (3.14)$$

The exit relative flow angle:

$$\beta_6 = \beta_{b6} + \delta_6 \quad (3.15)$$

The enthalpy:

$$\Delta h_0 = C_p (T_{04} - T_{06}) = (U_4 C_{\theta 4}) - (U_6 C_{\theta 6}) \quad (3.16)$$

The relative velocity:

$$W_6 = [C_{m6}^2 + (C_{\theta 6} - U_6)^2]^{1/2} \quad (3.17)$$

The relative exit and exit Mach numbers:

$$M_{6,rel} = W_6 / (kRT_6)^{1/2} \quad (3.18)$$

$$M_6 = C_6 / (kRT_6)^{1/2} \quad (3.19)$$

The exit and relative exit temperatures:

$$T_{06} / T_6 = 1 + [(k - 1) / 2] M_6^2 \quad (3.20)$$

$$T_{06,rel} / T_6 = 1 + [(k - 1) / 2] M_{6,rel}^2 \quad (3.21)$$

The exit and relative exit pressures:

$$p_{06} / p_6 = [1 + ((k - 1) / 2) M_6^2]^{(k-1)/k} \quad (3.22)$$

$$p_{06,rel} / p_6 = [1 + ((k - 1) / 2) M_{6,rel}^2]^{(k-1)/k} \quad (3.23)$$

In Figure 17 the rotor exit velocity triangle is shown. Usually  $\alpha_6 = 0$ , because the velocity triangle is often arranged so that the exit absolute velocity  $C_6$  is in the axial direction. This can be important when matching the next component downstream (for example, another turbine stage). Other things being equal, it will minimize the exit kinetic energy loss  $0.5mC_6^2$  (Baines, 2003). Some designers might opt for some exit swirl, thus  $C_{\theta 6} \neq 0$ . This can be beneficial in a subsequent diffusion process aimed at recovering exhaust kinetic energy. Even if very high power output is required, some negative swirl will aid that process.

[Equations 3.1 – 3.23 are from Baines, 2003]

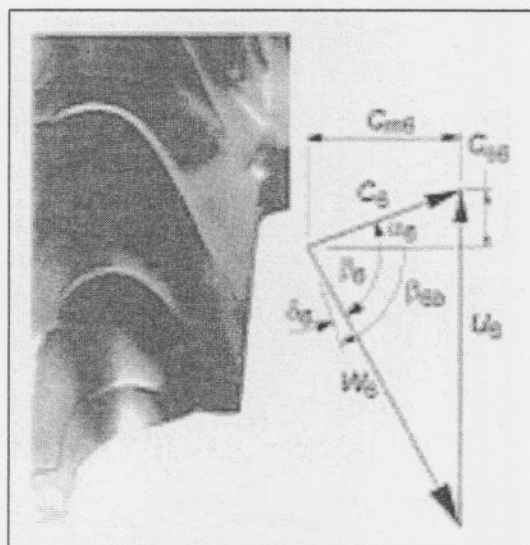


**Figure 17:** Rotor exit velocity triangle. (From Baines, 2003)

## 3.2 Nozzle vanes

### 3.2.1 The nozzle vane design

The nozzle of a radial flow turbine consists of an annular ring of vanes, which set the angle of approach of the working fluid to the rotor. The form of the vanes depends on whether the nozzle ring is preceded by a volute or by a simple collector. If a volute precedes it, the volute will impart some swirl to the gas. The nozzle vanes will work in conjunction with the volute to accelerate the fluid and they must therefore be set at the correct incidence for the swirl leaving the volute. The nozzle vanes will therefore need only a little camber or possibly none at all, as illustrated in Figure 18a. In cases such as these, the radial turbine nozzle vanes are often made straight. This is not to say that they are not aerodynamically loaded. A straight vane set at some angle to the radial direction will actually turn the flow toward the tangent as it moves inwards and a pattern of vane loading will follow (Baines, 2003).

If the nozzle is preceded by a collector, in which no swirl is generated, the fluid will approach the nozzle from the radial direction and the nozzle vanes are then required to do all of the acceleration and turning of the fluid, as illustrated in Figure 18b. Significant losses may be incurred due to nozzle incidence if in both cases attention is not given to matching the vane geometry to the flow upstream of the nozzle.

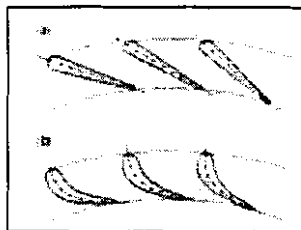


**Figure 18:** (a) *Uncambered* (b) *Cambered radial turbine nozzle guide vanes.*  
(From Baines, 2003)

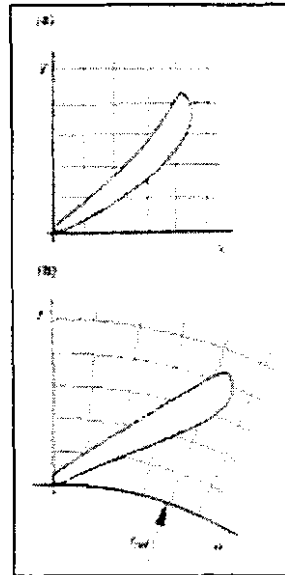


**Figure 19:** Co-ordinated transformation of blade design from (a) Cartesian to (b) radial plane. (From Baines, 2003)

Both types of vane airfoil sections can be used, although for straight vanes a simple profile that consists of a straight taper from the leading edge to the trailing edge circle is often found to be quite adequate, such as shown in Figure 19a.

A design method for airfoil sections, which is quite common, is that of conformal transformation. An axial turbine blade is first designed in the Cartesian ( $x, y$ ) plane using standard methods developed for that type of blade and then the geometry is transformed into the required annular ( $r, \theta$ ) plane, as in Figure 19b (Baines, 2003). The transformation equations are:

$$\theta = x / r_{ref} \quad (3.24)$$

$$r = r_{ref} \exp (y / r_{ref}) \quad (3.25)$$

where  $r_{ref}$  is a suitable reference radius which is similar to the trailing edge radius of the vanes.

The approach mainly used today is to design and analyze nozzle blades directly in the polar plane by making use of appropriate geometry generation and flow field analysis tools. However, the former method offers the security of starting from a well-known and tested profile (Baines, 2003).

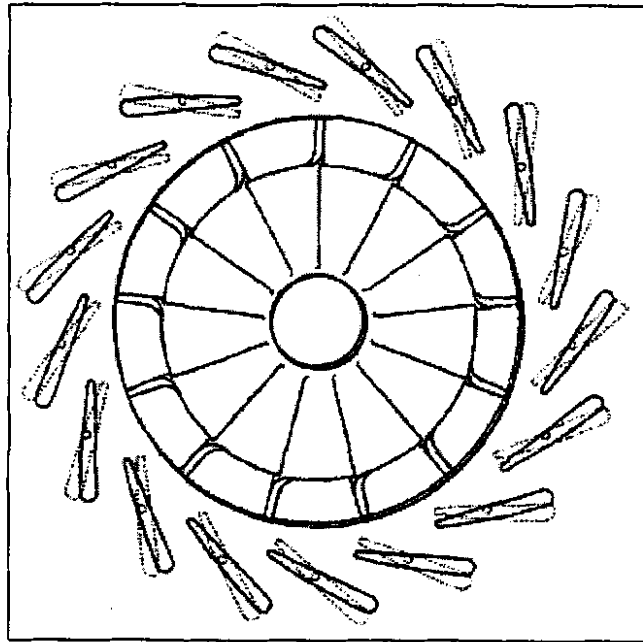


**Figure 20:** *Swing-vane variable-geometry turbine. (From Flaxington and Swain)*

[Refer to Hawley, Wallace, Cox, Horrocks & Bird (1999) and Murray (1989) for further discussions on variable vanes and their advantages.]

### 3.2.2 Deviation

Deviation occurs at the trailing edge of the blade, where the flow leaves the blade passage at an angle that is different from the metal angle (Baines, 2003). On leaving the nozzle, the flow does not follow the vanes exactly, but turns by an amount known as the deviation. This is actually a combination of two effects. A sudden expansion occurs, as the flow leaves the nozzle vanes, as a result of the finite trailing edge thickness of the vanes and the blockage caused by this. The sudden expansion results in a drop in the radial component of velocity and this causes the flow to tend to overturn. In addition, there is some under-turning

caused by the less than perfect guidance given to the flow by the vanes, particularly in the uncovered region of the suction surface from the throat to the trailing edge where there may be some diffusion and boundary layer growth (Baines, 2003).

By using a simple approach, it is not possible to predict the deviation. It can, however, be predicted reasonably well by using a properly set up CFD analysis, as tests suggest. Something more than this is required for preliminary design purposes. According to Baines, a rule borrowed from axial turbine tests is often used to quantify this, in which the angle of gas leaving the nozzle is given by:

$$\alpha_3 = \cos^{-1} (o/s) \quad (3.26)$$

where  $o$  is the throat opening and  $s$  is the vane spacing, as illustrated in Figure 21.

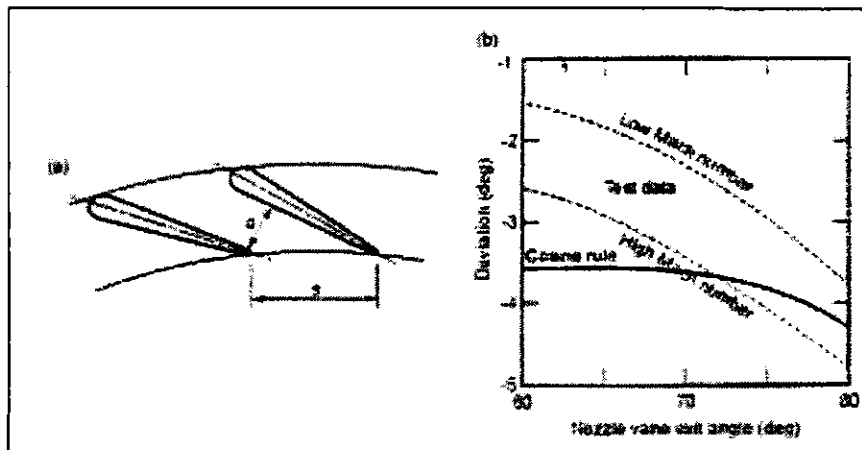


**Figure 21:** Comparison of predicted and measured deviation. (From Baines, 2003)

As can be seen, deviation is important in the design of a radial-inflow turbine, particularly during the detail design faze. For this reason, it was decided not to take in consideration during the preliminary design of a radial-inflow turbine.

### 3.3 The nozzle-rotor interspace

It is advantageous to leave a space between the nozzle and the rotor in order for the nozzle vane wakes to mix out and give a uniform flow at inlet to the rotor. A space between the blade rows reduces the mechanical coupling between the two, which can excite blade resonances and can lead to premature failure. However, the overall size of the turbine will be increased by a large space and can also lead to excessive pressure losses in this region. Jansen (1964) (as stated by Baines, 2003) recommends a minimum radius ratio between the nozzle trailing and rotor leading edges of 1.04. This is adequate for aerodynamic purposes at subsonic conditions. However, when using thin vanes and blades, it is prudent to increase this value to about 1.1 for added insurance against high cycle fatigue.

The optimum distance between the nozzle and the rotor is a compromise between blade row interactions, which reduces with distance, fluid friction and boundary layer growth, which increase with fluid path length (and hence radial distance). It is suggested that the maximum efficiency of a radial turbine occurs at a value of:

$$\Delta r / b_3 \cos \alpha_3 \approx 2 \quad (3.27)$$

where  $\Delta r$  is the radial distance between the nozzle exit and the rotor tip (Baines, 2003).





Maximum efficiency occurs for flow coefficients in the range 0.2 - 0.3 (Baines, 2003).

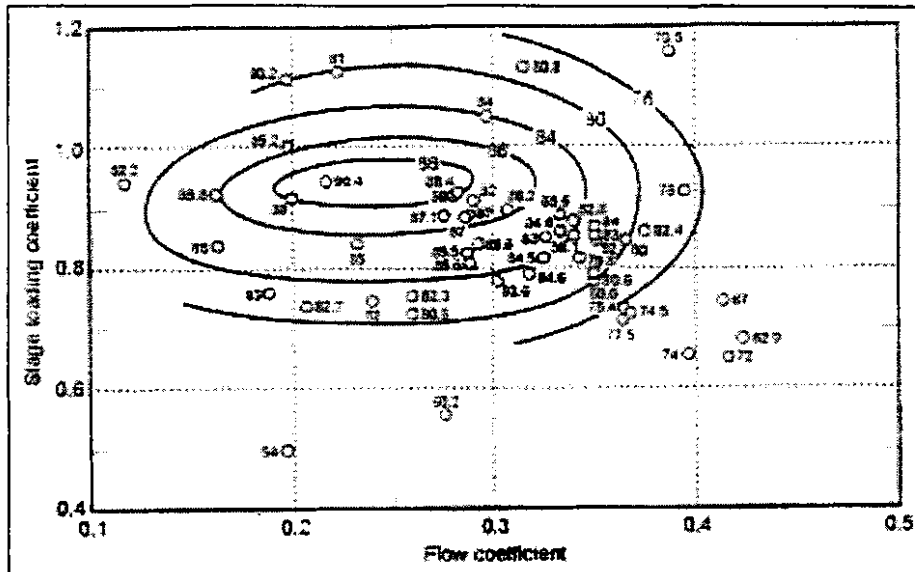


**Figure 22:** Correlation of blade loading and flow coefficients for radial-inflow turbines.  
(From Baines, 2003)

Using the definition of  $C_s$ , where  $C_s$  is the isentropic 'spouting' velocity, the turbine efficiency can be written as:

$$\eta_{ts} = 2 \Delta h_0 / U_4^2 (U_4 / C_s) = 2 \psi v^2 \quad (3.30)$$

Thus for an ideal turbine ( $\eta_{ts} = 1.0$ ),  $\psi = 1.0$  implies  $v = 0.7$ , where  $v$  is the velocity ratio  $U/C_s$ . For realistic values of efficiency,  $v$  will be lower, but for lower values of  $\psi$ ,  $v$  will be higher and so the two effects will tend to cancel each other out, according to Baines.

A means for choosing suitable starting design values for any rotational combination of specified performance parameters is provided by the combination of specific speed, specific diameter, loading and flow coefficients and this forms the basis of a simple design procedure which enables the designer to determine the key geometric parameters of the stage. By using a more detailed analysis,

these starting values can subsequently be refined, but that analysis will be considerably speeded by the choice of suitable starting values that this method provides.

By making use of Figure 22 as a guide, the design procedure begins by choosing suitable values of the loading and flow coefficients, but noting that other limitations restrict these choices. It is also necessary to specify the rotor meridional velocity ratio  $\xi$ , because the flow coefficient is defined in terms of the rotor exit velocity:

$$\xi = C_{m4} / C_{m6} \quad (3.31)$$

The meridional velocity ratio normally has a value near unity. The rotor inlet area is influenced by it and therefore the inlet blade height for fixed inlet radius. It therefore has some posture on the rotor incidence and it may be necessary to vary  $\xi$  in order to achieve an acceptable angle (Baines, 2003).

It is also necessary to establish the mass flow rate and the rotor tip blade speed  $U_4$ . The rotor tip blade speed is normally part of the turbine specification or may be determined by specific speed considerations. The mass flow rate may be determined in one of several ways. The turbine power output is given by  $P = m\Delta h_0$  and if power forms part of the specification, then the choice of loading coefficient immediately determines the blade speed, because  $\psi$  can also be defined as  $\Delta h_0 / U^2$  (Baines, 2003). The blade speed may alternatively be limited by stress considerations. This is particularly so in high temperature applications where the designer's experience will play an important role in choosing the maximum blade speed which is acceptable for the chosen rotor material. It may be necessary in such cases to refine this first estimate when a full structural analysis is done. Because high levels of swirl cannot be diffused effectively, the rotor exit swirl at the design condition should normally be small and will thus give rise to high exit

kinetic energy losses. It is therefore possible to write the Euler turbo-machinery equation as:

$$C_{\theta 4} \approx \psi U_4 \quad (3.32)$$

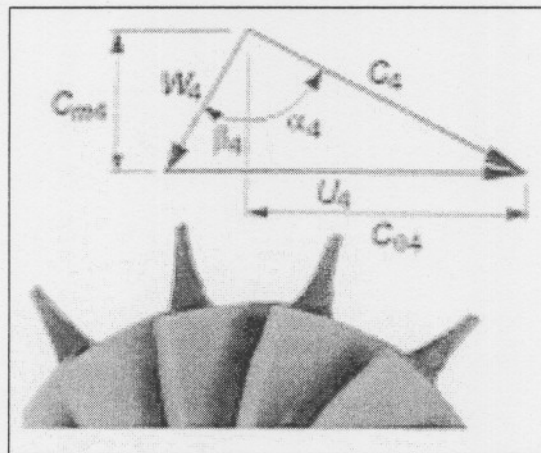


Figure 23: Rotor inlet velocity triangle. (From Baines, 2003)

Hence the rotor inlet velocity triangle is defined as shown in Figure 23 by:

$$C_{m4} = \xi \phi U_4 \quad (3.33)$$

where  $C_{m4}$  is the inlet meridional absolute velocity,  $\xi$  the inlet/outlet absolute velocity ratio,  $\phi$  the flow coefficient and  $U_4$  the inlet blade speed.

$$C_4 = (C_{m4}^2 + C_{\theta 4}^2)^{1/2} \quad (3.34)$$

where  $C_4$  is the inlet absolute velocity and  $C_{\theta 4}$  the inlet tangential absolute velocity.

$$\alpha_4 = \tan^{-1} (C_{\theta 4} / C_{m4}) \quad (3.35)$$

$$\beta_4 = \tan^{-1} [(C_{\theta 4} - U_4) / C_{m4}] \quad (3.36)$$

The rotor incidence angle is:

$$i_4 = \beta_4 - \beta_{b4} \quad (3.37)$$

where  $\beta_4$  is the inlet flow angle and  $\beta_{b4}$  is the inlet blade angle of the rotor.

The static temperature and pressure at the inlet to the rotor are:

$$T_4 = T_{04} - C_4^2 / 2 C_p \quad (3.38)$$

$$p_4 = p_{04} (T_4 / T_{04})^{k/(k-1)} \quad (3.39)$$

where  $T_{04} = T_{01}$  and  $p_{04} = p_{01} - \Delta p_0$ . Here  $\Delta p_0$  is the total pressure loss in the stator, which may be determined by flow tests. It may alternatively be justified to ignore it completely and treat the stator as isentropic, as the stator loss is usually only a small fraction of the overall turbine loss. The inlet area follows as:

$$A_4 = mRT_4 / p_4 C_{m4} \quad (3.40)$$

At exit, the total and static temperatures are:

$$T_{06} = T_{04} - \Delta h_0 / C_p \quad (3.41)$$

$$T_6 = T_{06} - C_6^2 / 2C_p \quad (3.42)$$

where, for axial or near axial flow at exit,  $C_6 \approx C_{m6} = \Phi U_4$ . The exit pressure  $p_6$  can then be calculated from the turbine efficiency estimate obtained from specific speed, loading and flow coefficient correlations.

$$p_6 / p_{01} = [1 - 1 / \eta_{ts} (1 - T_{06} / T_{01})]^{k/(k-1)} \quad (3.43)$$

From continuity the exit area follows:

$$A_6 = mRT_6 / C_6 p_6 \quad (3.44)$$

These equations enable the designer to obtain preliminary estimates of the important geometric parameters and flow states at the inlet and exit of the rotor.

Another parameter that must be kept in mind is the incidence angle. The incidence angle should be investigated to ensure that it is consistent with the general experience that in radial turbines the best efficiency occurs at some negative incidence, usually in the region of 20 - 30° (Baines, 2003). The rotor blade angle at inlet may or may not be open to the designer's choice, depending on the nature of the application. For all applications that demand a high level of rotor stress relative to the material yield strength, radial blade sections are required in order to keep the centrifugal stress within the blade material limits. For a radial-inflow turbine this implies a blade inlet angle of zero.

The designer must thus examine the calculated rotor inlet relative flow angle and must decide whether this gives a suitable rotor incidence. It can be set so as to achieve any desired incidence, if the designer has the freedom to modify the inlet blade angle. Non-zero inlet blade angles can be achieved in radial-inflow turbine rotors as long as they are lightly stressed, because high stresses will cause premature failure. It is possible to vary the inlet blade angle from zero, for a mixed flow turbine, while maintaining radial blade sections and this might be another reason for preferring this configuration (Baines, 2003). Figure 24 illustrates the above-mentioned.

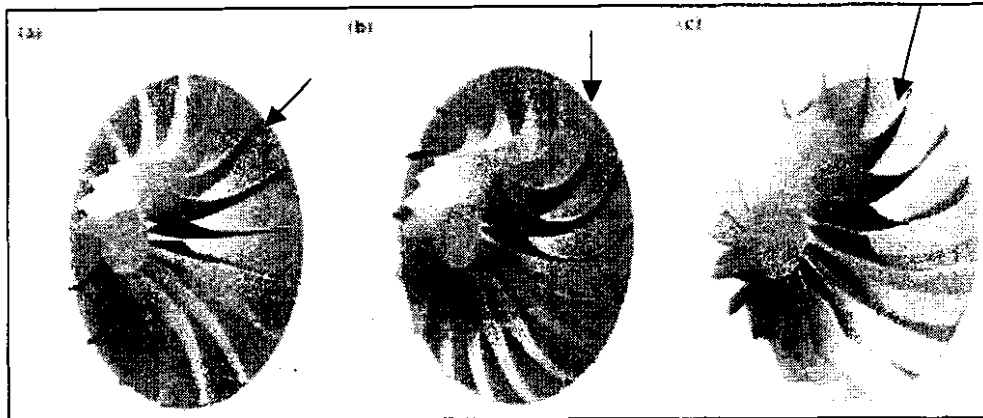


**Figure 24:** Rotor blade geometry at inlet (a) radial turbine with zero inlet blade angle and radial blade sections (b) radial turbine with non-zero inlet blade angle and non-radial blade sections (c) mixed flow turbine with non-zero inlet blade angle and radial blade sections. (From Baines, 2003)

The rotor inlet and exit areas must also be carefully examined, as these are each functions of the mean radius and the blade height. The blade speed and the speed of rotation determine the inlet radius. It can also be selected from the specific diameter or by setting  $U_4 / C_s = 0.7$ . The rotor blade height  $b_4$  is then fixed. The minimum blade hub radius at exit is normally limited by shaft size or by crowding of the blade roots. The tip radius and the blade height can thus be determined. The inlet and exit blade tip radii must now be compared, as the ratio of these two quantities determines the curvature of the rotor shroud contour in the meridional plane. According to Baines, a very modest curvature, in high efficiency conditions, will typically require exit / inlet tip radius ratios of about 0.7. Compact turbines may have values up to about 0.85, as it is quite difficult to achieve values near 0.7 for high specific speed designs. It is frequently required for some iteration with different rotational speeds, loading and flow coefficients in order to determine the best geometry.

The exit RMS radius is found and thus the exit blade speed, once this has been done. If it is assumed that the flow at exit is axial, the exit velocity triangle is fully determined (Figure 25) and hence the exit blade angle can be determined:

$$\beta_6 = \tan^{-1} (W_{\theta 6} / C_{m6}) = \tan^{-1} [(C_{\theta 6} - U_6) / C_{m6}] \quad (3.45)$$

The rotor inlet absolute flow angle  $\alpha_4$  is finally determined by the stator. In dealing with nozzled turbines, the nozzle exit blade angle fixes this value and in turn is determined by it, with some correction for nozzle deviation as necessary. In the case of nozzleless turbines, this angle is determined mainly by the volute geometry ( $A_0 / r_0$ ) ratio, which is thus fixed (Baines, 2003).

(Equations 3.28 – 3.45 are from Baines, 2003)

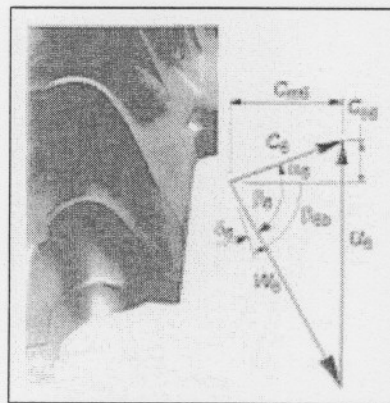


Figure 25: Rotor exit velocity triangle. (From Baines, 2003)

Abdel-Rahim (1994) also discusses a method for the design of a radial-inflow turbine and can also be used for the preliminary design thereof. It is, however, not discussed in this paper.

### 3.4.2 Rotor design optimization

The loading coefficient is a particularly simple concept to understand and it is also powerful in its direct relationship with incidence, according to Baines. Incidence has a major influence on turbine performance and data from a variety of sources suggests that the range of loading coefficients for radial inflow turbines is normally limited to a narrow band. Therefore suitable values can readily be chosen as a basis for design and analysis.

The method described here is based on the loading coefficient. The object of the method is to determine fundamental geometry parameters of the rotor such as diameters, blade heights, angles etc. and to achieve the best efficiency, given a required power output and mass flow rate. The most important underlying assumption here is that the majority of internal rotor passage losses are functions of the fluid velocity and so efficiency improvements are obtained by minimizing the fluid velocities at inlet and exit of the rotor, which are subject to other constraints (Baines, 2003). It is unnecessary to specify any internal losses in order to perform the optimization, if the procedure is only based on a loading coefficient. Doing so will provide an optimum according to the strategy here, but will not quantify the actual efficiency of the stage. If estimates of rotor and stator loss or efficiency are made, this can be done subsequently. It is mostly easier to calculate the stage efficiency, once the overall geometry is determined, by using a meanline modelling method (Baines, 2003). [See Ebaid & Al-Hamdan (2004) for other techniques to optimize the design of an inward-flow radial turbine.]

#### 3.4.2.1 Rotor inlet

According to Baines, the components of the velocity triangle at inlet (Figure 23) are related by,

$$C_4^2 + U_4^2 - 2C_4U_4 \sin\alpha_4 - W_4^2 = 0$$

and from the definition of loading coefficient it follows that,

$$\psi^2 - 2\psi \sin^2\alpha_4 - (W_4 / U_4)^2 = 0$$

the solution of which yields,

$$\psi = \sin^2\alpha_4 \pm \sin\alpha_4 [(W_4 / U_4)^2 - \cos^2\alpha_4]^{1/2} \quad (3.46)$$



One root of this equation is discarded, because it does not allow  $\psi$  to be greater than unity. If  $\psi$  is to be real, the condition

$$(W_4 / U_4)^2 \geq \cos^2 \alpha_4$$

must be satisfied and the minimum value of  $W_4 / U_4$  occurs when

$$W_4 / U_4 = \cos \alpha_4 \quad (3.47)$$

Under this condition the remaining inlet parameters are simple functions of  $\psi$  as follows (Baines, 2003):

$$\sin \alpha_4 = \psi^{1/2} \quad (3.48)$$

$$\tan \beta_4 = -[(1 - \psi) / \psi]^{1/2} \quad (3.49)$$

$$W_4 / U_4 = \cos \alpha_4 = (1 - \psi)^{1/2} \quad (3.50)$$

$$C_4 / U_4 = \psi^{1/2} \quad (3.51)$$

$$C_{m4} / U_4 = [\psi(1 - \psi)]^{1/2} \quad (3.52)$$

As Baines discusses, the implication of this optimization is that, with the blade loading  $\psi$  specified, the magnitudes of the relative and absolute velocities will be minimized if the two velocities are normal to each other, i.e.  $W^2 + U^2 = C^2$ . If the loading coefficients are in the region of 0.9, both the absolute and relative flow angles have values typical of those used, which are about 70° stator exit and -20° rotor inlet flow angles. In the case of working with radial turbines with  $\psi = 0.8 - 0.9$  and zero blade angle at rotor inlet, the optimum relative flow angle expressed in Equation 3.49 is very close to the value required for minimum incidence loss. If high loading is required ( $\psi > 0.95$ ), however,  $\beta_4$  approaches

zero (from the negative direction) and a positive blade angle is necessary to satisfy the requirements of maintaining sufficient incidence as well as minimizing the rotor inlet relative velocity. As  $\Psi$  approaches unity, which will be in the case of high loading, the optimum velocity triangle collapses as  $\alpha_4$  tends to  $90^\circ$ .

### 3.4.2.2 Rotor exit

The condition of zero exit swirl, which will minimize the exit kinetic energy of the rotor, might be regarded as one of the optimum conditions for the rotor exit (Baines, 2003). However, considering that the internal losses of the rotor are likely to be some function of the velocity of flow in the rotor passage, the goals of a rotor exit optimization will most probably be to minimize both the absolute exit velocity (to limit the exit kinetic energy) and the relative exit velocity (to limit the rotor passage loss). Other constraints may mean that it is not possible and perhaps not even desirable to minimize both simultaneously. A large proportion of the exit kinetic energy may be recovered and a greater priority can thus be placed on minimizing the internal losses, if the application allows sufficient space downstream of the rotor for an effective exhaust diffuser. By keeping with the assumption of zero exit swirl, the relation between the absolute and relative exit Mach numbers is (Baines, 2003),

$$M_{\delta,rel}^2 = M_{\delta}^2 + (K / M_{\delta}^2) \quad (3.53)$$

where  $K$  is a function of the loading coefficient and the rotor inlet to exit radius and area ratios. Its value is determined by the operating point and other parameters which values have previously been calculated in the optimizing procedure. The variable  $t$  can therefore be regarded as constant for the purposes of optimizing the exit velocity triangle (Baines, 2003).

Equation 3.53 is plotted in Figure 26 for a set of typical values of  $K$ . The exit flow angles, which these combinations of Mach numbers imply, are also shown here. It is clearly not possible to minimize both the relative and absolute Mach numbers

simultaneously. Smaller magnitudes of exit angles favour the relative Mach number at the expense of the absolute, whereas larger angles have the opposite effect. According to Baines, most practical radial turbine designs have an exit angle in the order of  $-60^\circ$ , which appears to strike a good compromise for many applications.

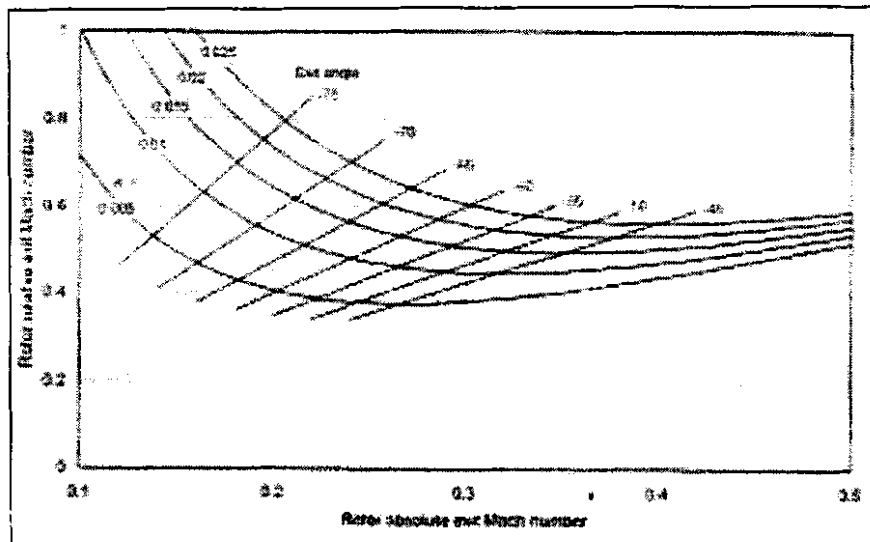


**Figure 26:** Rotor exit Mach numbers for zero exit swirl. (From Baines, 2003)

The Mach number situation is complicated by the addition of exit swirl, at least as far as any analytical determination of optimum is concerned. It is sufficient to say that designers usually add exit swirl, for most practical purposes, only when it is necessary to increase or reduce the power output without changing the speed of rotation (Baines, 2003). This can immediately be seen from the effect of positive or negative  $C_{\theta 6}$  in the Euler turbo-machine equation. Evidence suggests that a limited amount of swirl actually improves the performance of an exhaust diffuser, most probably because the swirl acts to centrifuge flow outwards and keep the boundary layers of the diffuser energized, thereby delaying the onset of stall. However, diffuser performance falls again when the exit swirl exceeds about  $15^\circ$  –  $20^\circ$  in conventional diffusers or up to  $40^\circ$  in diffusers designed specifically to work well in high levels of swirl (Baines, 2003). These limits should thus be respected when exhaust diffusion is used.

### 3.4.3 Scaling

This paragraph will look at the basic equations and assumptions concerning scaling, as this study concentrates on the preliminary design of a radial turbine and not the scaling method of design. The scaling procedure that follows is described as by Baines (2003).

The use of similitude to scale an existing design to a new application is the first level of design. Similitude should only be employed if an appropriate turbine is available and can be scaled for a new application. The term 'appropriate' includes requirements of flow, expansion ratio, power output and efficiency. Life requirements and economics are also essential considerations and in hostile environments may dominate the design process. The use of the similitude parameters is fully appropriate only if all of these needs can be met with an existing stage that can be scaled to a larger or smaller size. This can most effectively be used when working with a stage that was designed for the same working fluid that the new requirement demands. According to Baines, scaling can sometimes also be used with care to apply a stage from one working fluid to another, but often it is necessary to rely on a more complex level of analysis to verify the scaled variant.

Frequently scaling or verification testing is done using air for convenience, although several common applications of radial turbines require them to work with the exhaust gasses of hydrocarbon combustion. Fortunately both exhaust gasses of this type and air at and above ambient temperatures are near-perfect in behaviour and so the scaling rules can be applied with confidence, providing it is recognized that the gasses have different specific heat ratios  $k$  and gas constants  $R$ . Applications such as process expanders work with a variety of organic and refrigerant fluids, often complex mixtures with many components and with a behaviour which is far from ideal. In the case of working with steam turbines in which condensation occurs, or even where the expansion line only approaches the saturation line, constitute other non-ideal cases. It would be

inappropriate to apply the simple scaling rules to an air turbine to work with condensing steam, a refrigerant gas or an organic fluid, for the results of the scaled machine would almost certainly differ from the original design in ways which are very difficult to predict. Recognizing the quite different fluid properties, a higher level of design is required in cases like this.

The rules of scaling and similitude are summarized as follows (Baines, 2003):

Flow coefficient:

$$\Pi_1 = \frac{Q}{ND^3} = \frac{m}{\rho ND^3} \propto \frac{m}{\rho UD^2}$$

where,

- $m \approx$  mass flow rate,
- $N \approx$  rotational speed,
- $D \approx$  diameter,
- $U \approx$  blade speed, and
- $\rho \approx$  density.

Head coefficient:

$$\Pi_2 = \psi = \frac{\Delta h_0}{U^2}$$

where,

- $\Delta h_0 \approx$  total enthalpy.

Power coefficient:

$$\Pi_3 = \frac{P}{\rho N^3 D^5}$$

where,

- $P$  is power.

Reynolds number:

$$Re = \frac{\rho U D}{\mu}$$

where,

$\mu$  is kinematic viscosity.

Velocity ratio:

$$\Pi_s = \frac{ND}{a}$$

where,

$a$  is velocity.

For these all the familiar turbomachinery parameters can be derived, for example,

$$m_{ref} = \Pi_1 \times \Pi_s = \frac{m \sqrt{RT/k}}{D^2 p}$$

Thus, the application of simple scaling reveals that the flow rate varies linearly with the square of the turbine radius and the speed varies inversely with radius. Small variations in  $R$  and  $k$  can be used to modify these proportionalities. The turbine size necessary to accommodate a given flow rate as well as the shaft speed that this requires or the size related to a given shaft speed and the flow rate that this implies, are thus readily established. In cases like these, the power output of the scaled machine can then be calculated by using the power coefficient equation (Baines, 2003).

The Reynolds number is one parameter that usually cannot be scaled correctly, because it is a function of turbine speed and diameter, which are chosen as described above. The gas density and velocity are the only remaining

parameters. The velocity is a function of the gas composition and temperature and the designer can usually not control it. It is possible to scale the Reynolds number correctly, only if the density can be independently varied. This is only possible in a few highly specialized closed-circuit test facilities, but not in regular test facilities or in general applications (Baines, 2003).

The effect of Reynolds number on performance is often small and may in some circumstances be neglected, although it is not always the case. The definition of Reynolds number is important here and is mostly inconsistent. According to Hiett and Johnston (1963) (as stated by Baines, 2003), one can choose to define it in terms of the rotor inlet parameters and a kinematic viscosity based on the turbine inlet density:

$$Re_{Ricardo} = \frac{U_4 b_4}{\nu_1}$$

NASA defined it using the flow rate measured at inlet to the turbine:

$$Re_{NASA} = \frac{m}{\mu r_4}$$

The relationship between these two is:

$$\frac{Re_{NASA}}{Re_{Ricardo}} = 2\pi\phi_4 \left( \frac{\rho_4}{\rho_1} \right)$$

where  $\phi_4 = C_{m4} / U_4$  is the rotor inlet flow coefficient. It can thus be seen that the two Reynolds numbers are similar in magnitude, at least for normal design point operation, but care must be taken in interpreting the data to use the correct definition.

Hiett and Johnston describe their data as fitted by the equation:

$$\eta_{tt} = 1 - \frac{1}{\text{Re}_{Ricardo}^{0.16}}$$

with  $\eta_{tt}$  as the total-to-total efficiency.

It would, however, appear that the efficiency is constant with Reynolds number above about  $2 \times 10^5$ . This equation lacks generality, because it is specific to the level of efficiency determined for this turbine at this point. Somewhat theoretically, a more general formulation that includes the reference value of efficiency at specific Reynolds number of  $2 \times 10^5$  would take the form:

$$\frac{1 - \eta}{1 - \eta_{ref}} = \left( \frac{\text{Re}_{ref}}{\text{Re}} \right)^{0.16}_{Ricardo}$$

According to Holeski and Futral (1967) (as stated by Baines, 2003), it can be proposed that the overall loss be divided into viscous friction, so they correlated their data with an expression of the form:

$$\frac{1 - \eta}{1 - \eta_{ref}} = K + (1 - K) \left( \frac{\text{Re}_{ref}}{\text{Re}} \right)^{0.2}_{NASA}$$

where  $K$  is a constant which depends on the assumed split. Values of  $K$  between 0.3 and 0.4 were recommended as fitting their data well.

According to Baines, it should finally be noted that other effects might also prevent a precise geometric scaling. For example, blade fillet radii and thicknesses may have to be modified to meet manufacturing or structural requirements. Operating clearances, and particularly the rotor tip and back face clearances, may have to be modified. In these cases efficiency correlations may be made using suitable leakage models with the stipulation that they may not be exact unless carefully calibrated against appropriate test data.



According to Harvey, scaling allows us to utilize an already tested and proven component for a new engine, as long as the size difference does not result in a significantly compromised engine. It would be expected from a scaled component to be lower risk and therefore needs reduced development time, but the major advantage in using scaled components in different engines, is that lessons learned in one application can be used to improve both engines. The opposite is also true, as the risk exists where flaws from the original design can be carried over to the new design.

An engine that uses scaled components can, at least theoretically, never be as good as one designed for a specific application. Scaling a component up will usually result in a heavier than optimum engine and scaling a component down may result in a more complicated and costly engine than the engine size merits (Harvey).

Kurzke & Riegler (2000) also discuss a new compressor map scaling procedure for preliminary conceptual design of gas turbines, which will not be discussed in this study.

#### **3.4.4 EES radial-inflow turbine design**

Now that the basic literature for the design of a radial-inflow turbine has been discussed, a tool for the calculation of the initial design parameters of a radial-inflow turbine can be constructed. This can be achieved by making use of the Engineering Equation Solver (EES) and the design procedure discussed.

The design equations for a radial-inflow turbine were used to construct a tool in EES for the preliminary design of a radial-inflow turbine. In order to make the constructed program user friendly, a "design window" was constructed (Figure 27).

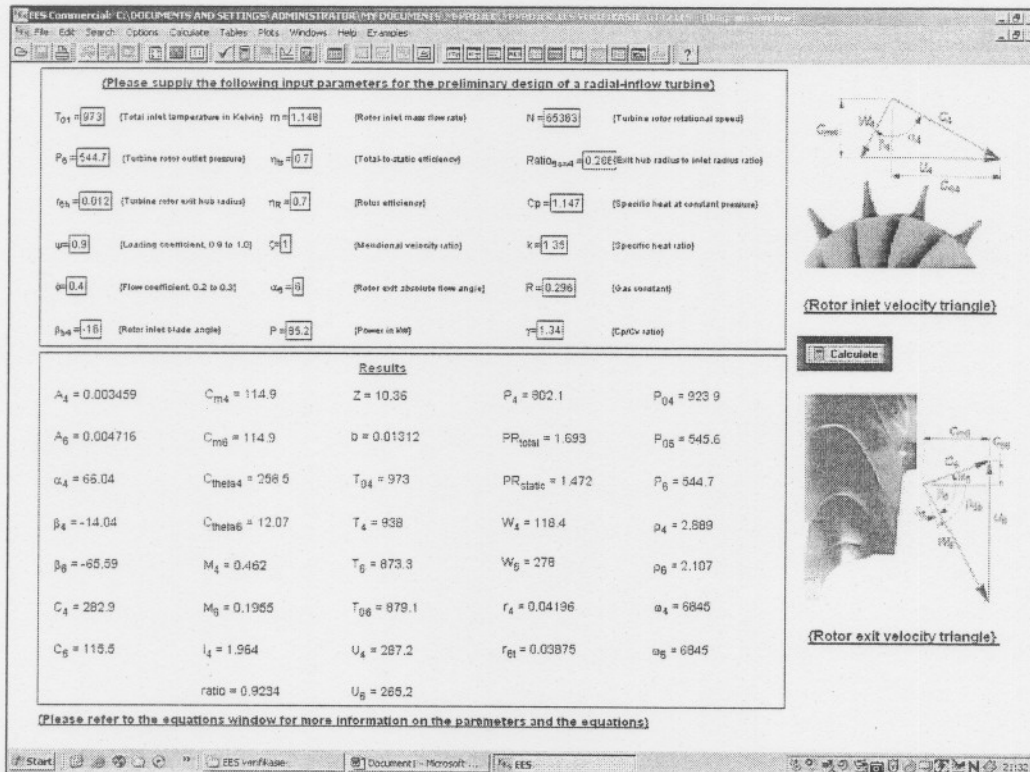


**Figure 27:** *Constructed EES design window for a radial-inflow turbine.*

In order to do a preliminary radial-inflow turbine design, the designer must enter the input parameters necessary to calculate the design parameters. After this has been completed, the “calculate” button is pushed and the results are shown. These results can then be used as input parameters for detail radial-inflow turbine design software packages such as *Concepts NREC Rital*®. In order to help the designer in choosing meaningful input parameters, a short description of each input parameter is given next to it.

See Appendix A for further detail concerning the constructed EES design program as well as an example for the design of a radial-inflow turbine by making use of the constructed EES design program.

### 3.4.5 Volute preliminary design

The volute is a unique component of turbo-machines and demands a design procedure that is separate from the designs of vanes and blades, according to Baines. The principal parameter in the design of a volute is the inlet area to centroid radius area  $A/r$ , as illustrated in Figure 28. This relationship determines the angle of flow at the exit of the volute, which is also the angle at which the flow approaches the rotor in a nozzleless turbine.

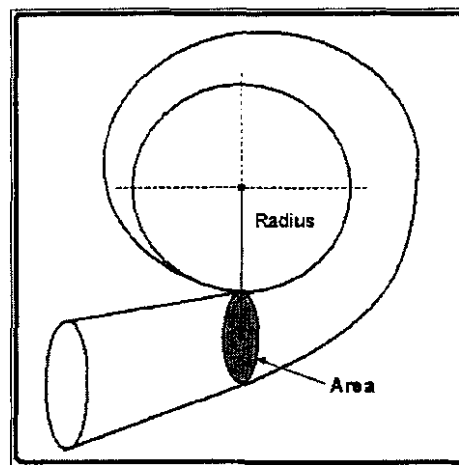


Figure 28:  $A/r$  ratio of a volute.

During the design procedure of the volute, the principal outputs are the section areas around the volute and it is the designer's choice of how many sections he/she wants to calculate (see Figure 29). The section area and centroid radius are inter-dependent of each other and it will be necessary for the designer to iterate the calculation with different choices of the centroid radius until an acceptable volute shape is achieved, according to the designer.

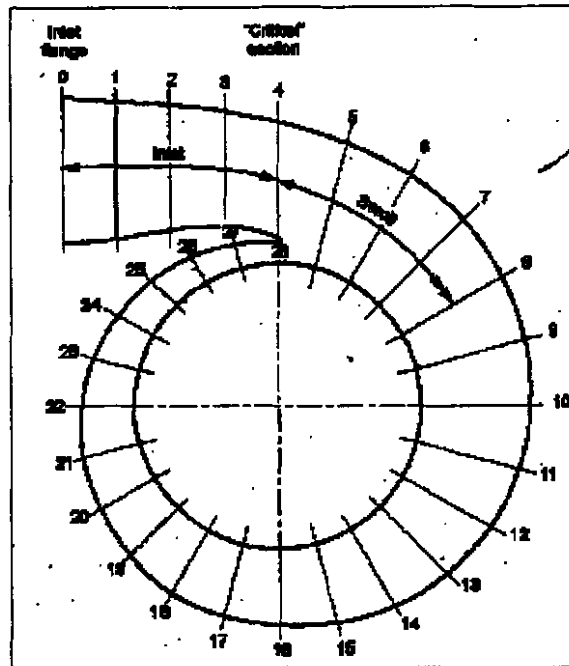


Figure 29: Volute sections. (From Baines, 2003)

According to Baines, the design procedure can then be described as follows:

### 3.4.5.1 Flange to Critical section

The Mach number can be solved at each section by the following equation,

$$\frac{m\sqrt{RT_0/k}}{A(1-B)p_0} = M \left( 1 + \frac{k-1}{2} M^2 \right)^{-\frac{1}{2} \left( \frac{k+1}{k-1} \right)}$$

From this, the following parameters can be calculated,

$$T = T_0 \left( 1 + \frac{k-1}{2} M^2 \right)^{-1}$$

$$C = M\sqrt{kRT}$$

$$p = p_0 \left( \frac{T}{T_0} \right)^{\frac{k}{k-1}}$$

### 3.4.5.2 Scroll section

The mass flow through any section of the volute can be calculated with,

$$m = m_{inlet} \left( 1 - \frac{\theta}{2\pi} \right)$$

where  $\theta$  is the angle measured in radians from the critical section.

The meanline velocity of flow through any section is given by the following equation,

$$C_\theta = SC \frac{r_c C_{\theta c}}{r}$$

where SC is the swirl coefficient.

The other parameters can then be calculated,

$$T = T_0 - \frac{C^2}{2C_p}$$

$$p = p_0 \left( \frac{T}{T_0} \right)^{\frac{k}{k-1}}$$

$$\rho = \frac{p}{RT}$$

The mean flow velocity toward the nozzle can then be solved by,

$$C_m = \frac{\Delta m}{\rho b_1 r_1 \Delta \theta}$$

where  $b$  is the width of the scroll section.

With this known,  $\alpha$  can be calculated,

$$\alpha = \tan^{-1}\left(\frac{C_\theta}{C_m}\right)$$

$$A = \frac{m}{\rho C_\theta (1 - B)}$$

The area of the section can then be calculated, with a known blockage factor  $B$ .

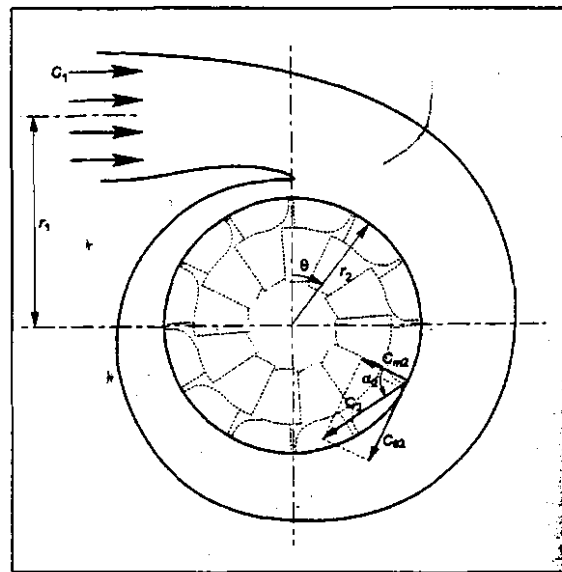


**Figure 30:** Sketch of the volute showing the velocity vectors. (From Baines, 2003)

A bend in the flow entering the volute is important in establishing a vortex flow about the axis of the turbine, but according to Hussain et al (as stated by Baines, 2003) the vortex motion is set up in about the first 20° of turning.

The basic design rule of the volute is to design the distribution of the flow around the periphery of the turbine so as to give a uniform mass flow rate and uniform static pressure at the volute exit. This must be achieved in order to ensure that each rotor blade passage flows to its proper capacity and also to ensure steady

radial loading, but in practice these conditions are only met approximately (Baines, 2003).

The calculation procedure is made much easier when a computational program such as EES is used, because the designer will have to do a couple of iterations before the correct volute shape is reached. Please refer to Appendix B for an example of the calculation procedure of the volute such as constructed in EES.

### 3.4.6 Blade loading and blade number

A single parameter can be considered in two ways, the blade loading and blade number. The integrated blade loading is simply the stage loading set by the turbine specification, divided by the blade number. In the case of radial turbines there are no simple rules for even the initial selection of a trial blade number with which to start the analysis, similar to the Zweifel coefficient for axial turbines. Given the usual radial turbine geometry, the optimum blade number at inlet will almost certainly be much larger than the optimum blade number at exit. Historical rules based on simple concepts of blade loading have been found to be quite inadequate (Baines, 2003).

A tool that can be used to determine an appropriate blade number is CFD analysis and fast solutions based on a coarse grid have proved adequate for this task. (Criteria for the minimum number of blades for a rotor have been developed by Jamieson, Glassman and Whitfield and can be found in *Fluid Mechanics and Thermodynamics of Turbomachinery* (chapter 8) by S.L. Dixon.)

In Figure 31 the relationship between the various criteria can be seen. For a certain inlet flow angle  $\alpha$ , a number of rotor vanes  $Z$  can be found.

According to Glassman (as stated by Dixon, 1998), the number of vanes can also be calculated from the following equation,

Bladsy 60



point”), which is commonly also the best efficiency point of the turbine, according to Baines. One can then analyze the turbine performance at all of the expected operating conditions, both design and off-design. On the other hand, a variable-geometry turbine may be “designed” at a range of conditions. Although the basic equations to model both the design and analysis functions are essentially the same, the techniques by which they are combined and organized differ (Baines, 2003). It is possible both to generate geometric configurations and to predict the performance of those configurations over a wide range of possible operating conditions, with a complete set of design tools.

According to Baines, the meanline analysis strategies for the solution of a radial-inflow turbine must proceed in one of several modes, depending on the way in which the operating point is specified:

- a) Mass flow rate and inlet total pressure are specified and the exit pressure is a free variable: no iterations are necessary.
- b) Inlet and exit pressures are specified: the mass flow rate is iterated until the exit pressure is correct.
- c) Mass flow rate and exit pressure are specified and the inlet pressure is a free variable: the inlet pressure is iterated until the exit pressure is correct.

One must take special precautions in case of choking. When either the nozzle or the rotor chokes, the mass flow remains constant for pressure ratios greater than the choking pressure ratio and thus the exit pressure is no longer uniquely defined (Baines, 2003). Under these conditions further constraints are necessary to define a unique solution. Radial turbines are rarely designed or required to operate in a supersonic regime, so that the problem of choking individual blade rows is not serious and can normally be handled by an assumption of supersonic turning about the trailing edge (Baines, 2003). It is quite easy for the solution to

wander into a transonic region or to set a trial value of mass flow rate that is greater than the choked value, during iterations for mass flow rate.

According to Baines, many of these problems can be eliminated if, instead of specifying mass flow rate and solving for pressure ratio, the situation is reversed and one specifies pressure ratio and calculates the mass flow rate. There is a unique value of mass flow rate for any pressure ratio and off limit problems simply do not appear. The pressure must be specified at each calculation station through the stage, in such a procedure, and the mass flow rates between each adjacent pair of stations are calculated. There is no guarantee that each component will then have the same mass flow rate and the individual pressures must be adjusted in a suitable numerical scheme in order to converge on a common mass flow rate. The number of calculations may be greater in this case, but overall the solution is numerically bettered conditioned and more stable (Baines, 2003).

There are two approaches to solving the flow in a turbo-machine. In the first one, known as the direct problem, the geometric configuration is specified and the flow and pressure fields are sought. The second approach is called the design problem and is based on specifying part of the geometry and part of the flow or pressure field. The solution provides the remaining part (Ghaly, 1990).

According to Zangeneh, there are two main approaches to the problem of aerodynamic design of turbo-machinery blades, the direct and the inverse approach. In the direct approach the flow is computed for a given blade geometry, while in the inverse approach the required flow distribution is specified and the corresponding blade geometry is computed.

### **3.5 Conclusion**

Chapter 3 discussed the basic analysis and design of a radial-inflow turbine as well as nozzle vane design. A simple tool to determine the initial design parameters of a radial-inflow turbine was constructed in EES and finally the volute design was discussed.

The final step in reaching the goal of this study is to verify the constructed EES design tool for determining the initial design parameters of a radial-inflow turbine. Verification is important in order to assure trust within the constructed EES design tool.

## CHAPTER 4

### EES VERIFICATION AND GUIDELINES

The final step in reaching the goal of this study is to verify the constructed EES design tool to determine the initial design parameters of a radial-inflow turbine. In order to accomplish this, the constructed EES design tool will be verified as follows:

- Compare it to an example design of a radial-inflow turbine sourced from S.L Dixon
- Compare it to the design specifications of a Garrett GT42 turbine unit
- Compare it to designs of radial-inflow turbines done in Concepts Rital

The verification will be followed by guidelines for the design of a radial-inflow turbine, which will give the designer basic information to keep in mind when doing a design.

#### **4.1 EES verification**

In order to verify whether the method to determine the initial design parameters for a radial-inflow turbine constructed in EES is acceptable, radial-inflow turbine design examples from various sources are used. These examples make use of other methods to do the preliminary design of a radial-inflow turbine than that used in this study.

The data from these examples are used to do a preliminary design in the constructed EES program and the results generated are then compared to the results given in the examples. By comparing the results, the EES design procedure can be verified and possible flaws in the program can be identified.

Another attempt to verify the constructed EES design procedure is to do a few radial-inflow turbine designs in Concepts Rital and to compare them to the same designs done in EES. Although Rital is a much more detailed design procedure in the sense that it incorporates losses and other factors not incorporated into the EES program, a comparison between the results generated by the two programs can be a sufficient way to verifying the constructed EES design procedure.

The following examples from two different sources were used in order to verify the constructed EES program for the design of a radial-inflow turbine. The data from the examples was used as input for the EES program and the results generated were compared to the results given by the examples used.

The first examples used were taken from Fluid Mechanics, Thermodynamics of Turbomachinery by S.L Dixon, which makes use of the *Optimum Efficiency Design* method in order to do a preliminary design of a radial-inflow turbine.

The second comparison is with a commercial Garrett GT42 radial-inflow turbine.

#### 4.1.1 Example 1

In order to compare the results of the example to that generated by the constructed EES program, a table was compiled. Table 1 contains the results of the EES program as well as the results of Example 8.3 – 8.6a (S.L. Dixon, P 244-263), which presents the design of a radial-inflow turbine. The percentage column illustrates the difference between the results compared and is calculated by dividing the results by each other and then multiplying that with 100%.

Because the methods used to do the EES design of a radial-inflow turbine differs from the example, some of the results of the example were used as input parameters for the EES program and visa versa. The results were, however, still kept separate. [See Appendix C for a copy of Example 8.3 – 8.6a used and the results generated by the EES design program.]

**Table 1: Comparison of EES and Example 1 results.**

Parameter	Example	EES	
Z	12	12.42	96.6%
$\alpha_4$	73.22°	72.41°	98.9%
$\beta_4$	33.56°	34.7°	96.7%
$\beta_6$	62.97°	66.9°	94%
PR	3.1	3.56	87%
$M_4$	0.77	0.75	97.4%
$U_4$	538.1 m/s	537.8 m/s	99.9%
$T_{06}$	840 K	765 K	91%
$T_6$	832.1 K	756 K	90.8%
$r_4$	0.117 m	0.1171 m	99.9%
$C_{\theta 4}$	448.9 m/s	441 m/s	98.2%
$C_{m4}$	135.4 m/s	139.8 m/s	96.9%
$C_4$	468.8 m/s	462.7 m/s	98.7%
$T_4$	954.5 K	956.3 K	99.8%
$P_4$	207 kPa	249.2 kPa	83.1%

From Table 1 it can be seen that all of the parameters have a comparison percentage of over 90 %, except the PR and the Inlet pressure. The 87% and 83.1% comparison of these two parameters can, however, still be regarded as acceptable.

The overall average comparison percentage is 95.26% and the results comparison can be concluded as acceptable.

#### 4.1.2 Garrett GT42

A Garrett GT42 radial-inflow turbine rotor as well as its operating conditions was obtained. The design specifications of the rotor such as the blade inlet angle and blade outlet angle could, however, not be found, as this is information that Garrett does not want to reveal.

In an attempt to gather the necessary information in order to perform the same design in EES, the rotor was measured by making use of a Vernier. Although the information gathered may not be completely accurate, as measuring inaccuracies may have occurred, it is seen as a good opportunity to compare a commercial

turbine to the constructed EES radial-inflow turbine design program. Table 2 gives a comparison of the EES and GT42 results.

[See Appendix D for a copy of the GT42 specifications and the results generated by the EES design program.]

**Table 2: Comparison of EES and GT42 results.**

Parameter	GT42	EES	Comparison
Z	10	10.36	96.5%
P <sub>4</sub>	799.2 kPa	802.1 kPa	99.6%
T <sub>4</sub>	700 °C	665 °C	95%
T <sub>6</sub>	635.9 °C	600.3 °C	94.4%
PR	1.47	1.69	87%
$\beta_4$	16.5°	14.04°	85%
$\beta_6$	60°	65.6°	91.5%
r <sub>4</sub>	0.043m	0.042m	97.7%
r <sub>6t</sub>	0.0392m	0.0388m	98.8%
b	0.0146m	0.0131	90%

From Table 2 it can be seen that the majority of parameters are once again above 90% comparison. The other parameters are the PR (87%),  $\beta_4$  (85%) and the blade height (90%). Even with the relative inflow-angle ( $\beta_4$ ), with the lowest percentage comparison, the overall comparison can be regarded as acceptable when taking into account that this is a comparison of a preliminary radial-inflow turbine design procedure with a commercial radial-inflow turbine.

The overall average comparison percentage is 93.3%.

#### 4.1.3 Concepts NREC Rital

As mentioned before, the need for the study originated from a lack of experience in radial-inflow turbine design. This identified the need for a basic design tool guiding the novice to meaningful initial design parameters that can be used as input in detail design packages commercially available.

In order to verify the acceptability of the answers supplied by EES, the results were compared to that obtained from such a commercial package. This was done using *Concepts Rital*<sup>®</sup>, a commercially accepted code for designing radial-inflow turbines.

The Concepts Rital design mode was selected as this gives the designer the option of entering the inlet temperature, the exit pressure, mass-flow rate, the power and the rotational speed. The Rital loss coefficients were also kept on during the comparison, as this will usually be the case during designs.

The radial-inflow turbine design in EES is done quicker compared to the same design in Concepts Rital. The main purpose of the constructed EES design method is, however, still to present the designer with a tool to do a quick radial-inflow turbine design and in doing this, stating the economic feasibility of the system without the need for a commercial package such as Concepts Rital.

The verification continued by doing the same design of a radial-inflow turbine in EES and Rital. In order to verify the constructed EES design tool, certain parameters such as the rotation speed, mass-flow rate and inlet temperature were varied and the results compared. The results are presented in column graphs, thereby making it easier to compare. Only selected parameters are shown in the comparison graphs to follow, as there are quite a number of parameters calculated by both programs.



#### 4.1.3.1 Rotational speed variation (N)

During the first four comparisons, the rotational speed was varied. The runs were done at 20 000 rpm, 50 000 rpm, 80 000 rpm and 110 000 rpm.

The inlet temperature was set at 500K, the exit pressure at 150 kPa and the power at 20 kW. For the first two comparisons, the mass-flow rate was set at 0.05 kg/s and for the last two comparisons at 0.07 kg/s and 0.1 kg/s. The total-to-static efficiency was taken as 90%.

The comparison results given in Figures 32 to 35 show the comparison between the Rital results and the EES results.

[See Appendix E for the design windows of the four comparisons.]

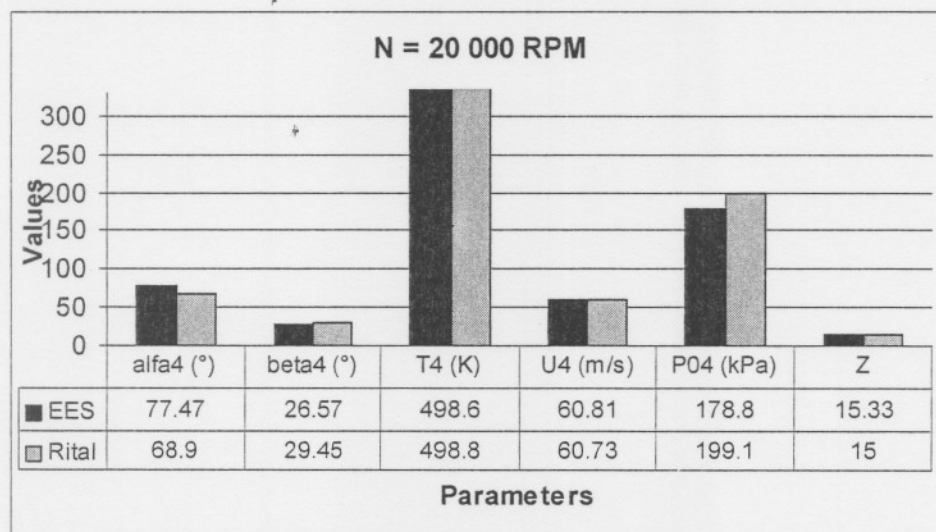


**Figure 32:** Rotational speed at 20 000 rpm.

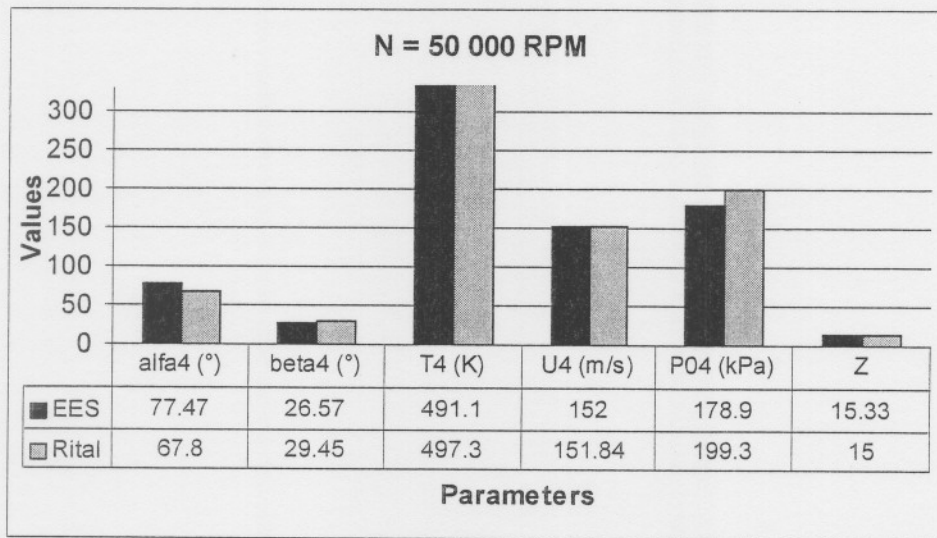


**Figure 33:** Rotational speed at 50 000 rpm.

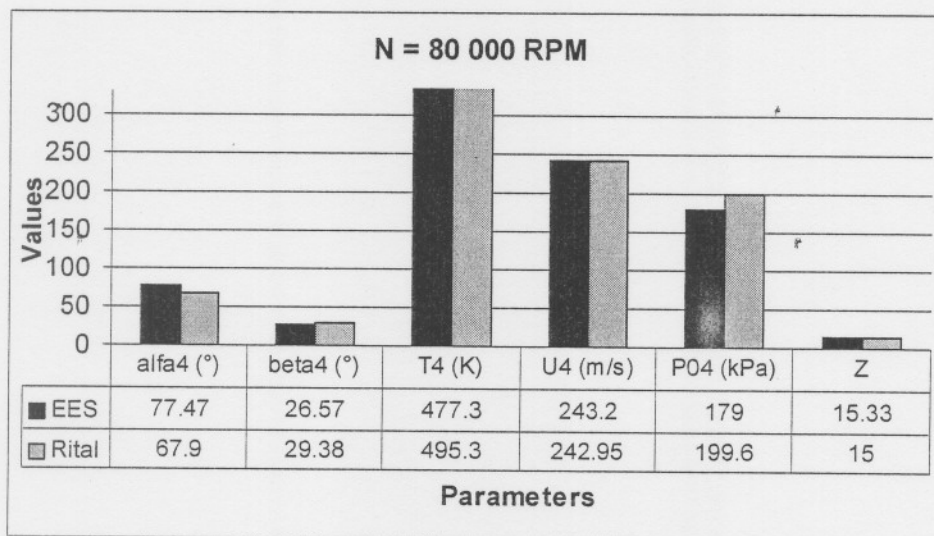


**Figure 34:** Rotational speed at 80 000 rpm.

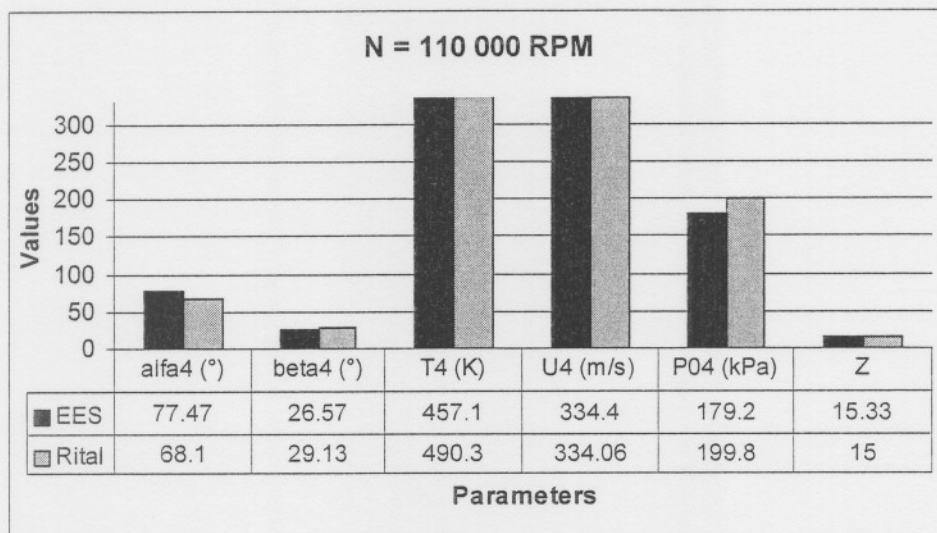


**Figure 35:** Rotational speed at 110 000 rpm.

#### 4.1.3.2 Mass-flow variation (m)

During the second three comparisons, the mass-flow rate was changed each time. The first run was done with a mass-flow rate of 0.1 kg/s, followed by a mass-flow rate of 0.125 kg/s and finally 0.15 kg/s.

The other input parameters, except the inlet temperatures, were kept as in Paragraph 4.1.3.1 and the rotational speed was kept constant at 60 000 rpm for all three comparisons.

The temperatures were set as follows for the different mass-flow rates:

- 600K for the mass-flow rate of 0.1 kg/s
- 500K for the mass-flow rate of 0.125 kg/s
- 360K for the mass-flow rate of 0.15 kg/s

The temperatures were decreased as the mass-flow rates were increased in order for the designs to solve. This is because an increase in temperature



causes an increase in energy and thus leads to a lower mass-flow rate required to operate (Author).

The comparison results are given in Figures 36 to 38 and shows what the comparison is of the Rital results and the constructed EES results.

[See Appendix E for the design windows of the four comparisons.]

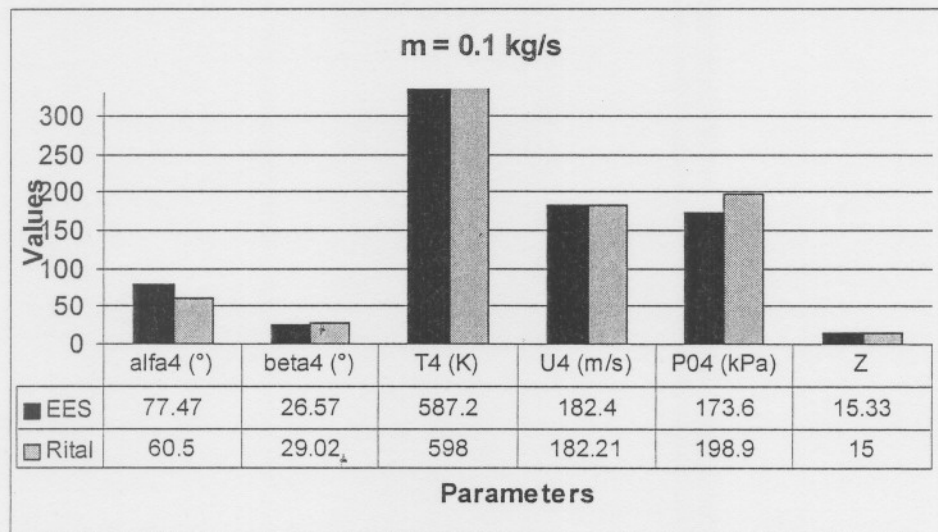


**Figure 36: Mass-flow rate at 0.1 kg/s.**

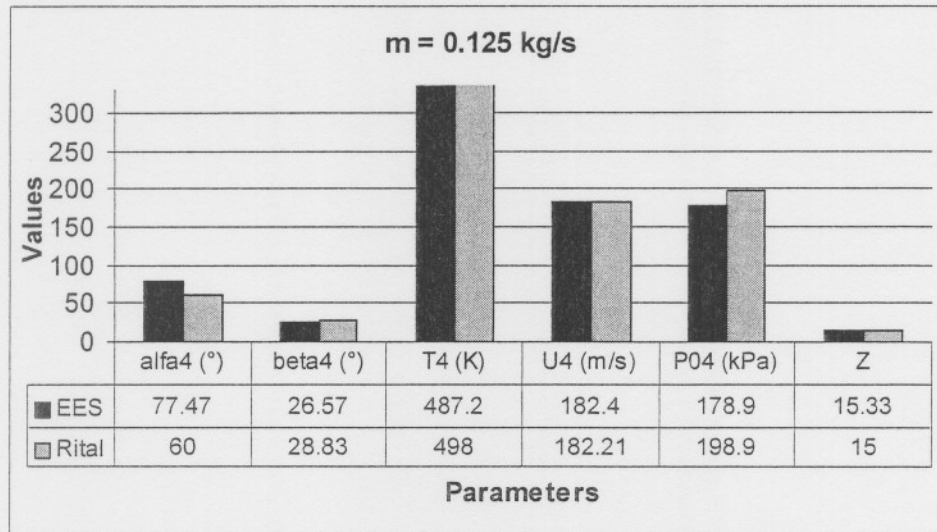


Figure 37: Mass-flow rate at 0.125 kg/s.

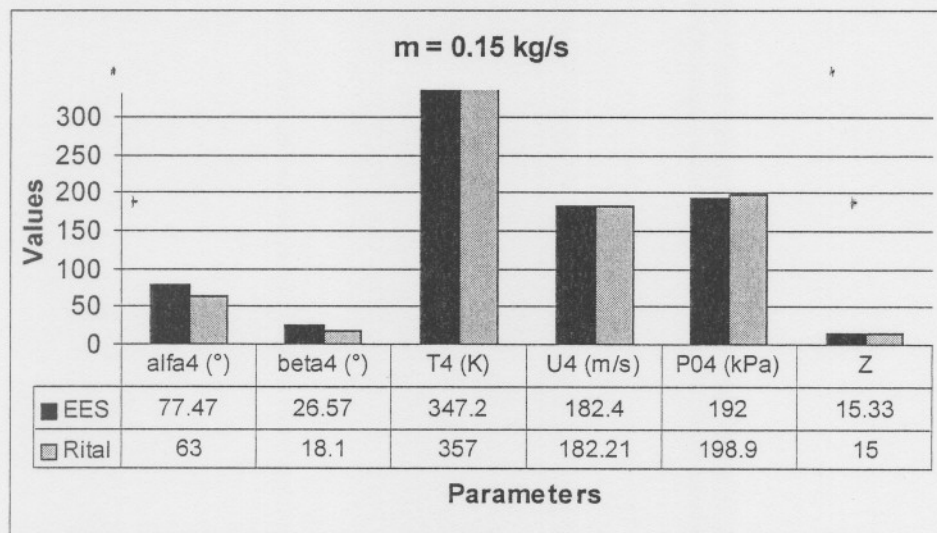


Figure 38: Mass-flow rate at 0.15 kg/s.

#### 4.1.3.3 Inlet temperature variation ( $T_{01} = T_{04}$ )

During the last three runs, the total inlet temperature was changed each time. The first comparison started with a total inlet temperature of 400 K, followed by total inlet temperatures of 600 K, 800 K and 1000K.

The mass-flow rate was kept at 0.06 kg/s, the rotational speed at 50 000 rpm and the exit pressure at 150 kPa. The other parameters were kept the same.

The comparison results given in Figures 39 to 42 show the comparison of the Rital results and the EES results.

[See Appendix E for the design windows of the four comparisons.]

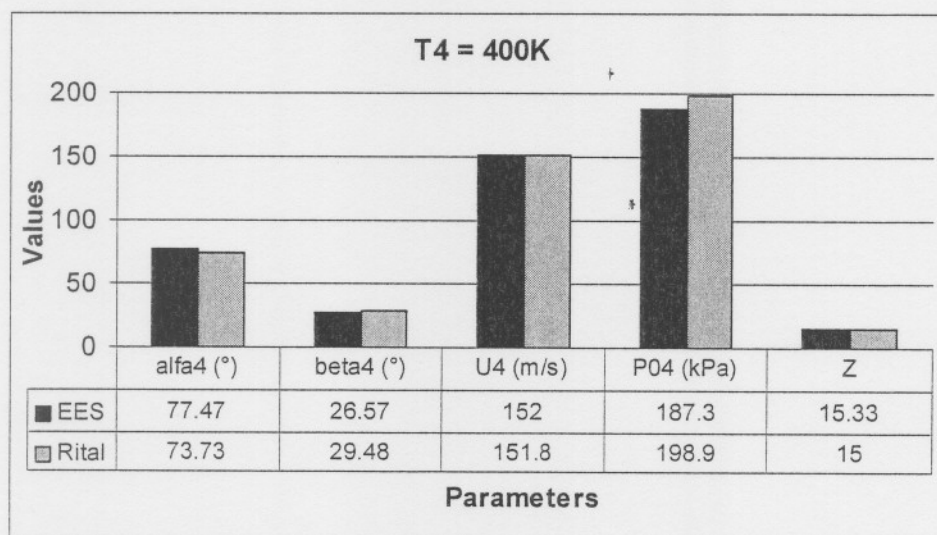


**Figure 39:** Inlet temperature at 400 K.

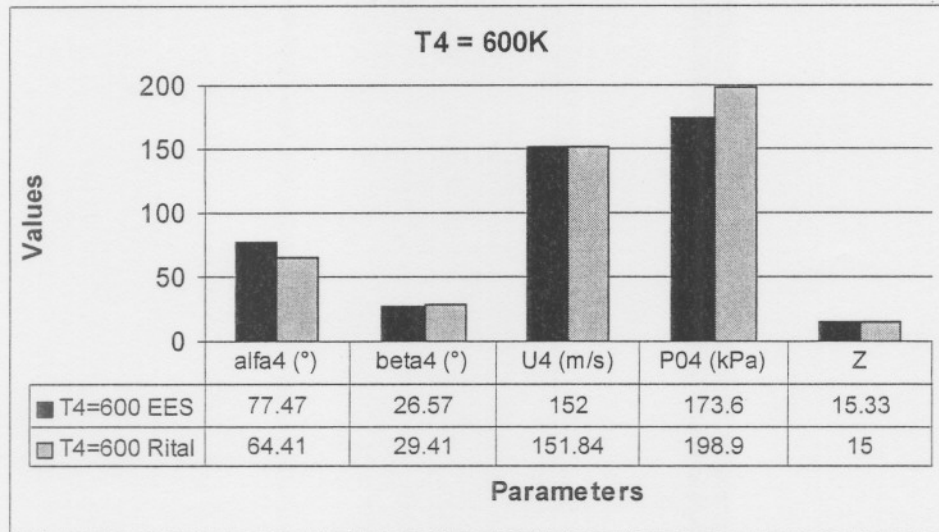


**Figure 40:** Inlet temperature at 600 K.

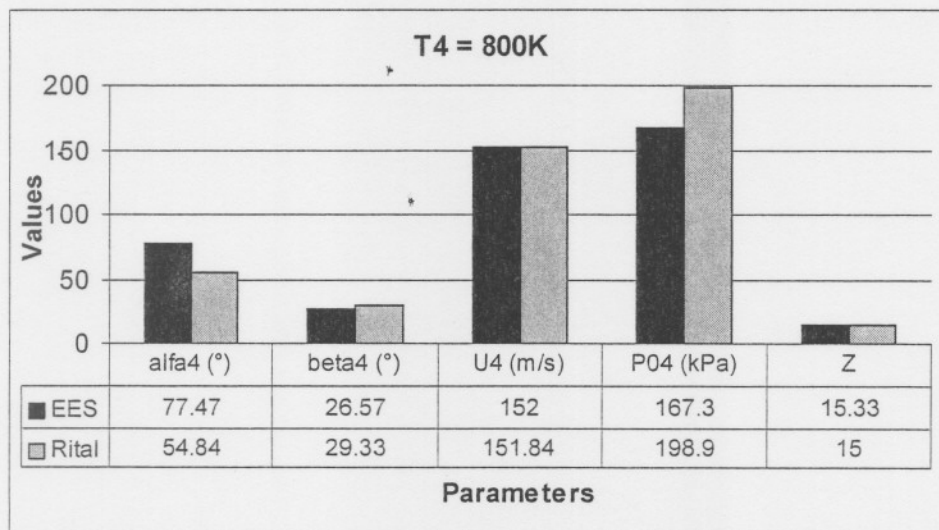


**Figure 41:** Inlet temperature at 800 K.



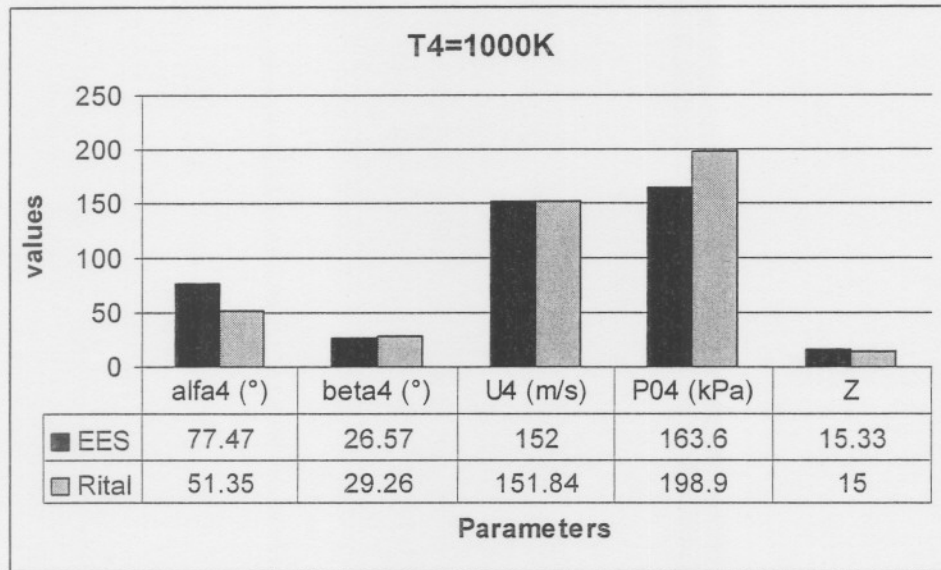


Figure 42: Inlet temperature at 1000K.

#### 4.1.3.4 Summary and Conclusion

During the variation of the rotational speed, the displayed parameters varied within acceptable tolerances. The inlet absolute flow angle ( $\alpha_4$ ) varied with a comparison percentage of 89%, 87.5%, 87.6% and 88% during the four different rotational speeds. The inlet relative flow angle ( $\beta_4$ ) varied with a comparison percentage of 90.2%, 90.2%, 90.4% and 91.2% respectively. The inlet static temperature ( $T_4$ ) varied between 99% and 93%. The comparison percentages for the inlet total pressure ( $P_{04}$ ) are 90%, 89.8%, 89.7% and 89.7%. The other parameters varied above a comparison percentage of 98%.

During the variation of the mass-flow rate, the displayed parameters once again varied within acceptable tolerances, with the exception of the inlet absolute flow angle. The inlet relative flow angle varied with a comparison percentage of 91.6%, 92.2% and 68.1% respectively. The inlet static temperature stayed constant above a comparison percentage of 97%. The inlet absolute flow angle, however, varied with a comparison percentage of 77.8%, 77.2% and 81% for the



three different mass-flow rates. The other parameters varied above a comparison percentage of 87%.

During the variation of the inlet temperature, the displayed parameters stayed within acceptable tolerances. The inlet absolute flow angle varied with a comparison percentage of 95.2%, 83.1%, 70.8% and 66.5% for the four different inlet temperatures. The inlet relative flow angle varied with a comparison percentage of 90.1%, 90.3%, 90.6% and 90.8% respectively. The inlet static pressure varied with comparison percentages of 94.2%, 87.3%, 84.1% and 82.3% for the four runs. The other parameters varied above a comparison percentage of 97%.

From the above results, it can be concluded that the constructed EES verification with the Concepts Rital program was acceptable. Most of the parameters varied above a comparison percentage of 82% with only the inlet absolute flow angle dropping to 66.5% during runs with the variation of the inlet temperature. However, for the rest of the comparisons it stayed above 77%.

It must be stated that the comparisons are only used as verification of the constructed EES design tool and by no means indicates the operating ranges of the constructed EES radial-inflow turbine design tool.

Although some variations were large, it is deemed acceptable, as this is only a preliminary design tool and the results proved to be close enough to give an acceptable ballpark value. Once obtained and fine-tuning is required, then Concepts Rital can be used.

## **4.2 EES design guidelines**

The procedure on how to do a preliminary radial-inflow turbine design using EES and operating it has been discussed in the preceding chapter. Paragraph 4.2.1 now provides an indication on the influence that each input parameter has during the design of a radial-inflow turbine using the constructed and verified EES design tool. Appendix F provides a short description on every parameter used in the EES radial-inflow turbine design tool and the role it plays within the design procedure.

In order to help the designer during the radial-inflow turbine design procedure, some information regarding materials and bearings is provided. It will help the designer in choosing meaningful input parameters when doing the design using the constructed EES design tool. The various materials will give the designer a good indication on realistic temperatures to use and the bearings on realistic rotational speeds.

### **4.2.1 EES input parameters**

Table 3 indicates the influence each input parameter has during the design of a radial-inflow turbine through the constructed EES design tool. It indicates which parameters are influenced and whether it's value will increase or decrease. The value of each input parameter was increased independently and the influence thereof recorded.

Table 3: Input parameters and their influences

Input Parameter		Result value	
Increase value		Increase	Decrease
$T_{01}$	$A_4$	$M_4$	
	$A_6$	$M_6$	
	$\beta_6$	$P_4$	
	$b$	$PR_{total}$	
	$T_{04}$	$PR_{static}$	
	$T_4$	$P_{04}$	
	$T_6$		
	$T_{06}$		
	$U_6$		
	$W_6$		
	$r_{6t}$		
$P_6$	$P_4$	$A_4$	
	$P_{04}$	$A_6$	
	$P_{06}$	$\beta_6$	
	$P_6$	$b$	
		$U_6$	
		$W_6$	
		$r_{6t}$	
$r_{6h}$	$C$	$A_4$	
	$M_4$	$A_6$	
	$M_6$	$\beta_6$	
	$U_4$	$b$	
	$P_4$	$T_4$	
	$W_4$	$T_6$	
	$W_6$	$T_{06}$	
	$r_4$	$U_6$	
		$PR_{static}$	
		$r_{6t}$	
$\psi$	$\alpha_4$	$\beta_4$	
	$C_4$	$i_4$	
	$C_{theta4}$		
	$Z$		
$\Phi$	$C$	$A_4$	
	$M_6$	$A_6$	
	$W_4$	$\alpha_4$	
		$\beta_4$	
		$\beta_6$	
		$Z$	
		$b$	
		$U_6$	
		$r_{6t}$	
Input Parameter		Result value	
Increase value		Increase	Decrease
$\beta_{b4}$	$i_4$	$M_6$	
$m$	$A_4$		
	$A_6$		
	$\beta_6$		
	$T_6$		
	$T_{06}$		
	$b$		
	$U_6$		
	$W_6$		
	$r_{6t}$		
$\eta$		$P_4$	
		$P_{04}$	
		$PR_{total}$	
		$PR_{static}$	
$\zeta$	$C_{m4}$	$A_4$	
	$W_4$	$\alpha_4$	
		$\beta_4$	
		$i_4$	
		$Z$	
		$b$	
$\alpha_6$	$C_6$	$\beta_6$	
	$C_{theta6}$	$W_6$	
$P$	$M_6$	$A_6$	
	$P_4$	$\beta_6$	
	$PR_{total}$	$U_6$	
	$PR_{static}$	$T_6$	
	$P_{04}$	$T_{06}$	
		$W_6$	
$N$	$C$	$A_4$	
	$M_4$	$A_6$	
	$M_6$	$\beta_6$	
	$U_4$	$T_4$	
	$U_6$	$T_6$	
	$W_4$	$T_{06}$	
	$W_6$	$P_4$	
	$\omega$	$PR_{static}$	
		$r_{6t}$	

## 4.2.2 Materials

The selection of a material for the turbine plays a very important role when selecting the temperature at which it will operate. Other factors such as stress and corrosion on the blades must also be acknowledged. The final selection of the material can only be done after a detail design of the radial turbine has been done and a stress analysis has been conducted using CFD or other methods. As this paper only describes the preliminary design of a radial-inflow turbine, it will only give a guideline to which materials the designer can use during the preliminary design. [More information on the effects that corrosion, temperature and stress play on the turbine blades can be found in Chapter 11 of Boyce, M.P.]

In practise, normal materials such as Stainless steel grade 304 can be used for temperatures up to 650°C. In the case where a higher temperature is used, the designer will have to make use of more expensive materials which can withstand the high temperatures with good service life up to 870°C. Coatings such as,

- Ni, 18% Cr, 12% Al, 0.3% Y,
- Co, 29% Cr, 3% Al, 0.3% Y or
- Co, 25% Ni, 20% Cr, 8% Al, 0.3% Y

can be used in temperatures up to 1000°C, but this is only in very extreme situations. A benchmark for preliminary design will be 600°C (873K), as most regular radial turbine wheels operate at this temperature (Baines, 2005).

Table 4 provides an estimate of the most commonly used turbine materials and their properties, published by Baines (2005). This table can be used in selecting the inlet temperature to the turbine rotor when using EES for the preliminary design of a radial-inflow turbine. The minimum tip clearance can also be found by using the % Elongation by adding this to the calculated turbine rotor radius.

[See Kawaura, Kawahara, Nishino & Saito (2002) for a new surface treatment of turbine blades.]

**Table 4: Properties of turbine materials. (Courtesy of Baines, 2005)**

Material	Temp. (°C)	$\sigma_y$ (MPa)	UTS (MPa)	Elongation (%)	$\rho$ (kg/m <sup>3</sup> )	E (GN/m <sup>2</sup> )	UTS/ $\rho$	E/ $\rho$
IN713LC	538	760	895	11	8000	183	0.11	0.023
	760	760	950	11		165	0.12	0.021
	871	580	750	12		157	0.084	0.02
	982	285	470	22		149	0.059	0.019
IN718	538	1020	1195	20	8200	200	0.15	0.024
	760	800	855	30			0.1	
MAR-M-247	538	825	1035	9	8500	172	0.12	0.02
	760	825	1035			159	0.12	0.019
	871	690	825			150	0.097	0.018
	982	380	550			142	0.065	0.017
$\gamma$ TiAl		400-	450-	3	4400	159	0.10-	0.036
		425	600	3	4400	159	0.14	0.036
Hot pressed Si <sub>3</sub> N <sub>4</sub>			690		3200	310	0.21	0.097
Hot pressed Beryllia			200		3030	400	0.068	0.132

### 4.2.3 Bearings

Bearings play a very important role in the design of a turbine, especially in a turbo unit. The bearing is responsible for keeping the turbo-unit in place while different forces are acting on it and while doing this, it still has to let the shaft rotate with the least amount of friction. This paragraph will not look at factors such as forces and friction concerning bearings, but will look at the maximum rotational speeds which a bearing can handle as it is one of the input parameters when doing a preliminary design of a radial-inflow turbine.

There are three types of bearings that are currently being used, namely the *Floating ring journal bearings*, *Rolling contact bearings* and *Air bearings*. In applications where bearing losses are very important, the designer will try and design the turbo-unit to rotate as slowly as possible, because the bearing power loss increases as the square of the shaft speed (Baines, 2005). In, for example, automotive applications where size and rotating inertia must be kept to the

minimum, this requirement is overridden and has driven the design to ever higher speeds. In normal applications the turbine will rotate at speeds reaching 80 000 rpm. In more extreme applications where the rotational speed must be as high as possible (as a result of turbine size limitations), speeds of 400 000 rpm can be achieved (Anonymous). It must however be acknowledged that the higher the rotational speed required, the more complicated the bearing becomes and thus more expensive. Other factors such as cooling and lubrication of the bearing must also be kept in mind, as these play very important roles in the service life of a bearing.

In automotive applications the most commonly used bearings are *Journal bearings* and *Ball bearings*. The Garrett ball bearing spools up 15 percent faster than traditional journal bearings (Garrett, 2005) and is therefore the preferred bearing to use when losses and reaction time are very important, although it is more expensive than regular journal bearings (see Figure 43).

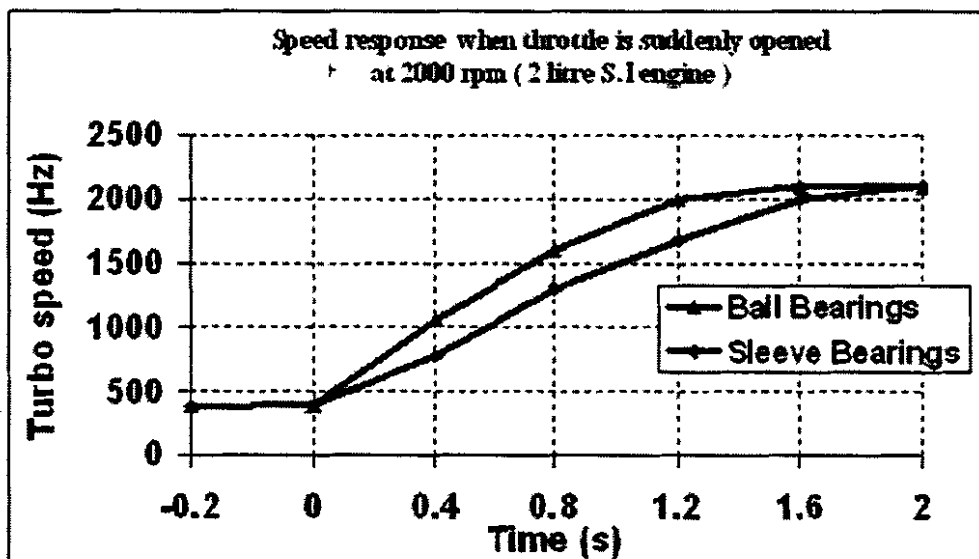


**Figure 43:** Speed response of a Ball bearing vs. a Sleeve bearing.  
(From Garrett website, 2005)

### **4.3 Conclusion**

In Chapter 4 the constructed EES design tool for determining the initial design parameters of a radial-inflow turbine was verified, as the comparisons were found acceptable. The chapter also discussed other parameters that must be kept in mind when doing a radial-inflow turbine design, such as material and bearing limitations and the influence each input parameter has during the EES design procedure.

The three steps in order to reach the goal of this study have now been completed, namely a thorough literature study, development of a simple design tool and finally verification of the constructed EES design tool. Chapter 5 will give a final conclusion regarding this study and will conclude with recommendations.

## CHAPTER 5

# CONCLUSION AND RECOMMENDATIONS

### 5.1 Conclusion

The problem statement stated that with the use of currently available turbo-machine simulation packages a need exists to guide young turbo-machine designers in making reasonable assumptions, based on previous experience, during the design of a new turbo-machine. The goal was to help develop the designer's background concerning radial-inflow turbine design and to construct a radial-inflow turbine design tool in EES. This would help prevent flaws carried over from an existing design to that of a new design. It would also make it possible to determine the feasibility of a system before continuing with a detail design through the much more expensive turbo-machine software packages.

The aim was to develop a tool to assist designers with the initial "ball-park" design of new radial-inflow turbine rotors. In doing so, giving the designer meaningful initial design parameters making it possible to start a new design within a current available simulation package with some degree of assurance that it will solve, from where further fine-tuning would be possible.

In order to reach this goal, the first step was to do a thorough literature study in order to determine which parameters are important during the design of a radial-inflow turbine. The second step was to develop a simple tool by making use of the Engineering Equation Solver (EES) in order to determine the initial design parameters of a radial-inflow turbine. This would make it possible for users to reach a first order design. In order to create trust within this tool, it had to be verified. This was accomplished through two different methods, the first being to compare it to design samples sourced from turbo-machine literature. The second method was to make use of the *Concepts NREC*® software package, which is accepted worldwide for the design of turbo-machines.



These steps were completed and the EES radial-inflow design program was constructed. Information gathered from various sources was used, most of it from the *Axial and Radial Turbines* handbook by Baines (2003). In order to verify the constructed EES design program, a radial-inflow turbine design example was used as well as the design specifications of a GT42 turbine. For further verification, the detail design software *Concepts Rital* was used. The same design was constructed in both the EES and Rital programs and some parameters were varied. The results of each run were then compared.

The results of the three different methods used showed that the comparisons are acceptable and it can therefore be concluded that the constructed EES preliminary radial-inflow turbine design tool is acceptable in determining the input parameters for radial-inflow turbine design software. It can also be concluded that time will be saved in the design cycle of a radial-inflow turbine. This is because better initial design parameters will lead to fewer runs being required to reach an acceptable detail designed radial-inflow turbine.

## **5.2 Recommendations**

During the verification of the constructed EES radial-inflow turbine design tool, normal radial-inflow turbine operating conditions were used. The design range of the EES design tool was not determined, for example very high and very low rotational speeds, very high and very low mass-flow rates and so forth.

It is thus recommended that a wide range of designs be created within Concepts and PCA, which can then be compared to the same designs in the EES design tool.

Another recommendation is to create an experimental set-up of a radial-inflow turbine and to compare the results with that generated by the EES design tool.

## References

- [1] Abdel-Rahim, Y.M. 1994. *Energy analysis of radial inflow expansion turbines for power recovery*. [Web:] <http://www.engineeringvillage.com> [Date of use: March 2005].
- [2] Anonymous. unknown date. *Eddy current sensor tests turbochargers at high speed*. Professional Engineering: p 42.
- [3] Baines, Nicholas C. 2005. *Fundamentals of Turbocharging*. Concepts NREC. USA: Edwards Brothers Incorporated.
- [4] Baines, Nicholas C. 2003. *Axial and Radial Turbines*. Concepts NREC. USA: Edwards Brothers Incorporated.
- [5] Baines, Nick. 2002. *Radial and mixed flow turbine options for high boost turbochargers*. [Web:] <http://www.engineeringvillage.com> [Date of use: March 2005].
- [6] Bell, Corky. 1997. *Maximum Boost*. USA.
- [7] Blanchard, B.S. & Fabrycky, W.J. 1998. *Systems Engineering and Analysis*. Third Edition.
- [8] Boyce, M.P. *Gas Turbine Engineering Handbook*. Second Edition. UK: Gulf Professional Publishing.
- [9] Daily, J.W. & Nece, R.E. 1960. *Chamber dimension effects on induced flow and frictional resistance of enclosed rotating discs*. Trans ASME Journ Basic Eng 82: 217-232.
- [10] Denton, J.D. & Xu, L. 1999. *The exploitation of three-dimensional flow in turbomachinery design*. [Web:] <http://www.engineeringvillage.com> [Date of use: April 2005].

- [11] Dixon, S.L. 1998. *Fluid Mechanics and Thermodynamics of Turbomachinery*. Fourth Edition.
- [12] Ebaid, M.S.Y. & Al-Hamdan, Q.Z. 2004. *Optimization techniques for designing an inward flow radial turbine rotor*. [Web:] <http://www.engineeringvillage.com> [Date of use: March 2005].
- [13] Garrett. 2005. *Bearings*. [Web:] <http://www.turbobygarrett.com> [Date of use: 20 October 2005].
- [14] Ghaly, W.S. 1990 / Jan / v 10 / nr 2 / p 179-197. *A Design Method for Turbomachinery Blading in Three-Dimensional Flow*. International Journal for Numerical Methods in Fluids.
- [15] Glassman, A.J. 1976. *Computer program for design and analysis of radial inflow turbines*. NASA TN 8164.
- [16] Gu, F., Engeda, A. & Benisek, E. *A comparative study of incompressible and compressible design approaches of radial inflow turbine volutes*. Mechanical Engineering Department, Michigan, USA.
- [17] Harvey, R.A. *Scaling of Gas Turbine Engines*. Pratt and Whitney, Canada.
- [18] Hawley, J.G., Wallace, F.J., Cox, A., Horrocks, R.W. & Bird, G.L. 1999. *Variable geometry turbocharging for lower emissions and improved torque characteristics*. [Web:] <http://www.sciencedirect.com> [Date of use: March 2005].
- [19] Hiett, G.F. & Johnston, I.H. 1963. *Experiments concerning the aerodynamic performance in inward radial flow turbines*. Proc Inst Mech Engrs 178(3I(ii)): 28-42.

- [20] Holeski, D.E. & Futral, S.M. 1967. *Experimental performance evaluation of a 6.02-inch radial inflow turbine over a range of Reynolds number*. NASA TN D-3824.
- [21] Hussain, M., Ilyas, M., & Bhinder, F.S. 1982. *A contribution to designing a nozzle-less volute casing for the inward flow radial gas turbine*. In *Turbocharging and Turbochargers*, Inst Mech Engrs, pp 49-54.
- [22] Jansen, W. 1964. *The design and performance analysis of radial-inflow turbines*. NREC Report 1067-1.
- [23] Karamanis, N. & Martinez-Botas, R.F. May 2002. *Mixed-flow turbines for automotive turbochargers: steady and unsteady performance*. Department of Mechanical Engineering, UK.
- [24] Kawaura, H., Kawahara, H., Nishino, K. & Saito, T. 2002. *New surface treatment using shot blast for improving oxidation resistance of TiAl-base alloys*. [Web:] <http://www.sciencedirect.com> [Date of use: March 2005].
- [25] Krylov, Y.P. & Spunde, Y.A. 1963. *About the influence of the clearance between the working blades and housing of a radial turbine on its exponent*. USAF Foreign Technology Division Translation FTD-MT-67-15.
- [26] Kurzke, J. & Riegler, C. 2000. *A new compressor map scaling procedure for preliminary conceptional design of gas turbines*. [Web:] <http://www.engineeringvillage.com> [Date of use: March 2005].
- [27] Miller, Harold. Edited by Kutz, Myer. 1998. *Mechanical Engineers Handbook*. Second Edition. John Wiley and Sons, Inc.
- [28] Murray, C.J. 1989 / Oct. / 02 / p 202-203 *'Smart' turbocharger responds to engine's needs*. Design News [Web:] <http://www.sciencedirect.com> [Date of use: March 2005].

- [29] Payne, S.J., Ainsworth, R.W., Miller, R.J., Moss, R.W. & Harvey, N.W. 2003. *Unsteady loss in a high pressure turbine stage*. [Web:] <http://www.engineeringvillage.com> [Date of use: April 2005].
- [30] Payri, F., Benajes, J. & Reyes, M. 1995. *Modelling of supercharger turbines in internal-combustion engines*. [Web:] <http://www.sciencedirect.com> [Date of use: March 2005].
- [31] Saravanamuttoo, H.H. , Rogers, G.F.C. & Cohen, H. 2001. *Gas Turbine Theory*. Fifth Edition. Pearson Education Limited.
- [32] Thakker, A. & Hourigan, F. 2004. *A comparison of two meshing schemes for CFD analysis of the impulse turbine for wave energy applications*. Wave Energy Research Team, Ireland.
- [33] Wilson, D.G. & Korakianitis, T. 1998. *The Design of High-Efficiency Turbomachinery and Gas Turbines*. Second Edition. Prentice-Hall.
- [34] Whitfield, A. & Baines, N.G. 1990. *Design of Radial Turbomachines*.
- [35] Zangeneh, M. 1991 / Sept / v 13 / nr 5 / p 599-624. *A Compressible Three-Dimensional Design Method for Radial and Mixed Flow Turbomachinery Blades*. International Journal for Numerical Methods in Fluids.

## Appendix A: EES rotor design and example

The goal is to construct a tool to determine the initial design parameters of a radial-inflow turbine. In order to accomplish this, EES was used in conjunction with the radial-inflow design equations discussed to create such a tool.

Appendix A present the constructed tool within EES by giving the input parameters and equations used to develop it. A short description of each "step" is given in order to make it easier for the designer to follow the constructed program for determining the initial design parameters of a radial-inflow turbine.

This is followed by a radial-inflow turbine design example in order to illustrate the EES design procedure constructed.

### **Program:**

{Please supply the following parameters for the preliminary design of a radial-inflow turbine}

T_01= 1073	{Total inlet temperature in Kelvin}
P_6= 101.3	{Pressure at the outlet of the turbine rotor in kPa}
N= 130000	{Rotational speed of the turbine rotor}
r_6h= 0.0082	{Exit hub radius of the turbine rotor}
psi= 0.95	{Loading coefficient, usually between 0.9 and 1.0}
phi= 0.3	{Flow coefficient, usually between 0.2 and 0.3}
beta_b4=0	{Inlet blade angle of the rotor}
m= 0.143	{Inlet mass flow rate to the rotor of the gas/fluid}
R= 0.287	{Gas constant}
k= 1.35	{Specific heat ratio}
Cp= 1.148	{Specific heat at constant pressure}
eta_R= 0.8	{Rotor efficiency}
eta_ts= 0.7	{Total-to-static efficiency}
alpha_6=10	{Absolute flow angle at the exit of the rotor}

zeta= 1 {Meridional velocity ratio,  $C_{m4} / C_{m6}$ }  
 Ratio\_6on4=0.3 {Exit hub radius to inlet radius ratio}  
 P= 20 {Power in kW}  
 gamma=1.333 {Cp/Cv ratio, usually 1.333 (combustion gas) or 1.4 (air)}

{ }

r\_6h/r\_4=Ratio\_6on4  
 omega\_4=(2\*PI\*N)/60 {Calculate omega, rotational velocity}  
 U\_4=omega\_4\*r\_4 {Calculate U\_4, inlet blade speed}  
 C\_4=(C\_m4^2+C\_theta4^2)^0.5 {Calculate C\_4, inlet absolute velocity}  
 C\_m4=zeta\*phi\*U\_4 {Calculate C\_m4, inlet meridional velocity}  
 psi=C\_theta4/U\_4 {Calculate C\_theta4, inlet tangential velocity}  
 phi=C\_m6/U\_4 {Calculate C\_m6, outlet meridional velocity}  
 alpha\_4=ARCTAN(C\_theta4/C\_m4) {Calculate alpha\_4, absolute flow angle at inlet}  
 beta\_4=ARCTAN((C\_theta4-U\_4)/C\_m4) {Calculate beta\_4, relative flow angle at inlet}  
 i\_4=beta\_4-beta\_b4 {Calculate i\_4, incidence angle at inlet}  
 W\_4=(C\_m4^2+(U\_4-C\_theta4)^2)^0.5 {Calculate W\_4, relative velocity at inlet}  
 A\_4=(m\*R\*T\_4)/(P\_4\*C\_m4) {Calculate A\_4, inlet area}  
 A\_4=2\*PI\*r\_4\*b {Calculate r\_4, inlet radius}  
 P=m\*Cp\*deltaT {Calculate deltaT, difference in temperature}  
 P=T\_01\*eta\_R\*(1-(1/PR\_total)^((gamma-1)/gamma)) {Calculate PR, pressure ratio}  
 PR\_total=P\_04/P\_06 {Calculate P\_04, inlet stagnation pressure}  
 P\_04/P\_4=(1+((k-1)/2)\*(M\_4^2))^(k/(k-1)) {Calculate P\_4, inlet static pressure}  
 rho\_4=P\_4/(R\*T\_4) {Calculate rho\_4, density of the gas/fluid at inlet}  
 M\_4=C\_4/(k\*R\*1000\*T\_4)^0.5 {Calculate M\_4, inlet Mach number}  
 T\_04/T\_4=1+(((k-1)/2)\*M\_4^2) {Calculate T\_4, inlet static temperature}  
 T\_04=T\_01 {Assume isentropic}  
 m=rho\_6\*PI\*(r\_6t^2-r\_6h^2)\*(1-B\_6)\*W\_6\*cos(beta\_6) {Calculate B\_6, blockage factor at exit}





$$\phi = \frac{C_{m6}}{U_4}$$

$$\alpha_4 = \arctan \left[ \frac{C_{\theta 4}}{C_{m4}} \right]$$

$$\beta_4 = \arctan \left[ \frac{C_{\theta 4} - U_4}{C_{m4}} \right]$$

$$i_4 = \beta_4 - \beta_{b4}$$

$$W_4 = (C_{m4}^2 + (U_4 - C_{\theta 4})^2)^{0.5}$$

$$A_4 = \frac{m \cdot R \cdot T_4}{P_4 \cdot C_{m4}}$$

$$A_4 = 2 \cdot \pi \cdot r_4 \cdot b$$

$$P = m \cdot C_p \cdot \delta T$$

$$P = T_{01} \cdot \eta_R \cdot \left[ 1 - \left( \frac{1}{PR_{total}} \right)^{\left( \frac{\gamma - 1}{\gamma} \right)} \right]$$

$$PR_{total} = \frac{P_{04}}{P_{06}}$$

$$\frac{P_{04}}{P_4} = \left[ 1 + \left( \frac{k - 1}{2} \right) \cdot M_4^2 \right]^{\left[ \frac{k}{k - 1} \right]}$$

$$\rho_4 = \frac{P_4}{R \cdot T_4}$$

$$M_4 = \frac{C_4}{(k \cdot R \cdot 1000 \cdot T_4)^{0.5}}$$

$$\frac{T_{04}}{T_4} = 1 + \left[ \frac{k - 1}{2} \right] \cdot M_4^2$$

$$T_{04} = T_{01}$$

$$m = (\rho_6 \cdot \pi \cdot (r_{6t}^2 - r_{6h}^2) \cdot (1 - B_6)) \cdot W_6 \cdot \cos(\beta_6)$$

$$\rho_6 = \frac{P_6}{R \cdot T_6}$$

$$W_6 = (C_{m6}^2 + (C_{\theta 6} - U_6)^2)^{0.5}$$

$$U_6 = \omega_6 \cdot r_{6t}$$

$$\omega_6 = \omega_4$$

$$C_6 = C_{m6} \cdot \frac{1}{\cos(\alpha_6)}$$

$$\beta_6 = \arctan \left[ \frac{C_{\theta 6} - U_6}{C_{m6}} \right]$$

$$C_{\theta 6} = C_{m6} \cdot \tan(\alpha_6)$$

$$M_{6rel} = \frac{W_6}{(k \cdot R \cdot 1000 \cdot T_6)^{0.5}}$$

$$M_6 = \frac{C_6}{(k \cdot R \cdot 1000 \cdot T_6)^{0.5}}$$

$$\delta T = T_4 - T_6$$

$$\frac{T_{06}}{T_6} = 1 + \left[ \frac{k-1}{2} \right] \cdot M_6^2$$

$$\frac{P_{06}}{P_6} = \left[ 1 + \left( \frac{k-1}{2} \right) \cdot M_6^2 \right]^{\left[ \frac{k-1}{k} \right]}$$

$$A_6 = \frac{m \cdot R \cdot T_6}{C_6 \cdot P_6}$$

$$A_6 = \pi \cdot r_{6t}^2$$

$$\text{ratio} = \frac{r_{6t}}{r_4}$$

$$Z = \frac{\pi}{30} \cdot (110 - \alpha_4) \cdot \tan(\alpha_4)$$

$$PR_{static} = \frac{P_4}{P_6}$$

### Example (Baines, 2003)

This example illustrates the preliminary design of a radial turbine for a turbocharger, as displayed in Figure 45. The mass flow rate, speed and power are set by the need to match the compressor and the exhaust gas temperature of the engine sets the inlet temperature to the turbine. The performance specification is therefore:

- Mass flow rate                      0.143 kg/s
- Speed                                      130 000 rpm
- Power                                      30 kW
- Inlet total temperature              873 K

The gas properties used are  $C_p=1.147$ ,  $k=1.35$ ,  $R=0.296$  and  $\gamma=1.34$ . The inlet blade angle ( $\beta_{b4}$ ) is taken as  $0^\circ$  (radial) and the exit flow angle ( $\alpha_6$ ) as  $10^\circ$ . The exit pressure is set to 400 kPa, the pressure to which the turbine exhausts, so that the inlet total pressure is eventually determined by the turbine equation. The constructed EES design program is used to do the necessary calculations.

The first attempt at a solution was made using optimum values of stage loading and flow coefficients as given in Figure 23,  $\Psi = 0.9$  and  $\Phi = 0.3$ . A total-to-total efficiency of 0.8 was assumed for the stage. The design procedure provides an estimate of the rotor exit area and in order to relate this to the hub and tip radii at this point, one or the other must be defined. The outlet hub radius was defined and from this the outlet tip radius could be calculated. The hub radius is limited by crowding of the blades and so it was set as a ratio of the rotor inlet radius to 0.3,  $r_{6h}/r_4$ , which is a likely minimum attainable for a rotor of this type (Baines, 2003). From this ratio the inlet tip radius can be calculated.

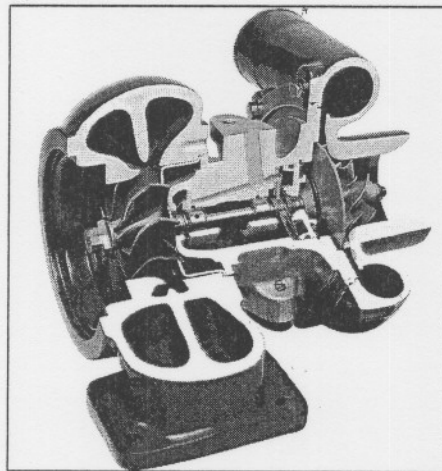


**Figure A1:** An illustration of a turbocharger, similar to that of the example.

The equations from Chapter 3 were used to do the necessary calculations using EES.

The results of this analysis are shown in Column A of Table A1. The blade speed is 394.8m/s, which is fairly high but should be acceptable for common rotor materials. A benchmark of 400m/s for the inlet blade speed is common, after which special materials must be used if it increases (Baines, 2003). A final decision must be made on this basis when a structural analysis is available, which will depend on the duty cycle and the life requirements of the turbocharger. The value calculated here gives confidence that it is safe to proceed. The rotor inlet flow angle  $\beta_4$  is in a range to give good incidence on to a radial-inlet blade. One of the most important answers here is the rotor exit tip to inlet radius ratio, which should be less than unity, as it will give a better aerodynamic solution, according to Baines.

In the case where the rotor exit tip to inlet radius ratio is very small,  $r_{6t}$  will be too low and thus also the exit area. In order to increase the exit area, the flow coefficient was increased to 0.3. The rotational speed was also set at 100 000 rpm. The results for this situation are shown in Column B of Table 4. This has the effect of increasing the meridional velocity at exit and since the meridional velocity ratio is unchanged, the corresponding velocity at inlet is increased. However, the inlet velocity triangle is also changed and the flow angle is increased to  $-18.43^\circ$ . The exit to inlet radius ratio is now 0.53. It would be necessary to make a careful approach to blade design backed up with CFD analysis of the blade passage flow for this geometry.

The speed was again set at 130 000 rpm and the stage loading coefficient was reduced to 0.8, as further gains might be possible. An increase in blade speed to 417.5 m/s can be seen in Column C, since the power output and mass flow rate are fixed. A careful structural analysis would be necessary to ensure an adequate service life, as experience suggests that this is now going close to the material limits (Baines, 2003). The inlet velocity triangle is quite acceptable with a larger value of  $U_4$ , because then  $C_{\theta 4}$  is reduced. The exit to inlet tip radius ratio is now 0.32, which suggests that this is a better aerodynamic solution.

**Table A1:** Results for the preliminary design of a radial-inflow turbine.

Rotor inlet	A	B	C	D
$U_4$	394.8	303	417.5	417.5
$C_{m4}$	197.4	91.11	208.7	208.7
$C_{\theta 4}$	355.3	273.3	334	334
$\alpha_4$	60.95	71.57	57.99	57.99
$\beta_4$	-11.31	-18.43	-21.8	-21.8
$C_4$	406.5	288	393.9	393.9
$W_4$	201.3	96.03	224.8	224.8
$T_4$	800.6	836.6	805.1	805.1
$P_{04}$	477.5	476.8	479.4	491.7
$A_4$	0.0005	0.00096	0.00047	0.00045
$r_4$	0.029	0.029	0.031	0.031
Rotor exit				
$T_6$	617.7	653.7	622.2	622.2
$P_{06}$	401.7	401	403.2	403.2
$P_6$	400	400	400	400
$A_6$	0.00033	0.00075	0.00031	0.00031
$r_{6h}$	0.0087	0.0087	0.0092	0.0092
$r_{6t}$	0.01	0.015	0.0099	0.0099
$r_{6t}/r_4$	0.35	0.53	0.32	0.32
$U_6$	138.7	161.6	135.4	135.4
$\beta_6$	-27.76	-57.95	-25.27	-25.27
$W_6$	223.1	171.7	230.8	230.8

Columns B and C thus contain two potential solutions that might be carried forward for detailed analysis, but the final choice will almost certainly depend on the maximum blade speed that can be tolerated by the materials. One or both designs must be developed to the point where a complete structural analysis can be made, if the designer does not have sufficient experience of other similar designs to make a clear decision.

In Columns B and C the exit stagnation pressures are 4 bar, which is likely to be too high for exhausting to ambient pressure with some exhaust system loss. If the exit static pressure has appreciably higher or lower than ambient, as is the case here, corresponding adjustments to the inlet total pressure should be made and the calculations repeated. The final values of stage loading and flow coefficient are well away from the region of optimum efficiency, as shown in

Figure 23, and it is possible that a total-to-total efficiency as high as 0.8 cannot be achieved. The calculations were therefore repeated with an efficiency of 0.7 in Column D to see what impact this had on the results. The only big changes were made to the inlet stagnation temperature that increased and the inlet area that decreased a little.

## Appendix B: EES volute design

In Appendix B the preliminary design of the volute for a radial-inflow turbine as programmed in EES is displayed. The parameters specified can, however, be renamed, as it is the designers choice. The formatted equations follow the equations as constructed in EES, for better understanding thereof.

{Please supply the following parameters for the preliminary design of a radial inflow volute}

P_0=	820	{Inlet total pressure}
T_0=	973	{Total inlet temperature}
R=	0.296	{Gas constant}
k=	1.333	{Specific heat ratio}
SC=	0.85	{Swirl coefficient}
Cp=	1.1472	{Specific heat at constant pressure}
b=	0.05	{Width of the scroll section}
A_begin=	0.06	{Inlet area}
m_begin=	1.2	{Inlet mass flow rate}
r_begin =	0.1	{Inlet radius of scroll section}
r_einde =	0.05	{Outlet radius of scroll section}
Intervalle =	10	{Number of sections (intervals) for the scroll section}
Intervalle_i=	3	{Number of sections (intervals) for the inlet section}
B_b=	0.000001	{Blockage of the inlet section}

{=====}

{Program equations}

```

r[1] = r_begin
m[1]=m_begin
theta[1]=0
R_m=287
    
```

{Loop calculations for the inlet section}

Y[1]=A_begin	{Area at section 1 of the inlet section}
Duplicate t=1,Intervalle_i	{Function for the iteration of the calculations}

```

Y[t+1]=Y[t]-0.005                                {Section area}

(m_begin*(R*T_0/k)^0.5)/(Y[t+1]*(1-B_b)*P_0)=N[t]*(1+(k-1)/2*N[t]^2)^(-0.5*((k+1)/(k-1)))
                                                    {Section Mach number}

W[t]=T_0*(1+((k-1)/2)*N[t]^2)^(-1)                {Section temperature}
C[t]=N[t]*(k*R*W[t])^0.5                           {Section absolute velocity}

Q[t]=P_0*((W[t]/T_0)^(k/(k-1)))                    {Section pressure}

end

C_begin=C[intervalle_i]

{Loop calculations for the scroll section}

DELTAR= r_begin - r_einde                          {Difference between inlet radius and outlet radius}

R_step = DELTAR/Intervalle                          {Value at which the radius diminishes for each following
                                                    section}

theta_step=(2*pi)/Intervalle                        {Value of angular steps in radians}

Duplicate i =1, Intervalle                          {Function for the iteration of the calculations}

    r[i+1]=r[i]-R_step                               {Starting value for the first section radius}

    theta[i+1]=theta[i]+theta_step                   {Starting value for the first section angle}

    m[i+1] = m_begin*(1-(theta[i+1]/(2*pi)))          {Starting value for the first section mass flow rate}

    C_theta[i]=SC*((r_begin*C_begin)/r[i+1])         {Section mean velocity}

    T[i]=T_0-(C_theta[i]/(2*Cp))                     {Section temperature}

    P[i]=P_0*((T[i]/T_0)^(k/(k-1)))                  {Section pressure}

    rho[i]=P[i]/(R*T[i])                             {Section density}

    C_m[i]=(m[i]-m[i+1])/(rho[i]*b*r_begin*(theta[i+1]-theta[i])) {Section mean flow velocity}

    alpha[i]=ARCTAN(C_theta[i]/C_m[i])                {Section absolute flow angle}

    A[i]=m[i]/(rho[i]*C_theta[i]*(1-B_b))             {Section area}

    C_abs[i]=(((C_theta[i]^2)+(C_m[i]^2))^0.5)*10       {Section absolute velocity}

    Mach[i]=C_abs[i]/((k*R_m*T[i])^0.5)              {Calculate section Mach number}

end

{%%%%%%%%%%%%%%%%%%%%%%%%%%%%%%%%%%%%%%%%%%%%%%%%%%%%%%%%%%%%%%%%%%%%%%%%%%%%%%%%%%%%%%%%%%%%%%%%%%%%%%%%%%%%%%%%%%%%%%%%%%%%%%%%%%%%%%%%%%%%%%%%}
    
```



## Appendix C: EES verification window

Figure C1 displays the constructed EES window during the design comparison of Example 1. It illustrates the input parameters used as well as the results generated.

EES Commercial: C:\DOCUMENTS AND SETTINGS\ADMINISTRATOR\MY DOCUMENTS\PROJECT\PROJECTS\EES VERIFIKASIE\EXAMPLE 1.3 - 0.6A.EES - [Program Window]

File Edit Search Options Calculate Tables Plots Windows Help Examples

(Please supply the following input parameters for the preliminary design of a radial-inflow turbine)

$T_{01} = 1050$ (Total inlet temperature in Kelvin)	$m = 1$ (Rotor inlet mass flow rate)	$N = 43843$ (Turbine rotor rotational speed)
$P_0 = 100$ (Turbine rotor outlet pressure)	$\eta_{ts} = 0.81$ (Total-to-static efficiency)	$\text{Ratio}_{0.014} = 0.7$ (Exit hub radius to inlet radius ratio)
$r_{0h} = 0.082$ (Turbine rotor exit hub radius)	$\eta_R = 0.81$ (Rotor efficiency)	$C_p = 1.15$ (Specific heat at constant pressure)
$\psi = 0.82$ (Loading coefficient, 0.0 to 1.0)	$\zeta = 1$ (Meridional velocity ratio)	$k = 1.35$ (Specific heat ratio)
$\phi = 0.26$ (Flow coefficient, 0.2 to 0.3)	$\alpha_0 = 0$ (Rotor exit absolute flow angle)	$R = 0.296$ (Gas constant)
$\beta_{b4} = 0$ (Rotor inlet blade angle)	$P = 230$ (Power in kW)	$\gamma = 1.33$ (Cp/Cv ratio)

**Results**

$A_4 = 0.008124$	$C_{m4} = 139.8$	$Z = 12.42$	$P_4 = 249.2$	$P_{04} = 357.4$
$A_6 = 0.01601$	$C_{m6} = 139.8$	$b = 0.01104$	$PR_{\text{total}} = 3.564$	$P_{06} = 100.3$
$\alpha_4 = 72.41$	$C_{\theta 4} = 441$	$T_{04} = 1050$	$PR_{\text{static}} = 2.492$	$P_6 = 100$
$\beta_4 = -34.7$	$C_{\theta 6} = 0$	$T_4 = 956.3$	$W_4 = 170.1$	$\rho_4 = 0.8803$
$\beta_6 = -66.89$	$M_4 = 0.7484$	$T_6 = 756.3$	$W_6 = 356.3$	$\rho_6 = 0.4467$
$C_4 = 462.7$	$M_6 = 0.2544$	$T_{06} = 764.8$	$r_4 = 0.1171$	$\omega_4 = 4591$
$C_6 = 139.8$	$i_4 = -34.7$	$U_4 = 537.8$	$r_{6t} = 0.07138$	$\omega_6 = 4591$
	ratio = 0.6094	$U_6 = 327.7$		

(Please refer to the equations window for more information on the parameters and the equations)

Start [Icons] EES verifikasie Document1 - Microsoft ... EES [Icons] 21:30

**Rotor inlet velocity triangle**

**Rotor exit velocity triangle**

Figure C1: Example 1 EES design window.

## Appendix D: EES verification window

Figure D1 displays the constructed EES window during the design comparison of the GT42 turbine unit. It illustrates the input parameters used as well as the results generated.

The following page displays some of the specifications regarding the GT42 turbine.

EES Commercial: C:\DOCUMENTS AND SETTINGS\ADMINISTRATOR\MY DOCUMENTS\M-PROJECT\M-PROJECT\EES-VERIFIKASIE\GT42.EES - [Diagram Window]

File Edit Search Options Calculate Tables Plots Windows Help Examples

(Please supply the following input parameters for the preliminary design of a radial-inflow turbine)

$T_{01} = 973$ [Total inlet temperature in Kelvin]	$\dot{m} = 1.148$ [Rotor inlet mass flow rate]	$N = 65383$ [Turbine rotor rotational speed]
$P_6 = 544.7$ [Turbine rotor outlet pressure]	$\eta_{ts} = 0.7$ [Total-to-static efficiency]	$Ratio_{a_{out4}} = 0.286$ [Exit hub radius to inlet radius ratio]
$r_{0h} = 0.012$ [Turbine rotor exit hub radius]	$\eta_R = 0.7$ [Rotor efficiency]	$C_p = 1.147$ [Specific heat at constant pressure]
$\psi = 0.9$ [Loading coefficient, 0.9 to 1.0]	$C = 1$ [Meridional velocity ratio]	$k = 1.35$ [Specific heat ratio]
$\phi = 0.4$ [Flow coefficient, 0.2 to 0.3]	$\alpha_6 = 6$ [Rotor exit absolute flow angle]	$R = 0.296$ [Gas constant]
$\beta_{b4} = -16$ [Rotor inlet blade angle]	$P = 85.2$ [Power in kW]	$\gamma = 1.34$ [Cp/Cv ratio]

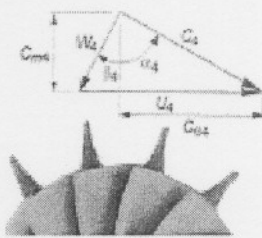
**Results**

$A_4 = 0.003459$	$C_{m4} = 114.9$	$Z = 10.36$	$P_4 = 802.1$	$P_{04} = 923.9$
$A_6 = 0.004716$	$C_{m6} = 114.9$	$b = 0.01312$	$PR_{total} = 1.693$	$P_{06} = 545.6$
$\alpha_4 = 66.04$	$C_{theta4} = 258.5$	$T_{04} = 973$	$PR_{static} = 1.472$	$P_6 = 544.7$
$\beta_4 = -14.04$	$C_{theta6} = 12.07$	$T_4 = 938$	$W_4 = 118.4$	$\rho_4 = 2.889$
$\beta_6 = -65.59$	$M_4 = 0.462$	$T_6 = 873.3$	$W_6 = 278$	$\rho_6 = 2.107$
$C_4 = 282.9$	$M_6 = 0.1955$	$T_{06} = 879.1$	$r_4 = 0.04196$	$\omega_4 = 6845$
$C_6 = 115.5$	$i_4 = 1.964$	$U_4 = 287.2$	$r_{0t} = 0.03875$	$\omega_6 = 6845$
	ratio = 0.9234	$U_6 = 265.2$		

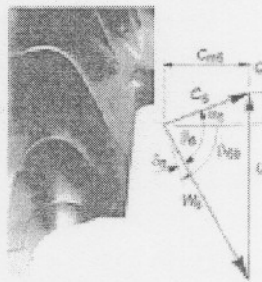
(Please refer to the equations window for more information on the parameters and the equations)

Calculate

Start | EES verifikasie | Document1 - Microsoft ... | EES | 21:32



{Rotor inlet velocity triangle}

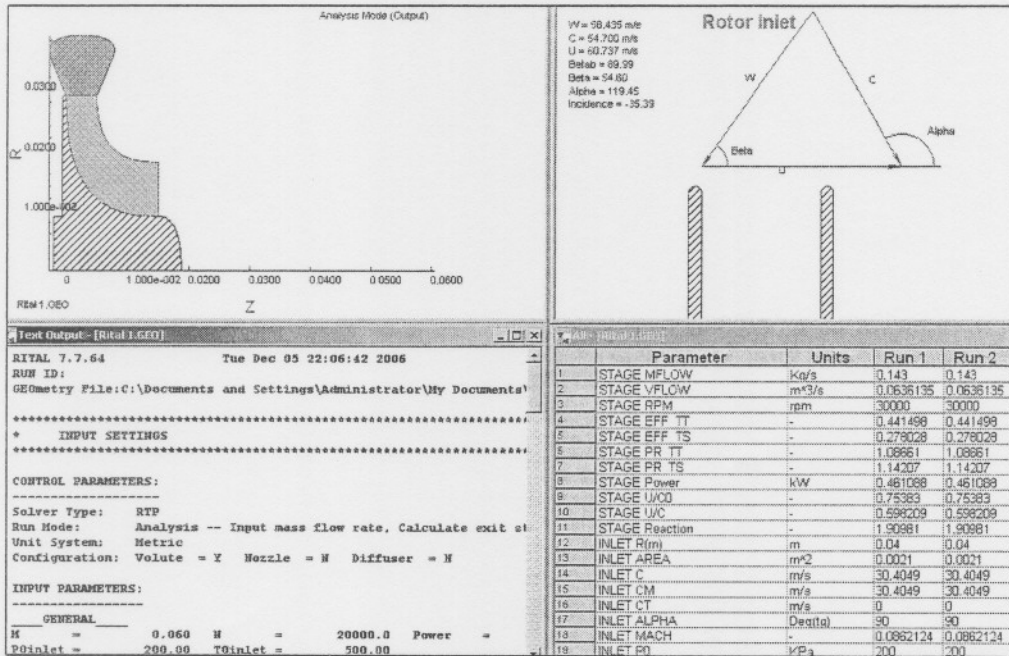


{Rotor exit velocity triangle}

Figure D1: GT42 EES design window.







N = 50 000 rpm:

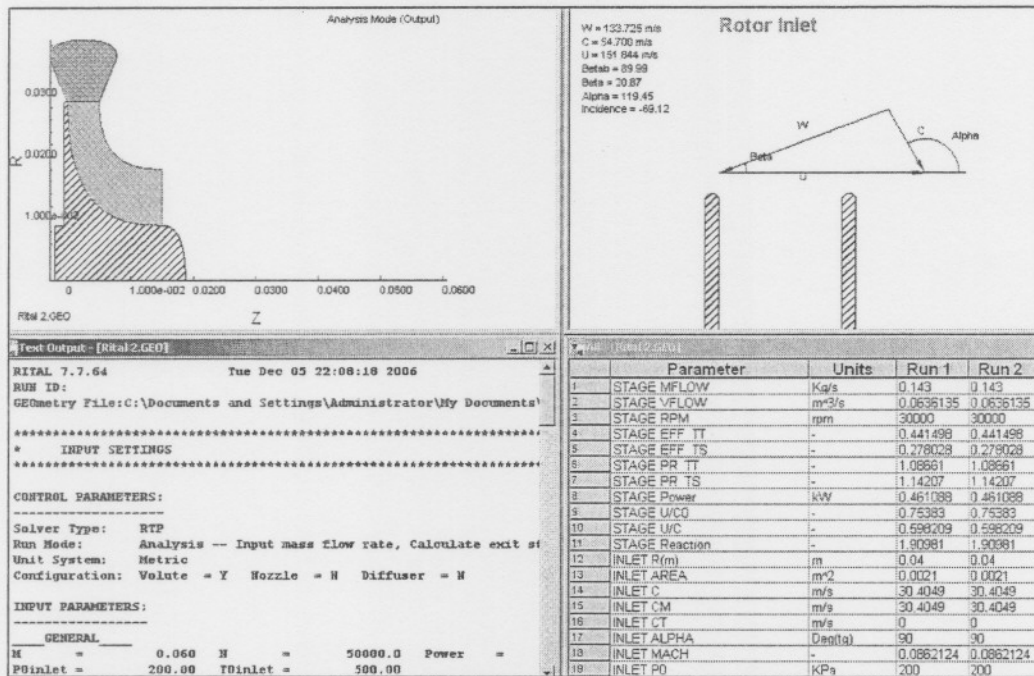
T <sub>01</sub> = 500 (Total inlet temperature in Kelvin)	m = 0.06 (Rotor inlet mass flow rate)	N = 50000 (Turbine rotor rotational speed)		
P <sub>0</sub> = 150 (Turbine rotor outlet pressure)	η <sub>ts</sub> = 0.9 (Total-to-stator efficiency)	Ratio <sub>0.95</sub> = 0.31 (Exit hub radius to inlet radius ratio)		
r <sub>0h</sub> = 0.009 (Turbine rotor exit hub radius)	η <sub>tt</sub> = 0.9 (Rotor efficiency)	C <sub>p</sub> = 1.147 (Specific heat at constant pressure)		
w = 0.9 (Loading coefficient, 0.0 to 1.0)	C <sub>1</sub> = 1 (Dimensional velocity ratio)	k = 1.35 (Specific heat ratio)		
ψ = 0.2 (Flow coefficient, 0.2 to 0.3)	α <sub>0</sub> = 30 (Rotor exit absolute flow angle)	R = 0.287 (Gas constant)		
β <sub>04</sub> = 0.01 (Rotor inlet blade angle)	P = 20 (Power in kW)	γ = 1.35 (C <sub>p</sub> /C <sub>v</sub> ratio)		

Calculate

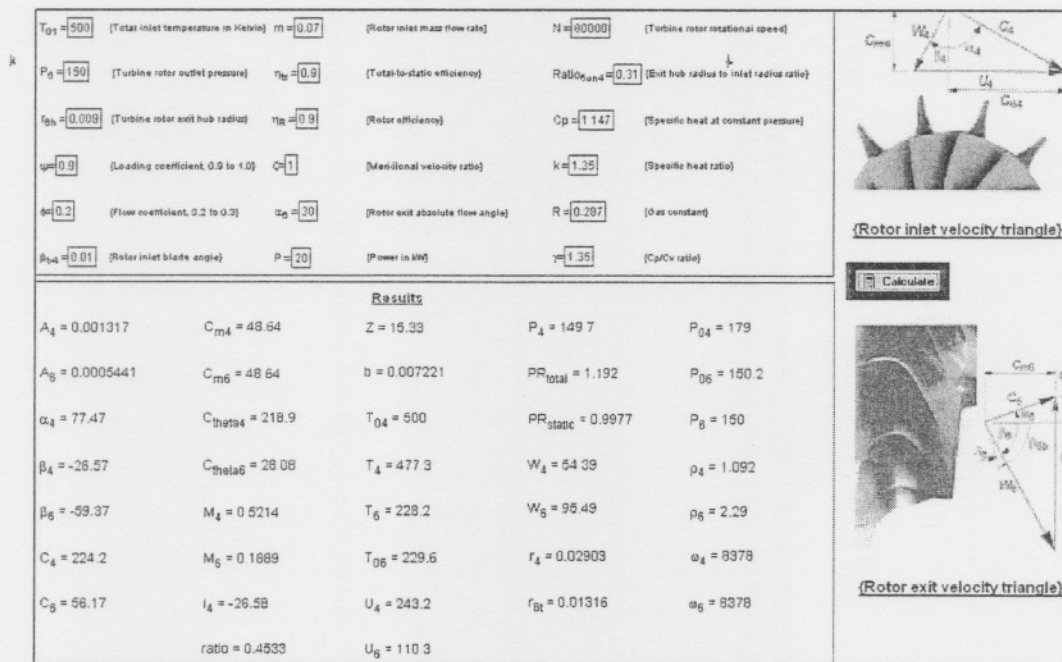
Results				
A <sub>4</sub> = 0.001666	C <sub>m4</sub> = 30.4	Z = 15.33	P <sub>4</sub> = 169.9	P <sub>04</sub> = 178.9
A <sub>8</sub> = 0.0006557	C <sub>m8</sub> = 30.4	b = 0.009135	PP <sub>total</sub> = 1.192	P <sub>08</sub> = 150.1
α <sub>4</sub> = 77.47	C <sub>theta4</sub> = 136.8	T <sub>04</sub> = 500	PR <sub>stac</sub> = 1.113	P <sub>0</sub> = 150
β <sub>4</sub> = -26.57	C <sub>theta8</sub> = 17.55	T <sub>4</sub> = 491.1	W <sub>4</sub> = 33.99	ρ <sub>4</sub> = 1.194
β <sub>8</sub> = -62.37	M <sub>4</sub> = 0.3213	T <sub>0</sub> = 200.5	W <sub>8</sub> = 65.57	ρ <sub>8</sub> = 2.607
C <sub>4</sub> = 140.1	M <sub>8</sub> = 0.1259	T <sub>08</sub> = 201.1	r <sub>4</sub> = 0.02903	ω <sub>4</sub> = 5236
C <sub>8</sub> = 35.11	i <sub>4</sub> = -26.58	U <sub>4</sub> = 152	r <sub>0t</sub> = 0.01445	ω <sub>8</sub> = 5236
	ratio = 0.4976	U <sub>0</sub> = 75.64		

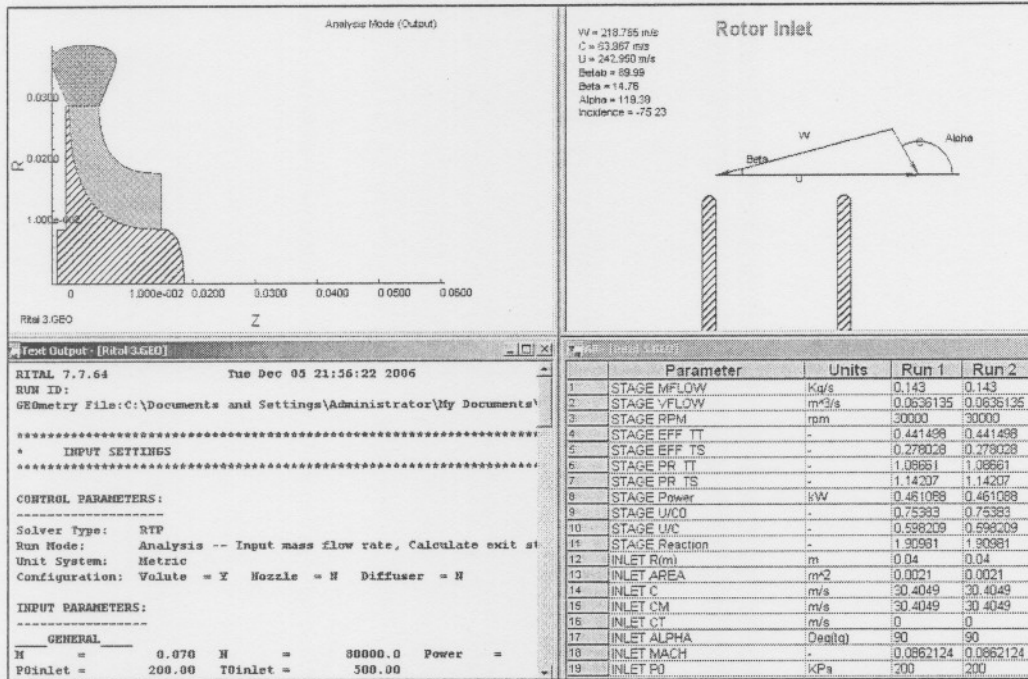
(Rotor inlet velocity triangle)

(Rotor exit velocity triangle)



$N = 80\ 000\ \text{rpm}$ :





N = 110 000 rpm:

T <sub>04</sub> = 500 [Total inlet temperature in Kelvin]	m = 0.1 [Rotor inlet mass flow rate]	N = 110000 [Turbine rotor rotational speed]
P <sub>0</sub> = 150 [Turbine inlet outlet pressure]	η <sub>ts</sub> = 0.9 [Total-to-static efficiency]	Ratio <sub>0.04</sub> = 0.31 [Exit hub radius to inlet radius ratio]
r <sub>0h</sub> = 0.009 [Turbine rotor exit hub radius]	η <sub>r</sub> = 0.9 [Rotor efficiency]	C <sub>p</sub> = 1.147 [Specific heat at constant pressure]
ψ = 0.9 [Loading coefficient, 0.9 to 1.0]	C = 1 [Mach number velocity ratio]	k = 1.35 [Specific heat ratio]
β = 0.2 [Flow coefficient, 0.2 to 0.3]	α <sub>0</sub> = 30 [Rotor exit absolute flow angle]	R = 0.287 [Gas constant]
β <sub>04</sub> = 0.01 [Rotor inlet blade angle]	P = 20 [Power in MW]	γ = 1.35 [C <sub>p</sub> /C <sub>v</sub> ratio]

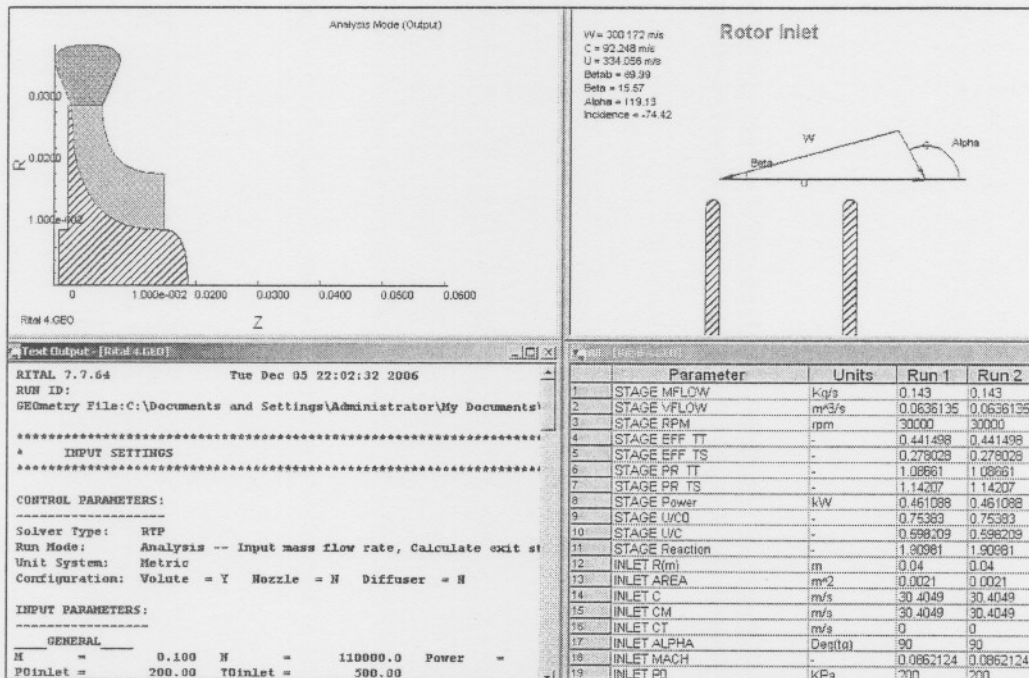
(Rotor inlet velocity triangle)

**Results**

A <sub>4</sub> = 0.001547	C <sub>m4</sub> = 66.89	Z = 15.33	P <sub>4</sub> = 126.7	P <sub>04</sub> = 179.2
A <sub>5</sub> = 0.0007003	C <sub>m5</sub> = 66.89	b = 0.008483	PR <sub>total</sub> = 1.192	P <sub>05</sub> = 150.4
α <sub>4</sub> = 77.47	C <sub>theta4</sub> = 301	T <sub>04</sub> = 500	PR <sub>static</sub> = 0.8449	P <sub>0</sub> = 150
β <sub>4</sub> = -26.57	C <sub>theta5</sub> = 38.62	T <sub>4</sub> = 457.1	W <sub>4</sub> = 74.78	p <sub>4</sub> = 0.9662
β <sub>5</sub> = -53.37	M <sub>4</sub> = 0.7327	T <sub>05</sub> = 282.7	W <sub>5</sub> = 149.2	p <sub>0</sub> = 1.849
C <sub>4</sub> = 308.3	M <sub>5</sub> = 0.2334	T <sub>06</sub> = 285.4	r <sub>4</sub> = 0.02903	ω <sub>4</sub> = 11519
C <sub>0</sub> = 77.23	i <sub>4</sub> = -26.58	U <sub>4</sub> = 334.4	r <sub>01</sub> = 0.01493	ω <sub>5</sub> = 11519
ratio = 0.5143		U <sub>R</sub> = 172		

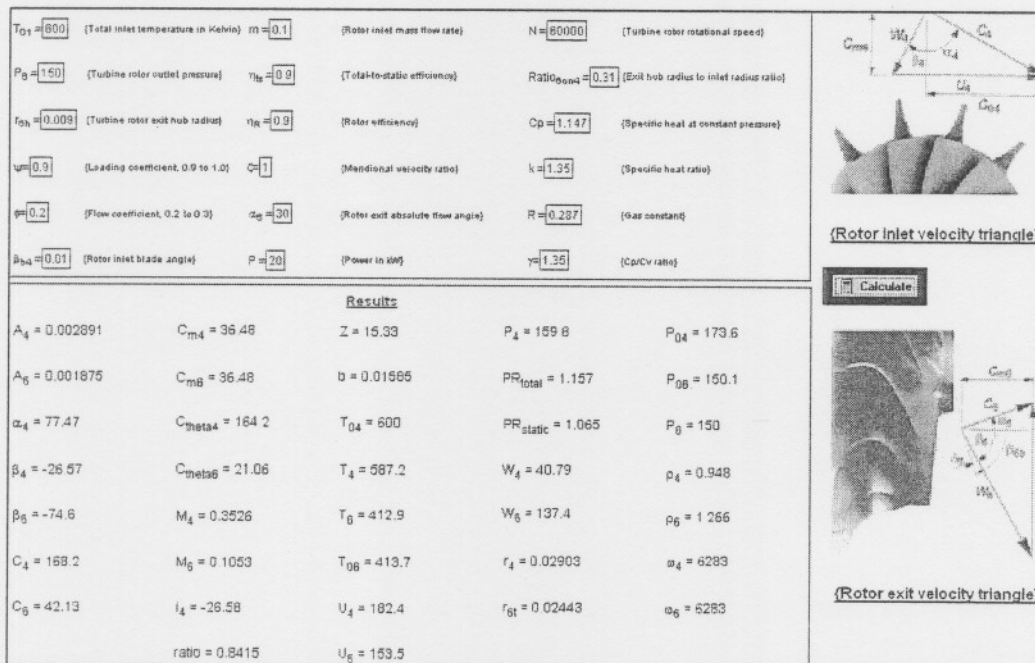
(Rotor exit velocity triangle)

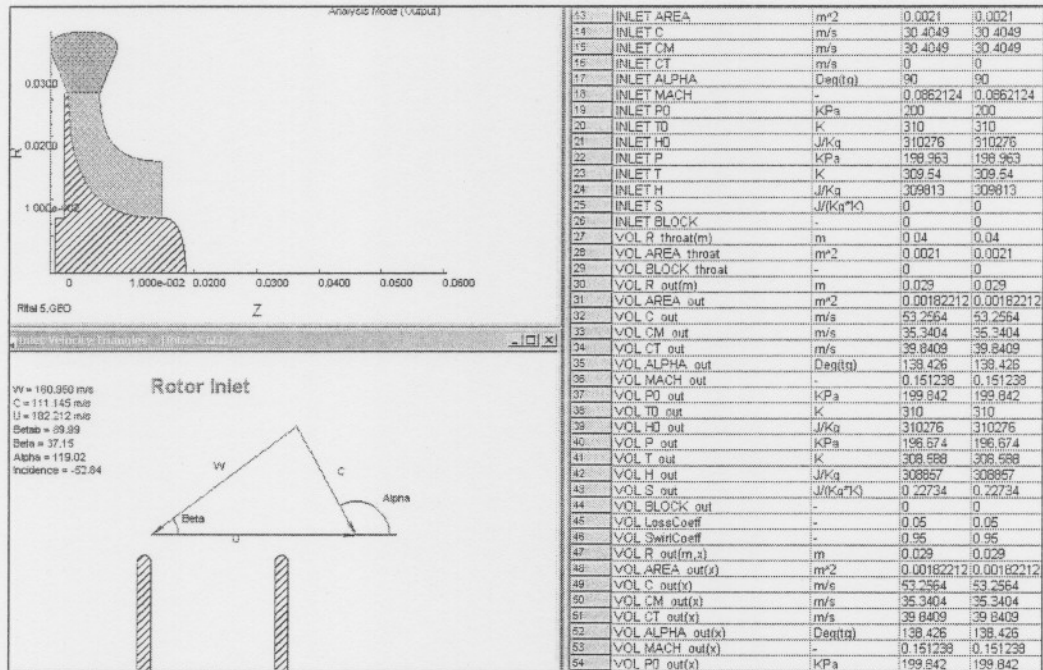




## Mass-flow variation

$$M = 0.1 \text{ kg/s}$$





$M = 0.125 \text{ kg/s:}$

$T_{01} = 500$ (Total inlet temperature in Kelvin)	$\dot{m} = 0.125$ (Rotor inlet mass flow rate)	$N = 80000$ (Turbine rotor rotational speed)
$P_0 = 150$ (Turbine rotor outlet pressure)	$\eta_{ts} = 0.9$ (Total-to-static efficiency)	$\text{Ratio}_{0.04} = 0.31$ (Exit hub radius to inlet radius ratio)
$r_{01} = 0.009$ (Turbine rotor exit hub radius)	$\eta_R = 0.9$ (Rotor efficiency)	$C_p = 1.147$ (Specific heat at constant pressure)
$\psi = 0.8$ (Loading coefficient, 0.9 to 1.0)	$C = 1$ (Meridional velocity ratio)	$k = 1.35$ (Specific heat ratio)
$\beta = 0.2$ (Flow coefficient, 0.2 to 0.3)	$\alpha_0 = 30$ (Rotor exit absolute flow angle)	$R = 0.287$ (Gas constant)
$\beta_{04} = 0.01$ (Rotor inlet blade angle)	$P = 20$ (Power in kW)	$\gamma = 1.35$ (Cp/Cv ratio)

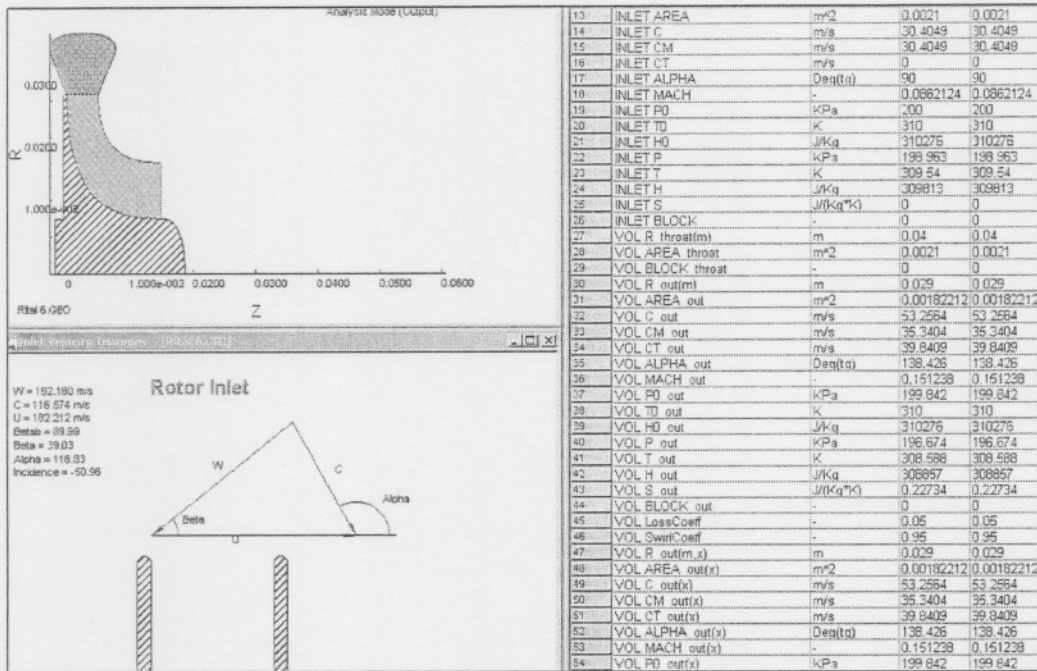
Results					
$A_4 = 0.00295$	$C_{m4} = 36.48$	$Z = 15.33$	$P_4 = 161.9$	$P_{04} = 178.9$	
$A_8 = 0.001974$	$C_{m8} = 36.48$	$b = 0.01623$	$PR_{\text{total}} = 1.192$	$P_{08} = 150.1$	
$\alpha_4 = 77.47$	$C_{\text{theta}4} = 164.2$	$T_{04} = 500$	$PR_{\text{static}} = 1.079$	$P_8 = 150$	
$\beta_4 = -26.57$	$C_{\text{theta}8} = 21.06$	$T_4 = 487.2$	$W_4 = 40.79$	$\rho_4 = 1.158$	
$\beta_8 = -75.03$	$M_4 = 0.3871$	$T_8 = 347.7$	$W_8 = 141.2$	$\rho_8 = 1.503$	
$C_4 = 168.2$	$M_8 = 0.1148$	$T_{08} = 348.5$	$r_4 = 0.02903$	$\omega_4 = 6283$	
$C_8 = 42.13$	$i_4 = -26.58$	$U_4 = 182.4$	$r_{81} = 0.02507$	$\omega_8 = 6283$	
	ratio = 0.8634	$U_8 = 157.5$			

**{Rotor inlet velocity triangle}**

**{Rotor exit velocity triangle}**





M = 0.15 kg/s:

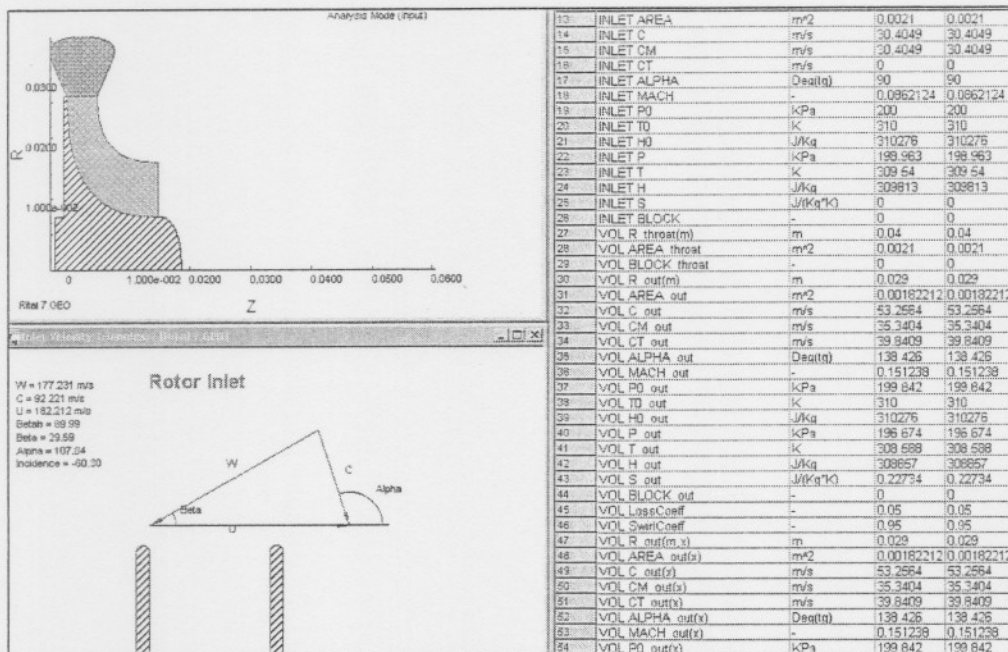
$T_{01} = 360$ (Total inlet temperature in Kelvin)	$m = 0.15$ (Rotor inlet mass flow rate)	$N = 6000$ (Turbine rotor rotational speed)
$P_0 = 150$ (Turbine rotor outlet pressure)	$\eta_{tp} = 0.9$ (Total-to-static efficiency)	$Ratio_{out/in} = 0.31$ (Exit hub radius to inlet radius ratio)
$r_{0h} = 0.008$ (Turbine rotor exit hub radius)	$\eta_R = 0.9$ (Rotor efficiency)	$C_p = 1.147$ (Specific heat at constant pressure)
$\psi = 0.9$ (Loading coefficient, 0.9 to 1.0)	$C = 1$ (Meridional velocity ratio)	$k = 1.35$ (Specific heat ratio)
$\phi = 0.2$ (Flow coefficient, 0.2 to 0.3)	$\alpha_0 = 30$ (Rotor exit absolute flow angle)	$R = 0.297$ (Gas constant)
$\beta_{04} = 0.01$ (Rotor inlet blade angle)	$P = 20$ (Power in kW)	$\gamma = 1.35$ (Cp/Cv ratio)

Results					
$A_4 = 0.002454$	$C_{m4} = 36.48$	$Z = 15.33$	$P_4 = 167$	$P_{04} = 192$	
$A_5 = 0.001574$	$C_{m5} = 36.48$	$b = 0.01345$	$PR_{total} = 1.279$	$P_{05} = 150.1$	
$\alpha_4 = 77.47$	$C_{theta4} = 164.2$	$T_{04} = 360$	$PR_{static} = 1.113$	$P_5 = 150$	
$\beta_4 = -26.57$	$C_{theta5} = 21.06$	$T_4 = 347.2$	$W_4 = 40.79$	$p_4 = 1.676$	
$\beta_5 = -79.03$	$M_4 = 0.4585$	$T_5 = 231$	$W_5 = 125$	$p_5 = 2.263$	
$C_4 = 168.2$	$M_5 = 0.1408$	$T_{05} = 231.8$	$r_4 = 0.02903$	$\omega_4 = 6283$	
$C_5 = 42.13$	$i_4 = -26.58$	$U_4 = 182.4$	$r_{E4} = 0.02238$	$\omega_5 = 6283$	
ratio = 0.7709		$U_5 = 140.6$			

(Rotor inlet velocity triangle)

(Rotor exit velocity triangle)



## Inlet temperature variation

$$T_{01} = 400 \text{ K}$$

(Please supply the following input parameters for the preliminary design of a radial-inflow turbine)

$T_{01} = 400$  (Total inlet temperature in Kelvin)  $m = 0.06$  (Rotor inlet mass flow rate)  $N = 50000$  (Turbine rotor rotational speed)

$P_0 = 150$  (Turbine inlet outlet pressure)  $\eta_{01} = 0.9$  (Total to static efficiency)  $R_{01} = 0.31$  (Exit hub radius to inlet radius ratio)

$r_{01} = 0.009$  (Turbine rotor exit hub radius)  $\eta_R = 0.9$  (Rotor efficiency)  $C_p = 1.147$  (Specific heat at constant pressure)

$\psi = 0.9$  (Loading coefficient, 0.9 to 1.0)  $C = 1$  (Meridional velocity ratio)  $k = 1.35$  (Specific heat ratio)

$\phi = 0.2$  (Flow coefficient, 0.2 to 0.3)  $\alpha_0 = 30$  (Rotor exit absolute flow angle)  $R = 0.287$  (Gas constant)

$\beta_{01} = 0.01$  (Rotor inlet blade angle)  $P = 20$  (Power in kW)  $\gamma = 1.35$  (Cp/Cv ratio)

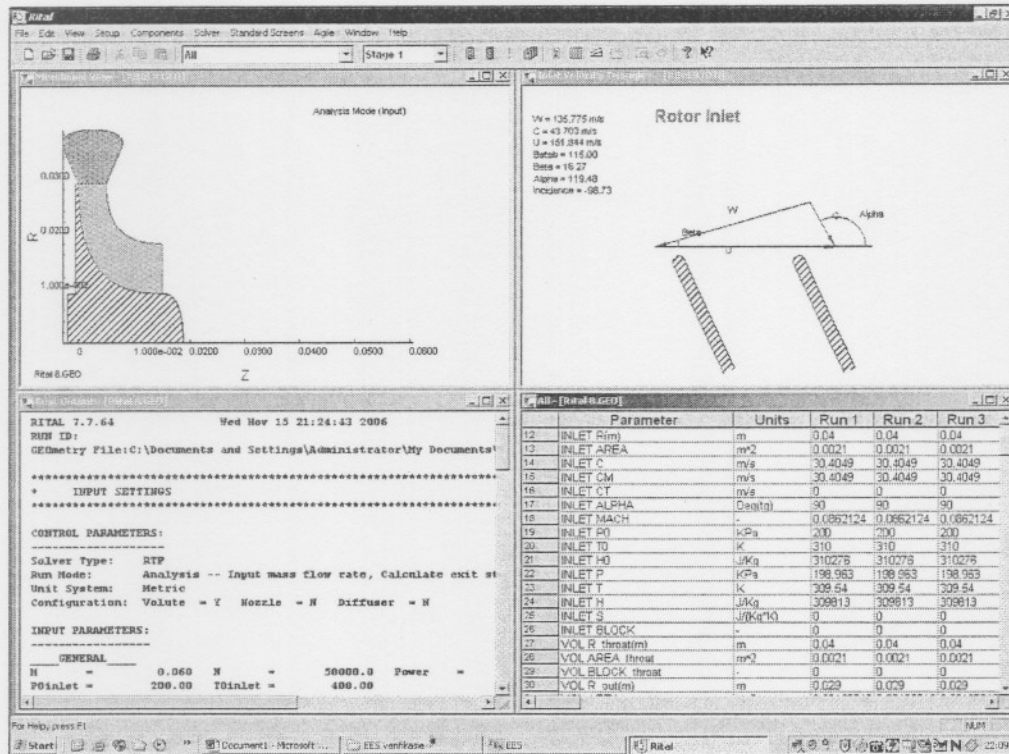
**Results**

$A_4 = 0.00129$	$C_{m4} = 30.4$	$Z = 15.33$	$P_4 = 171.7$	$P_{04} = 187.3$
$A_6 = 0.0003287$	$C_{m6} = 30.4$	$b = 0.007071$	$PR_{tot} = 1.247$	$P_{06} = 150.2$
$\alpha_4 = 77.47$	$C_{msta4} = 136.8$	$T_{04} = 400$	$PR_{stac} = 1.145$	$P_6 = 150$
$\beta_4 = -25.57$	$C_{msta6} = 17.55$	$T_4 = 391.1$	$W_4 = 33.99$	$p_4 = 1.53$
$\beta_6 = -49.82$	$M_4 = 0.36$	$T_6 = 100.5$	$W_6 = 47.12$	$p_6 = 5.2$
$C_4 = 140.1$	$M_6 = 0.1779$	$T_{06} = 101.1$	$r_4 = 0.02903$	$\alpha_4 = 5236$
$C_6 = 35.11$	$i_4 = -26.58$	$U_4 = 152$	$r_{04} = 0.01023$	$m_6 = 5236$
	ratio = 0.3523	$U_6 = 53.58$		

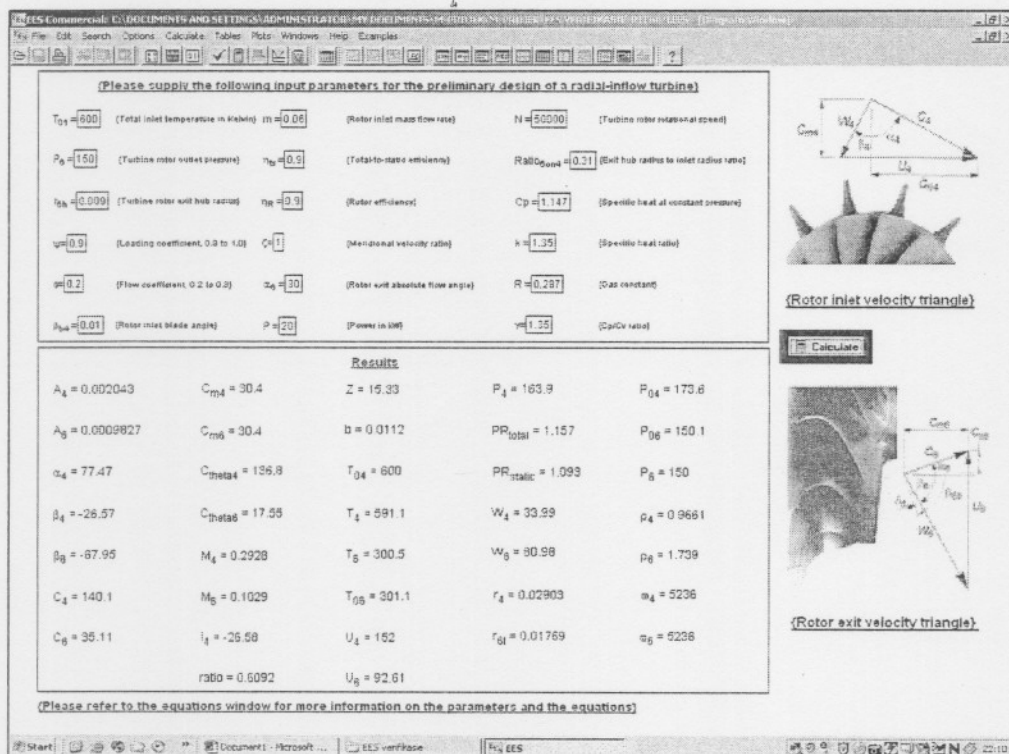
(Please refer to the equations window for more information on the parameters and the equations)

**(Rotor inlet velocity triangle)**

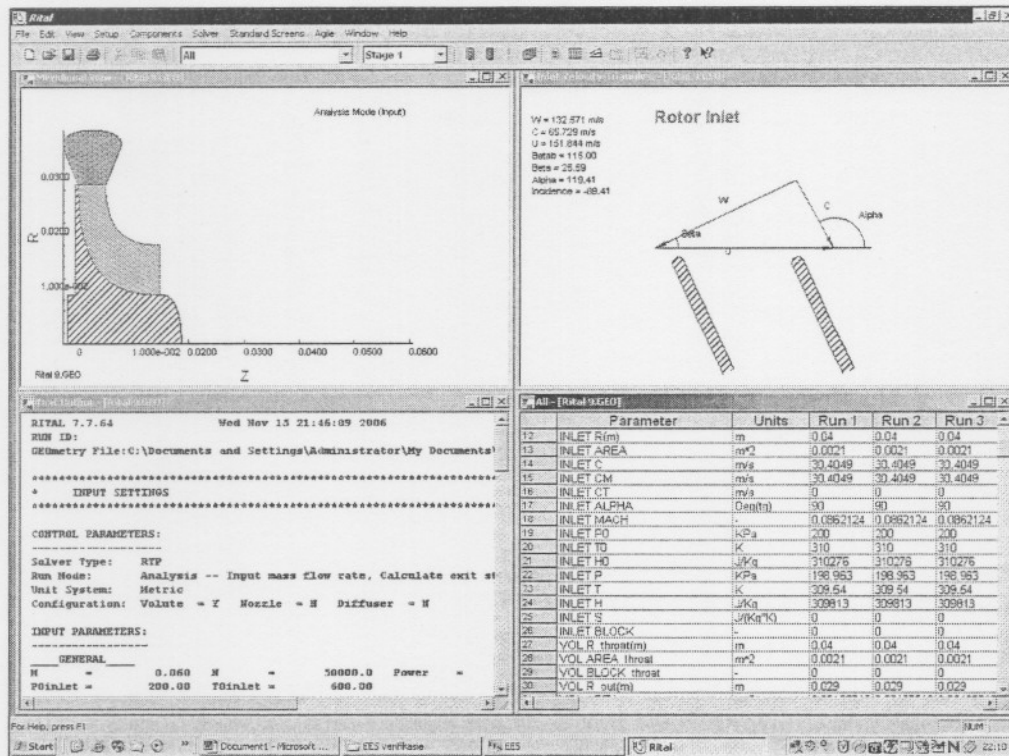
**(Rotor exit velocity triangle)**



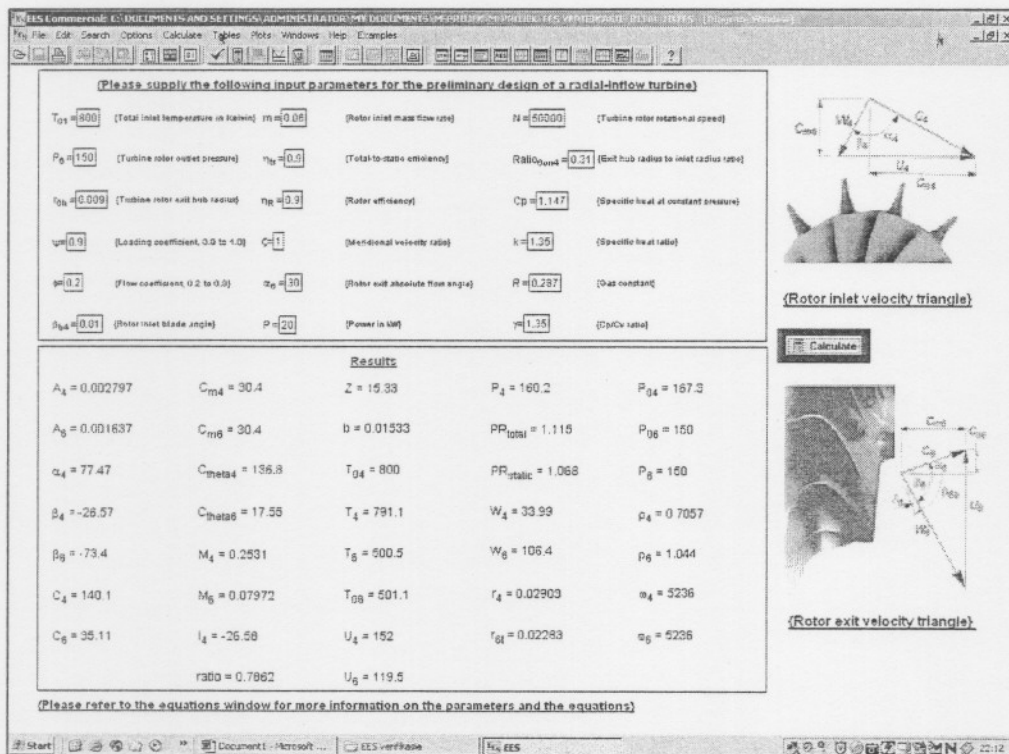
$$T_{01} = 600 \text{ K}$$

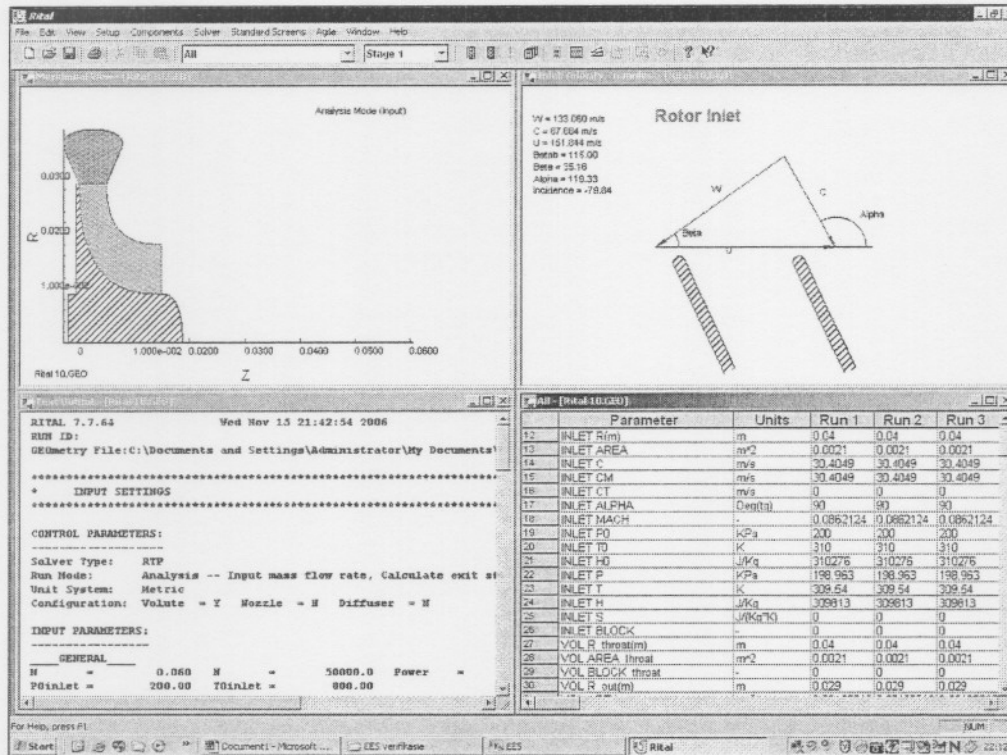






$$T_{01} = 800 \text{ K}$$





$$T_{01} = 1000 \text{ K}$$

**Inputs:**

$T_{01} = 1000$  (Total inlet temperature in Kelvin)  $m = 0.06$  (Rotor inlet mass flow rate)  $N = 50000$  (Turbine rotor rotational speed)

$P_0 = 150$  (Turbine rotor outlet pressure)  $\eta_b = 0.9$  (Total-to-static efficiency)  $Ratio_{0.04} = 0.31$  (Exit hub radius to inlet radius ratio)

$r_{0h} = 0.009$  (Turbine rotor exit hub radius)  $\eta_r = 0.9$  (Rotor efficiency)  $C_p = 1.147$  (Specific heat at constant pressure)

$w = 0.9$  (Loading coefficient, 0.9 to 1.0)  $\phi = 1$  (Meridional velocity ratio)  $k = 1.35$  (Specific heat ratio)

$\beta = 0.2$  (Vane coefficient, 0.2 to 0.3)  $\alpha_0 = 30$  (Rotor exit absolute flow angle)  $R = 0.207$  ( $\phi$  as constant)

$\beta_{04} = 0.01$  (Rotor inlet blade angle)  $P = 20$  (Power in kW)  $\gamma = 1.35$  ( $C_p/C_v$  ratio)

**Results:**

$A_4 = 0.003551$   $C_{m4} = 30.4$   $Z = 15.33$   $P_4 = 159.1$   $P_{04} = 163.6$

$A_6 = 0.002291$   $C_{m6} = 30.4$   $b = 0.01947$   $PR_{total} = 1.091$   $P_{06} = 150$

$\alpha_4 = 77.47$   $C_{theta4} = 136.8$   $T_{04} = 1000$   $PR_{static} = 1.054$   $P_6 = 150$

$\beta_4 = -26.57$   $C_{theta6} = 17.55$   $T_4 = 991.1$   $W_4 = 33.99$   $p_4 = 0.5558$

$\beta_6 = -78.21$   $M_4 = 0.2262$   $T_6 = 700.5$   $W_6 = 127.5$   $p_6 = 0.7461$

$C_4 = 140.1$   $M_6 = 0.06738$   $T_{06} = 701.1$   $r_4 = 0.02903$   $\alpha_4 = 3236$

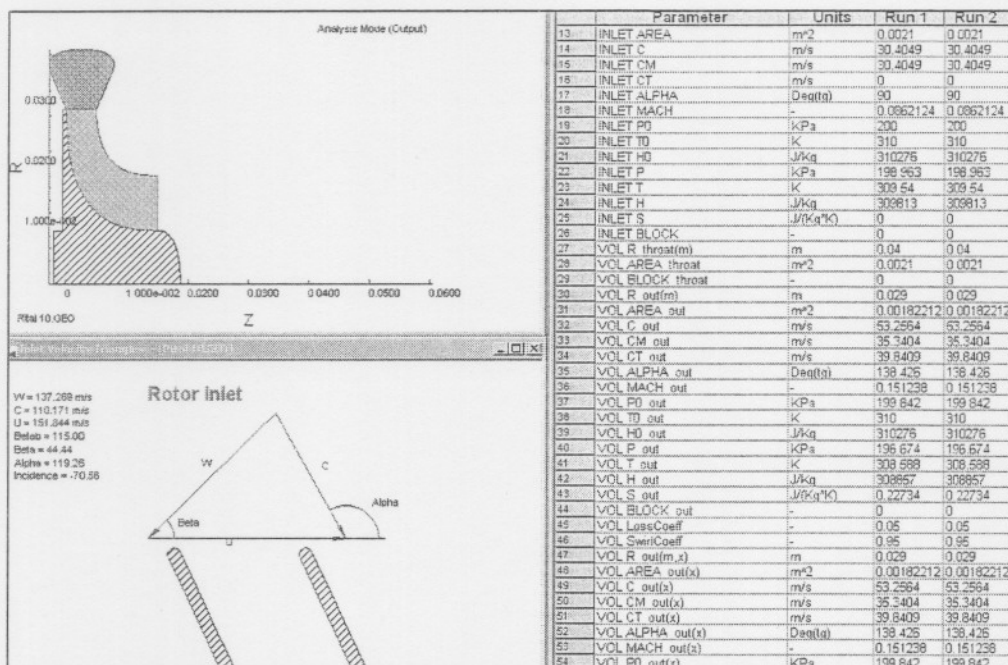
$C_6 = 35.11$   $i_4 = -26.58$   $U_4 = 152$   $r_{01} = 0.027$   $\alpha_6 = 5236$

$ratio = 0.9301$   $U_6 = 141.4$

**Diagrams:**

**Rotor inlet velocity triangle:**

**Rotor exit velocity triangle:**





## Appendix F: EES parameters

The design procedure for the rotor of a radial-inflow turbine, as discussed in Appendix A, was programmed in EES in order to create a procedure by which the inlet parameters for Concepts Rital can be calculated. The equations in Chapter 3 were used and combined with other turbo-machine and fluid analysis equations to create the EES program for the calculation of the input parameters.

After these equations were programmed in EES, a calculation window was created in EES in order to make it easier for the designer when doing a radial-inflow rotor design. This design window is linked to the equations used to create the procedure and gives exactly the same answers, but looks better than the equations previewed in Appendix A.

Although it may seem easy to do a preliminary design of a radial-inflow turbine rotor by making use of the design window created, caution must be taken in choosing the input parameters for the EES program. The designer must try and keep the input parameters as real as possible and this may be difficult if the designer does not have efficient experience in turbo-machine design or good guidelines to follow. In order to prevent this from happening, a basic manual on using the design procedure created in EES has been constructed.

The manual will be based on the design window created in EES and it is displayed in Figure F1. The manual is constructed by discussing each parameter as displayed in the design window.

EES Commercial: C:\DOCUMENTS AND SETTINGS\ADMINISTRATOR\MY DOCUMENTS\1-M-PROJECT\_HOOFPROGRAM 2.EES - [Diagram Window]

File Edit Search Options Calculate Tables Plots Windows Help Examples

(Please supply the following input parameters for the preliminary design of a radial-inflow turbine)

$T_{01} = 973.3$ (Total inlet temperature in Kelvin)	$\dot{m} = 1.148$ (Rotor inlet mass flow rate)	$N = 65363$ (Turbine rotor rotational speed)
$P_0 = 544.7$ (Turbine rotor outlet pressure)	$\eta_{ts} = 0.7$ (Total-to-static efficiency)	$Ratio_{0.004} = 0.3$ (Exit hub radius to inlet radius ratio)
$r_{0h} = 0.012$ (Turbine rotor exit hub radius)	$\eta_R = 0.75$ (Rotor efficiency)	$C_p = 1.147$ (Specific heat at constant pressure)
$\psi = 0.9$ (Loading coefficient, 0.9 to 1.0)	$C = 1$ (Mendional velocity ratio)	$k = 1.35$ (Specific heat ratio)
$\phi = 0.3$ (Flow coefficient, 0.2 to 0.3)	$\alpha_0 = 6$ (Rotor exit absolute flow angle)	$R = 0.296$ (Gas constant)
$\beta_{b4} = -16$ (Rotor inlet blade angle)	$P = 85.2$ (Power in kW)	$\gamma = 1.34$ (Cp/Cv ratio)

**Results**

$A_4 = 0.004946$	$C_{m4} = 82.14$	$Z = 12.07$	$P_4 = 789.5$	$P_{04} = 889.1$
$A_6 = 0.00664$	$C_{m6} = 82.14$	$b = 0.01968$	$PR_{total} = 1.631$	$P_{06} = 545.2$
$\alpha_4 = 71.57$	$C_{theta4} = 246.4$	$T_{04} = 973.3$	$PR_{static} = 1.449$	$P_6 = 544.7$
$\beta_4 = -18.43$	$C_{theta6} = 8.633$	$T_4 = 943.8$	$W_4 = 86.58$	$p_4 = 2.826$
$\beta_6 = -74.98$	$M_4 = 0.423$	$T_6 = 879$	$W_6 = 316.9$	$p_6 = 2.093$
$C_4 = 259.7$	$M_6 = 0.1394$	$T_{06} = 882$	$r_4 = 0.04$	$\omega_4 = 6845$
$C_6 = 82.59$	$l_4 = -2.435$	$U_4 = 273.8$	$r_{01} = 0.04597$	$\omega_6 = 6845$
	ratio = 1.149	$U_6 = 314.7$		

(Please refer to the equations window for more information on the parameters and the equations)

**Diagram Window:**

(Rotor inlet velocity triangle)

(Rotor exit velocity triangle)

Calculate

Figure F1: Design window for a radial-inflow turbine rotor in EES.

### 5.1.1 Input parameters

$T_{01}$  (Total inlet temperature)

The total inlet temperature is the inlet temperature that enters the radial turbine rotor as it exits the volute. Caution must be taken when choosing the material of which the rotor must be manufactured, as the inlet to the rotor is where the highest temperature of the working fluid is recorded. The inlet temperature is determined by a source of energy, for example an internal combustion chamber.



$P_6$  (Turbine outlet pressure)

The turbine rotor outlet pressure is the pressure exiting the rotor. The pressure at which the turbine exits, for example ambient pressure, determines the outlet pressure. In some cases the outlet pressure will not be available to the designer. In this situation, the designer chooses an acceptable outlet pressure and does the design of the rotor by changing the outlet pressure until a satisfactory design has been reached. The designer will then be forced to design the next component, to which the rotor exits, to give the desired outlet pressure as chosen during the design of the rotor.

$r_{6h}$  (Rotor exit hub radius)

The turbine rotor exit hub radius is the smaller of the two radii, the other being the turbine rotor inlet radius. The exit hub radius is the choice of the designer, but it is recommended that the designer look at other radial turbine examples in order to start with a realistic value thereof. It is usually limited by shaft size or by crowding together of the blade roots (Baines, 2003).

$\Psi$  (Loading coefficient)

In radial turbines there is a wide variation in blade speed due to the radius change between inlet and exit and therefore the choice of blade speed used to define the loading coefficient is arbitrary, according to Baines. It depends on the designer for which total-to-static efficiency of the rotor he wants to design and this then sets the value of the loading coefficient, as determined by Figure 35. A loading coefficient of 0.9 – 1 is usually used, as this is where the highest turbine efficiency is found, although this range is by no means a restriction during the design procedure. If a lower or higher loading coefficient is used, it will only result in a lower turbine efficiency with gains in other parameters. It all depends on the choice of the designer.

$\Phi$  (Flow coefficient)

Figure 35 can also be used in order to determine the value of the flow coefficient, after the designer has decided on the total-to-static efficiency of the rotor. A flow coefficient in the range of 0.2 – 0.3 is usually used, as this is where the highest turbine efficiency is found. If a lower or higher flow coefficient is used, it will only result in a lower turbine efficiency with gains in other parameters. It all depends on the choice of the designer.

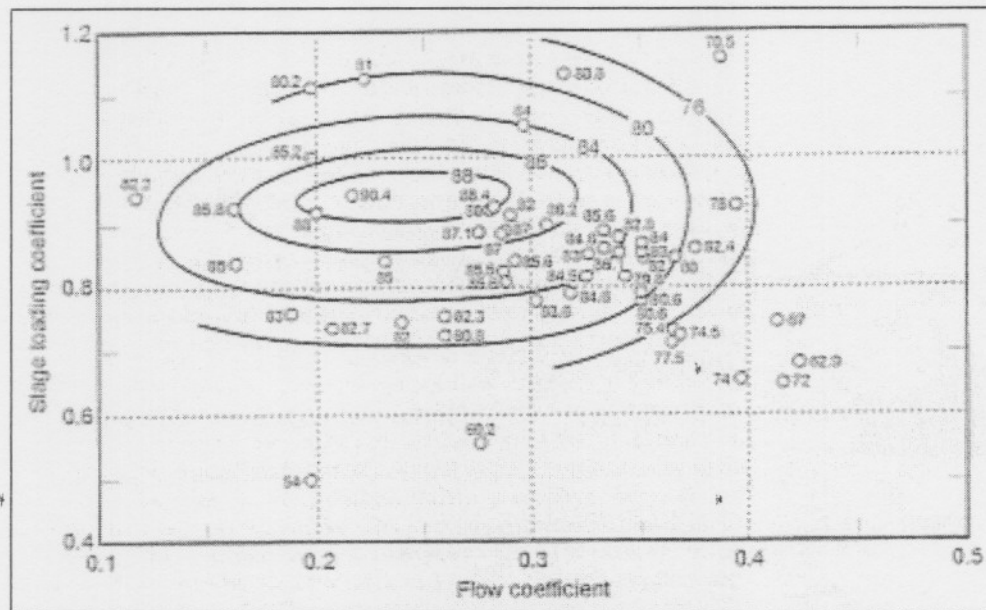


**Figure F2:** Correlation of blade loading and flow coefficients for radial-inflow turbines. Data points and contours show total-to-static efficiency. (From Baines, 2003)

$\beta_{b4}$  (Rotor inlet blade angle)

The rotor inlet angle is the angle at which the blade is situated at the rotor inlet and not the angle of the flow entering the rotor blade. The inlet to the rotor is a highly stressed region, because of the bending stress in the blade generated by the centrifugal force. For this reason the inlet blade angle is usually radial, but small variations in angle is possible when considering a stronger material.

$\dot{m}$  (Rotor inlet mass flow rate)

The rotor inlet mass flow rate is determined by the flow entering the rotor from the pre-attached element. This element can be the volute attached to the rotor or any other design.

$\eta_{ts}$  (Total-to-static efficiency)

The total-to-static efficiency is the efficiency of the turbine and can be written as  $\eta_{ts} = 2\Psi v^2$ . This implies that for an ideal turbine, where  $\eta_{ts} = 1$ ,  $\Psi = 1$  and  $v = 0.7$ . In practice and thus for realistic values of efficiency,  $v$  will be lower and for lower values of  $\Psi$ ,  $v$  will be higher (Baines, 2003). This shows that the two effects will tend to cancel out.

$\eta_R$  (Rotor efficiency)

The rotor efficiency is the efficiency of the rotor itself. It is used as a method to specify the rotor loss by calculating the rotor efficiency as the ratio of the actual work output and the theoretical work output based on the rotor pressure drop alone.

$\zeta$  (Meridional velocity ratio)

The meridional velocity ratio is the ratio of the inlet meridional velocity and the exit meridional velocity. It normally has a value near unity. It influences the rotor inlet area and therefore the inlet blade height for fixed inlet radius. The meridional velocity ratio therefore has some influence on the rotor incidence and it may be necessary to vary  $\zeta$  in order to achieve an acceptable incidence angle (Baines, 2003).

$\alpha_6$  (Rotor exit absolute flow angle)

The exit absolute flow angle is the flow angle of the exit absolute velocity  $C_6$ . This angle may be important in matching the next component downstream, for example another turbine or exhaust system. Other things being equal, it will minimize the exit kinetic energy loss (Baines, 2003).

## **P** (Power)

The power is defined in Kilowatt and is the power the designer wishes to achieve from the radial turbine design. In other words, this is the work that is expected to be delivered by the turbine.

## **N** (Turbine rotational speed)

The turbine rotational speed is the speed at which the rotor will spin. The ideal is to get the rotational speed as high as possible, but other factors such as material strength and fluid properties must be taken in consideration. In Paragraph 5.2 factors are discussed which limit the rotational speed to more realistic values.

## **Ratio<sub>son4</sub>** (Exit hub to inlet radius ratio)

The ratio of these two quantities determines the curvature of the rotor shroud contour in the meridional plane (Baines, 2003). This means that it determines the shape of the rotor blade and at which angles it is bended from the inlet to the outlet.

## **C<sub>p</sub>** (Specific heat)

The specific heat value is fluid dependable and the values for  $C_p$  for different fluids are usually available in most fluid dynamic books.

## **k** (Specific heat ratio)

The specific heat ratio is also fluid dependable and the values for  $k$  can be found in most fluid dynamic books.

## **R** (Gas constant)

The gas constant value depends on the fluid used for flow through the turbine. Most gas constant values for different fluids are available in fluid dynamic books.

$\gamma$  (Cp/Cv ratio)

The  $\gamma$  value is also fluid dependable and is available for most fluids in fluid dynamic books and literature.

### 5.1.2 Output parameters

$A_4$

The rotor inlet area is the annulus area at the rotor tip. The total inlet area is the sum of all the blade areas added together.

$A_6$

The exit area is the area where the working fluid exits the rotor. This area is the difference between the rotor outlet tip radius and the shaft radius of the rotor.

$\alpha_4$

The absolute inlet flow angle to the rotor is the angle at which the working fluid approaches the rotor. This angle is determined by the nozzle vanes, if it is present, or by the angle determined by the volute.

$\beta_4$

$\beta_4$  is the inlet relative flow angle of the working fluid. One would expect it to be the same as the inlet blade angle of the rotor, in order to give the best inlet to the rotor, but it is not the case. The optimum inlet flow angle is in the region of  $-20^\circ$  to  $-40^\circ$  (Baines, 2003) and this is explained in Figure F3. Cases *a* and *c* shows flow separation at the suction surface and pressure surface respectively. Case *b* however shows that the flow turns smoothly into the blade passage without fluid separation.

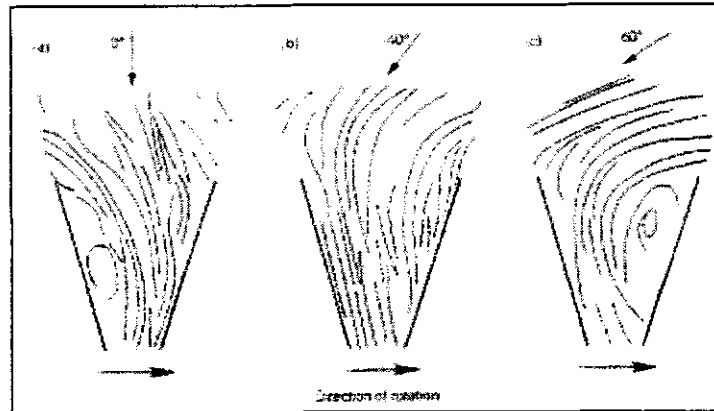


**Figure F3:** Results of three different relative inlet-flow angles. (From Baines, 2003)

### $\beta_6$

$\beta_6$  is the exit blade angle of the rotor. The exit blade angle with a deviation angle added to it, will give the exit fluid angle  $\beta_{6b}$ .

### $C_4$

The inlet absolute velocity is the velocity at which the working fluid approaches the rotor.

### $C_6$

The exit absolute velocity is the velocity at which the working fluid exits the rotor.

### $C_{m4}$

The meridional inlet absolute velocity is the radial component of the inlet absolute velocity  $C_4$ .

### $C_{m6}$

The meridional exit absolute velocity is the axial component of the exit absolute velocity  $C_6$ .

### $C_{\theta 4}$

$C_{\theta 4}$  is the tangential component of the inlet absolute velocity  $C_4$ .

#### **$C_{\theta 6}$**

$C_{\theta 6}$  is the radial component of the exit absolute velocity  $C_6$ .

#### **$M_4$**

The inlet Mach number is the Mach number of the working fluid as it approaches the rotor. It is important that the inlet Mach number be kept below one, as shock waves can appear if it is exceeded.

#### **$M_6$**

The exit Mach number is the Mach number of the working fluid as it exits the rotor.

#### **$i_4$**

The rotor incidence angle must be investigated by the designer to ensure that it is consistent with the general experience that in radial turbines the best efficiency occurs at some negative incidence in the region of  $20^\circ$ - $30^\circ$  in magnitude (Baines, 2003).

#### **ratio**

The rotor exit tip to inlet radius ratio  $r_{6t}/r_4$  should be less than unity when designing a radial-inflow turbine, as this will give a good aerodynamic solution (Baines, 2003).

#### **Z**

The number of rotor vanes can be determined by three widely used criteria; the Jamieson, Glassman and Whitfield criteria. In Figure 31 the relationship between the various criteria can be seen. For a certain inlet flow angle  $\alpha$ , a number of rotor vanes Z can be found.

#### **b**

The material determines the blade thickness the designer decides on, as the material's properties are very important. A material that has good strength

properties and which can handle high temperature will give the designer the choice of a thinner blade over that of a material with weaker properties.

#### $T_{04}$

The total inlet temperature is usually set equal to  $T_{01}$ , the total temperature exiting the energy source, for example a combustion chamber. If a volute is used, it will be the temperature exiting the volute and entering the rotor.

#### $T_4$

The static inlet temperature is the actual temperature entering the rotor.  $T_4$  is calculated by making use of the total inlet temperature  $T_{04}$ , the inlet absolute velocity and the inlet Mach number. The static inlet temperature must be kept in sequence with the material used, in order to insure that the material will not fail due to excessive working temperature.

#### $T_6$

The exit static temperature is the actual temperature exiting the rotor, calculated by making use of the exit absolute velocity, the exit Mach number and the working fluid properties. The exit temperature must be kept in mind during design, as this is the temperature of the working fluid as it enters the next component coupled to the rotor, for example a second stage rotor or exhaust system.

#### $T_{06}$

The exit stagnation temperature is calculated by making use of the exit static temperature, the exit Mach number and the specific heat ratio.  $T_{06}$  will in most cases be close to the exit static temperature, indicating the temperature on a specific point in time.

#### $U_4$

The inlet blade speed is the speed at which the rotor spins at the inlet tip of the rotor. This speed is very important when designing a radial-inflow turbine, as it influences the material used for the rotor. An inlet blade speed of 400 m/s is fairly



high for radial turbines, but should be acceptable for most common rotor materials such as Inconel 713 and 718 (Baines, 2003).

#### **$U_6$**

The exit blade speed is the speed at which the rotor spins at the outlet tip of the rotor.  $U_6$  will almost always be much less than the inlet blade speed, as the exit radius of the rotor will in most cases be less than the inlet radius, as can easily be seen from Figure 25.

#### **$P_4$**

The inlet static pressure is the pressure of the working fluid as it enters the rotor. The inlet static pressure is calculated by making use of the inlet stagnation pressure, the inlet Mach number and the specific heat ratio. The inlet stagnation pressure is usually designed according to certain requirements, such as to be less than the compressor delivery pressure.

#### **$PR_{total}$**

The total pressure ratio is the pressure ratio calculated with the power required, the inlet total temperature and the working fluid properties.

#### **$PR_{static}$**

The static pressure ratio is calculated by the ratio of the inlet static pressure and the exit static pressure. The pressure ratio for a radial-inflow turbine is usually between 1 and 2, but may exceed 2 in certain specific applications.

#### **$W_4$**

The inlet relative velocity is determined by the inlet absolute velocity and the rotor inlet blade speed  $U_4$ .

#### **$W_6$**

The exit relative velocity is determined by the exit absolute velocity and the rotor exit blade speed  $U_6$ .

**$r_4$** 

The inlet radius is calculated from the inlet area and determines, together with the exit tip radius, the tip ratio of the rotor.

 **$r_{6t}$** 

The exit tip radius is calculated from the exit rotor area and is used to determine the tip ratio. During design, it is favourable to keep the tip ratio  $r_{6t}/r_4$  less than unity, as this will give a desirable aerodynamic rotor solution (Baines, 2003).

 **$P_{04}$** 

The inlet stagnation pressure is calculated by using the total pressure ratio and the exit stagnation pressure.  $P_{04}$  is the pressure of the working fluid at a certain point in time.

 **$P_{06}$** 

The exit stagnation pressure is calculated from the exit static pressure, determined by the pressure necessary in the next component, the exit Mach number and the fluid properties.  $P_{06}$  is the pressure of the working fluid at a certain point in time.

 **$P_6$** 

The exit static pressure is usually determined by the component following the radial turbine. This component can be a second turbine or an exhaust system. The exit pressure must be kept in mind when exhausting to ambient pressure, in order to control the exhaust system loss (Baines, 2003). The higher the exit static pressure that exits to ambient pressure is, the higher the exhaust system loss.

 **$\rho_4$** 

The inlet density is the density of the working fluid as it enters the turbine rotor. The density is calculated by making use of the ideal gas equation,  $P = \rho RT$ . For preliminary design, this is adequate.

